Gain-of-function STAT1 mutations impair STAT3 function and underlie susceptibility to Chronic Mucocutaneous Candidiasis

Jie Zheng

Thesis submitted for the Doctor of Philosophy

Institute of Cellular Medicine

Newcastle University, UK

January 2014

Abstract

Background: Signal transducer and activator of transcription (STAT)3 activation triggers transcription of interleukin (IL)-17 which is crucial for mounting protective immune responses against fungi. Several mutations affecting the STAT3/IL-17 pathway have been reported, resulting in selective susceptibility to fungal (*Candida*) infection characteristic of Chronic Mucocutaneous Candidiasis (CMC). Patients with autosomal dominant (AD)-CMC have defective T helper (Th)-17 responses *(Ng et al, JACI 2010)* and harbour gain-of-function (GOF) STAT1 (rather than STAT3) mutations *(van de Veerdonk et al NEJM 2011)*, leading to hyper-phosphorylation of STAT1 *(Smeekens et al PLosOne 2011)*. How this affects STAT3 or leads to decreased IL-17 production is unknown.

Objective: To assess how GOF-STAT1 mutations affect STAT3 activation, DNA-binding, gene expression, cytokine production and whether this can be epigenetically modified.

Approaches: Peripheral blood mononuclear cells (PBMCs) or Epstein-Barr virus (EBV)-transformed cell lines were stimulated with various cytokines (IL-23, IL-6, IL-21, IL-27, IFN-α, IFN-γ) in the absence or presence of fludarabine (a STAT1 inhibitor) or trichostatin A (a histone deacetylase inhibitor, HDACi). Activation of STAT1 and STAT3 was measured by western blotting (WB). DNA-binding of STAT1 and/or STAT3 was evaluated using electrophoretic mobility shift assay (EMSA), TransAm STAT3 kit and chromatin immunoprecipitation (ChIP) assay. STAT3-inducible gene (RORc, IL-17, IL-22, IL-10, c-Fos, SOCS3, c-Myc) and STAT1-inducible gene (CXCL10, IRF1) expression was assessed using quantitative real time-polymerase chain reaction (qRT-PCR). Gene silencing was performed with small interfering RNA (siRNA) targeting HDAC1, 2 and 3. *Candida albicans*-induced cytokine (IL-17, IL-22, IL-10) production was measured by enzyme-linked immunosorbent assay (ELISA).

Key Findings: GOF-STAT1 mutations lead to hyper-phosphorylation of STAT1 and delayed dephosphorylation. Mutations decrease STAT3-induced gene expression and Th-17-mediated cytokine production without affecting STAT3 phosphorylation, nuclear accumulation or DNA-binding to a STAT-consensus binding site - human *sis*-inducible element (hSIE). The disrupted STAT3 function can be modified either by enhancing acetylation or inhibiting STAT1 activation.

Conclusion: GOF-STAT1 mutations impair STAT3 function, which can be rescued by enhancing acetylation and/or inhibiting STAT1. These findings are the likely mechanisms underlying decreased Th-17 (IL-17A and IL-22) cytokine production and susceptibility to fungal infections in CMC.

Acknowledgements

My PhD study has been a truly enjoyable experience. It would not have been possible without the guidance and support from my supervisors. Firstly, I would like to thank Dr Desa Lilic, who spent her time and shared her knowledge helping me to complete this PhD project. I am very grateful for the motivation and support she has provided throughout the past three years and for being not only a mentor but also a friend, giving me a learning environment so that I could develop personally as well as professionally. In addition, I would like to thank my second supervisor Prof. Drew Rowan, for his invaluable scientific and technical guidance during my PhD.

I would like to express my gratitude to Dr Mario Abinun and Dr Andrew Gennery for providing the samples of CMC patients with GOF-STAT1 mutations, to Dr Jelena Mann for providing her assistance with ChIP assay, to Dr Dennis Lendrem for his assistance with statistic analysis, to Dr Catherine Syddall for her assistance with EMSA, to Dr Amy Anderson for her assistance with Flow cytometry, to Dr Matt Barter for his assistance with cell transfection, and to all the members of the Musculoskeletal Research Group and Primary Immune Deficiency Group for their helps, friendship and donating blood to the project.

I would like to thank my parents for their immense understanding and encouragement. With all my heart, I must reserve my greatest thanks and deepest gratitude to my husband Tian for his endless love, patience, support, understanding and much more.

Finally, thanks to the UK-China Excellent Scholarship providing funding for this project, without which my PhD study would not have been possible.

Declaration

The candidate confirms that the work submitted is her own work under the guidance of supervisors, Dr Desa Lilic and Prof. Drew Rowan. Except for commonly held concepts, and where specific reference is made to other work, the content of the thesis is original. The work in this thesis was performed from January 2011 to January 2014. All work was carried out in Musculoskeletal Research Group, Institute of Cellular Medicine, Newcastle University, UK. No part of this thesis has been submitted for the award of any other degree.

Content

List of Figures and Tables

List of Figures

List of Tables

Abbreviations

ABI	Applied Biosystems
AD	Autosomal Dominant
AIDS	Acquired Immunodeficiency Syndrome
AIRE	Autoimmune Regulator
APECED	Autoimmune Polyendocrinopathy Candidiasis Ectodermal Dystrophy
APS1	Autoimmune Polyendocrinopathy Syndrome type I
APS	Ammonium Persulphate
AR	Autosomal Recessive
BSA	Bovine Serum Albumin
CARD9	Caspase Recruitment Domain-containing Protein 9
CCD	Coiled-coil Domain
cDNA	Complementary DNA
CI	Confidence Intervals
CMC	Chronic Mucocutaneous Candidiasis
CMV	Cytomegalovirus
ChIP	Chromatin Immunoprecipitation
ChIP-Seq	Chromatin Immunoprecipitation-sequencing
CLR	C-type Lectin Receptor
CXCL10	CXCL-motif Chemokine Ligand 10
CysA	Cyclosporine A
DBD	DNA-binding Domain
DC	Dentritic Cell
DC SIGN	DC Specific Intracellular Adhesion Molecule Grabbing Non-integrin
DMEM	Dulbecco’s Modified Eagle Medium
dNTP	Deoxy-Nucleotide Triphosphate
DOCK	Dedicator of Cytokinesis 8
DTT	DL-Dithiothreitol
EBV	Epstein-Barr Virus
ECL	Enhanced Chemiluminescence

EDTA	Ethylenediaminetetraacetic Acid
ELISA	Enzyme-Linked Immunosorbent Assay
EMSA	Electrophoretic Mobility Shift Assay
EtOH	Ethyl Alcohol
FcRγ	Fc Receptor gamma-chain
FCS	Fetal Calf Serum
FLU	Fludarabine
GAS	Interferon-gamma Activated Sequence
GFP	Green Fluorescent Protein
GOF	Gain-of-Function
HAT	Histone Acetyltransferase
HDAC	Histone Deacetylases
HDACi	Histone Deacetylases Inhibitor
HBSS	Hanks Buffered Saline Solution
HC	Healthy Control
HEPES	4-(2-hydroxyethyl)-1-piperazineethanesulfonic acid
HIES	Hyper-IgE Syndrome
HIV	Human Immunodeficiency Virus
hSIE	Human *sis*-inducible Element
IFN	Interferon
Ig	Immunoglobulin
IL	Interleukin
IMDM	Iscove's Modified Dulbecco's Medium
IPEX	Immunodysregulation Polyendocrinopathy Enteropathy X-linked Syndrome
IRAK	IL-1 Receptor Associated Kinase
IRF	Interferon Regulatory Factor
ISG	IFN-stimulated Gene
ISGF	IFN-stimulated Gene Factor
ISRE	Interferon-stimulated Response Element
JAK	Janus Kinase

KO	Knock-out
LD	Linker Domain
LGB	Low Gel Buffer
LOF	Loss-of-Function
MAL	Myeloid Differentiation Factor 88 Adaptor Like
MR	Mannose Receptor
MSMD	Mendelian Susceptibility to Mycobacterial Disease
MST1/STK4	Serine Threonine Kinase 4
MST	3-(4,5-dimethylthiazol-2-yl)-5-(3-carboxymethoxyphenyl)-2-(4-sulfophenyl)-2H-tetrazolium
MyD88	Myeloid Differentiation Factor 88
NF-κB	Nuclear Factor-κB
NLR	Nucleotide-binding Oligomerization Domain Receptor/NOD-like Receptor
NTD	Amino-terminal Domain
OPD	O-Phenylenediamine Dihydrochloride
PAGE	Polyacrylamide Gel Electrophoresis
PAMP	Pathogen-associated Molecular Pattern
PBMC	Peripheral Blood Mononuclear Cell
PBS	Phosphate Buffered Saline
PCR	Polymerase Chain Reaction
PHA	Phytohemagglutinin
PIAS	Protein Inhibitors of Activated STAT Proteins
PID	Primary Immunodeficiency Disease
PRP	Pattern Recognition Receptor
pSTAT	Phosphorylated STAT
PTP	Protein Tyrosine Phosphatase
PVDF	Polyvinylidene Difluoride
p300/CBP	Transcription Coactivator of p300 and CREB-Binding Protein
qRT-PCR	Quantitative Real Time-Polymerase Chain Reaction
ROR	Retinoic Acid Receptor (RAR)-related Orphan Receptor
RVI	Royal Victoria Infirmary

SCID	Severe Combined Immune Deficiency
SDS	Sodium Dodecyl Sulfate
SGB	Stacking Gel Buffer
SH2	Src Homology 2 Domain
SHP-2	Src Homology 2 Domain Containing PTP-2
siRNA	Small Interfering RNA
SOCS	Suppressor of Cytokines Signaling
STAT	Signal Transducer and Activator of Transcription
Staph A	Staphylococcus Aureus
SyK	Spleen Tyrosine Kinase
TAD	Transactivation Domain
TAK	TGF-β Activated Kinase
TBK	TRAF Family Member Associated NF-κB Activator Binding Kinase
TBE	Tris/Borate/EDTA
TBS/T	Tris-Buffered Saline-Tween
TC-PTP	T Cell Protein Tyrosine Phosphatase
TEMED	*N,N,N',N'*-Tetramethylethylenediamine
TGF-β	Transforming Growth Factor-β
TLR	Toll-like Receptor
TNF	Tumor Necrosis Factor
TRAF	TNF Receptor Associated Factor
TRIF	Toll-IL-1 Receptor Domain Containing Adaptor Inducing IFN-β
TRAM	TRIF Related Adapter Molecule
TS	Tail Segment
TSA	Trichostatin A
Th	T helper cell
TYK	Tyrosine Kinase
UGB	Upper Gel Buffer
WB	Western Blotting
YNB	Yeast Nitrogen Base

CHAPTER 1 GENERAL INTRODUCTION

1.1 *Candida* and Chronic Mucocutaneous Candidiasis

Candida albicans is a commensal ubiquitous fungal organism, found naturally in the intestinal tract of all people, often colonizing the skin and the mucosal surfaces of normal individuals, without causing disease. However, *Candida* is an opportunistic organism and in permissive circumstances it can cause infections [1].

1.1.1 Infections caused by Candida

In immunocompromised individuals such as those with primary or secondary immune deficiencies, *Candida* infections can cause a spectrum of clinical presentations, ranging from localized mucocutaneous infections to disseminated and/or invasive disease [2].

Primary versus secondary Candidiasis: Primary immunodeficiency diseases (PIDs) are genetic, inborn errors of innate and/or adaptive immunity that render their hosts susceptible to infections and other immune-mediated diseases including autoimmunity and exaggerated inflammatory responses [3]. Conventional PIDs were defined by a distinct immunological phenotype resulting in a broad susceptibility to range of microorganisms. As a conventional PID, Severe Combined Immune Deficiency (SCID) has been reported to predispose to candidiasis although, importantly, these patients are also simultaneously susceptible to a wide range of microorganisms [4, 5] i.e. do not have a selective susceptibility to *Candida*. Secondary *Candida* infections can be precipitated by a range of factors including dentures, antibiotics, immunosuppressive drugs and human immunodeficiency virus (HIV) infection/acquired immunodeficiency syndrome (AIDS) [6, 7], where permissive circumstances promote *Candida* growth.

Mucocutaneous Candidiasis is seen in patients with oral *Candida* infection, known as thrush, but can also present as persistent mucosal infections affecting vaginal, esophageal and gastrointestinal mucosae. More seriously, disseminated *Candida* infection - **Systemic Candidiasis** is encountered in patients with phagocytic defects affecting neutrophils, monocytes and macrophages [3]. It involves the hematogenous

spread of *Candida albicans* to multiple organs, including the brain, kidneys, heart, liver and lungs and leads to a high mortality [8].

1.1.2 Primary immunodeficiency syndromes of CMC as a model for studying the Candida immunity

Selective susceptibility to *Candida* infections is well recognized in PID syndromes of Chronic Mucocutaneous Candidiasis (CMC), where patients suffer with chronic, persistent or recurrent, debilitating infection of the skin, nails and mucous membranes with *Candida* (usually *albicans*) [9, 10]. As opposed to conventional PIDs, CMC is defined as a "non-conventional" PID [11], manifesting as narrow susceptibility to infection with weakly pathogenic microbes. Indeed, non-conventional PIDs are ideal models to understand individual susceptibility to common infections, which can elucidate the genetic basis of impaired immunity to specific infections with a genotype-to-phenotype approach [1]. As a good example of non-conventional PIDs, understanding the aetiology and pathogenesis of CMC can unravel the immunological pathways mediating human immunity to fungi. Until recently, classifications of CMC were mostly based on the time of onset and endocrine organ involvement, the largest subgroups being patients with autosomal dominant (AD)-CMC with or without thyroid disease, patients with the Autoimmune Polyendocrinopathy Syndrome type I (APS1) also known as the Autoimmune Polyendocrinopathy Candidiasis Ectodermal Dystrophy syndrome (APECED) and sporadic patients with isolated CMC.

1.2 Protective immunity to Candida infections

Protective immunity to *Candida* involves both innate and adaptive cellular and humoral immune responses. Current data suggest that protection against disseminated diseases is mediated primarily by innate immune mechanisms (such as neutrophils) [12]. In contrast, protection against mucocutaneous disease relies on cell-mediated immunity specially T cells [13].

1.2.1 Role of the innate immune system

The innate immune system can recognize a range of conserved fungal

pathogen-associated molecular patterns (PAMPs) [14] and initiate a rapid response to activate inflammatory cells that have a dual role of eliminating the invader and triggering the appropriate adaptive immune responses. Mannans, mannoproteins, β-glucans and chitin, considered to be PAMPs, are essential structures of *Candida* cell walls [15]. Chitin and β-glucans provide the necessary rigidity of the internal skeleton, whilst a heavily mannosylated layer of mannoproteins covers this layer and forms the surface. These different *Candida* cell wall components can be recognized by host pattern recognition receptors (PRRs), including the Toll-like receptors (TLRs), the C-type lectin receptors (CLRs) and the NOD-like receptors (NLRs) (Fig 1.1) [16, 17].

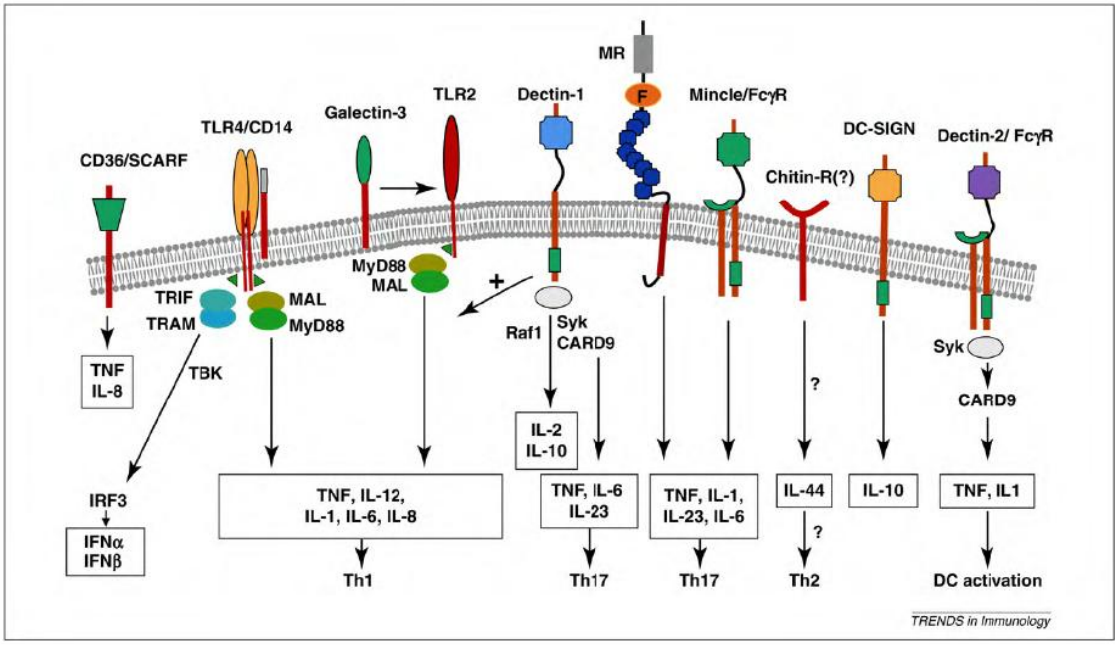

Figure 1.1 Pattern recognition receptors sensing *Candida albicans* at the innate immune system [18].
TLR, Toll-like receptor; MyD88, myeloid differentiation factor 88; Syk, spleen tyrosine kinase; CARD9, caspase recruitment domain-containing protein 9; MAL, MyD88 adaptor like; IRAK, IL-1 receptor associated kinase; TRAF, TNF receptor associated factor; TAK, TGF-β activated kinase; TRIF, Toll-IL-1 receptor domain containing adaptor inducing IFN-β; TRAM, TRIF related adapter molecule; TBK, TRAF family member associated NF-κB activator binding kinase; IRF, IFN response factor; MR, mannose receptor; DC SIGN, DC specific intracellular adhesion molecule grabbing non-integrin.

TLRs were the first PRRs to be identified [19]. Mammalian TLRs contain leucine-rich repeats in the extracellular domain of innate immune cells, which can recognize

microbial or fungal structures. TLRs share a cytosolic Toll-interleukin (IL)-1 receptor domain with IL-1 and IL-18 receptors responsible for activation of downstream signaling pathways [20]. Following the recognition of ligands by TLRs, it can activate the myeloid differentiation factor 88 (MyD88)-dependent pathways leading mainly to the stimulation of pro-inflammatory cytokines. Some TLRs stimulation of an alternative route through the Toll-IL-1 receptor domain containing adaptor inducing IFN-β (TRIF) - TRIF related adapter molecule (TRAM) pathways which trigger Type I interferons (IFNs) signaling [21]. Among the TLR families, TLR2, TLR4, TLR9 and heterodimers containing TLR1 and TLR6, have been reported to mediate the recognition of *Candida* PAMPs [22]. **TLR2** and **TLR4** were thought to have a host defense role against fungi via inducing cytokines such as TNF-α and IL-1β [23]. TLR2 from myeloid cells was reported to recognize the phospholipomannan component of *Candida albicans* cell walls [24], whilst TLR4 recognizes the mannan structures [25]. In addition, **TLR9** can recognize fungal DNA from *Candida albicans*, which subsequently can induce the production of inflammatory cytokines by dentritic cells (DCs) [26]. A partial role of **TLR1** and **TLR6** has been demonstrated in recognition of *Candida albicans in vitro* and induction of cytokines by macrophages. However, there was no increased susceptibility to infection observed from the absence of these receptors from genetically manipulated animals [27].

CLRs are central for fungal recognition of carbohydrate structures. CLR family members include Mannan receptor (MR), Dectin-1, Dectin-2, DC-SIGN, Mincle and Galectin-3. Among these receptors, Dectin-1 and Dectin-2 are important in inducing cytokines that drive inflammation and adaptive immunity to protect the host from *Candida* infections. This is dependent on the activation of a common signaling pathway involving spleen tyrosine kinase (Syk), caspase recruitment domain-containing protein 9 (CARD9) and nuclear factor (NF)-κB [28]. **Dectin-1** binds β-1,3-glucan and activates the **Syk-CARD9** signaling in innate immune cells, promoting interleukin IL-23 production and subsequent T helper type (Th)-17 cells induction in human *Candida* immunity [29, 30]. **Dectin-2** recognizes high-mannose structures that bind hyphal forms of fungi and activate NF-κB via the Fc receptor γ-chain **(FcRγ)-Syk-CARD9** pathway,

thus activating Th-17-inducing activity against *Candida* infections in murine models [31].

Collaborative responses between PRRs: Notably, certain TLRs cooperate with CLRs to mount antifungal immunity. Dectin-1 can collaborate with TLR2 or TLR4 to trigger cytokine production upon recognition of *Candida albicans* [32]. In addition, Galectin-3 and MR are also involved in supporting TLR2-mediated innate cell responses to *Candida* infections [18, 33]. However, further research is needed to better clarify the relationships between PRRs and their functions in *Candida* immunity.

1.2.2 Role of the adaptive immune system

Adaptive immunity to *Candida* infections relies on the induction of cellular immunity, appropriate cytokines and effector phagocytic cells. Studies suggest that the Th-1 and Th-17 cells and the induction of their associated cytokines are required for host resistance to *Candida*.

Th-1 cells and related cytokines implicated in *Candida* infections: Th-1 cells are induced by IL-12, regulated by the transcription factor T-bet and produce IFN-γ that confers immunity to intracellular pathogens. Experimental study in animal models highlighted Th-1-mediated immunity as crucial in immunosurveillance and protection against *Candida albicans* [34]. Previous research in humans suggested that patients with CMC have impaired production of Th-1-inducing cytokines, which could results in an inability to mount protective cell-mediated responses and failure to clear *Candida* [35]. However, the role of Th-1 cells in mucosal antifungal immunity has now largely been replaced by Th-17 cells [33].

Th-17 cells and related cytokines implicated in *Candida* infections: Th-17 cells develop in the presence of IL-1β, transforming growth factor (TGF)-β and IL-6 that requires several transcription factors including signal transducer and activator of transcription (STAT)3 and retinoic acid receptor (RAR)-related orphan receptor γt (RORγt) (a similar protein that in humans is encoded by the RORc gene) [36]. Th-17

cells are further expanded and maintained in the presence of the IL-12-related cytokine, IL-23 [37]. Cytokines produced by Th-17 cells including IL-17A, IL-17F and IL-22 can induce chemokine production at sites of *Candida* infections and initiate the recruitment of neutrophils. Therefore, Th-17 cells are believed to play a crucial role in fungal immunity [38, 39], although they are also associated with pathogenesis of many autoimmune and allergic disorders [36, 40]. Accumulating data regarding immune defects in CMC have highlighted IL-17 signaling in host defense against *Candida albicans* [41, 42] (see below).

1.3 Recent advances in understanding immune defects in PIDs with CMC

Studying patients with inborn errors of immunity has recently led to a major breakthrough in our understanding of immune defects underlying CMC (Fig 1.2).

1.3.1 Hyper IgE syndrome – STAT3, DOCK8 and Tyk2 mutations

Hyper IgE syndrome (HIES), also called Job's syndrome is a PID characterized by recurrent skin abscesses and severe lung infections that result in pneumatoceles, very high concentrations of the serum antibody immunoglobulin (Ig) E and CMC. Inheritance of HIES can be autosomal dominant (AD) or autosomal recessive (AR) [43].

AD-HIES with STAT3 mutations: In this group, CMC is the second most frequent presentation, affecting about 80% of AD-HIES patients [44]. Dominant-negative mutations in the STAT3 gene were found to be responsible for AD-HIES [45, 46]. It is of note that these mutations are heterozygous as homozygous STAT3 mutations are lethal and animal models of STAT3 gene knock-out (KO) are tissue specific. Several groups have shown STAT3 mutations result in a markedly reduced number and function of Th-17 cells and increased susceptibility to *Candida albicans* (but also *Staphylococcus*) in HIES [47, 48]. Murine models have confirmed the role of Th-17 T cells in immunity to both systemic and mucosal *Candida albicans* infections [49], and mouse STAT3-deficient $CD4^{+}$T cells are unable to differentiate into IL-17-producing T cells [50]. Therefore, identification of the genetic basis of AD-HIES paved the way for

cellular and molecular dissection of its associated CMC phenotype.

AR-DOCK8 mutations: Mutations in the gene encoding the dedicator of cytokinesis 8 protein (DOCK8) have been demonstrated in AR-HIES [51]. With AD-HIES, it shares hyper-IgE, eosinophilia, and recurrent *Staphylococcal* infections, but is distinguished from AD-HIES by increased susceptibility to viral infections (Herpes simplex, Molluscum contagiosum) and the lack of connective tissue and skeletal abnormalities. Similar to the heterozygous STAT3 mutations in HIES, the homozygous mutations in DOCK8 show substantially reduced numbers of Th-17 cells and present clinically with CMC infections [52]. It has been reported that this mutation impairs normal immunoglobulin class-switching responses, partly through STAT3-dependent signaling cascades [53], however, the function of DOCK8 is still unclear.

Tyk2 mutations: One patient who has tyrosine kinase (Tyk)2 deficiency [54] has been reported with characteristic of HIES and Mendelian susceptibility to mycobacterial disease (MSMD), which is also associated with defects in Th-17 cells and susceptibility to CMC [55]. However, a recent study reported a second patient with Tyk2 deficiency without HIES characteristics [56].

1.3.2 CMC – CARD9 and Dectin-1 mutations

The Dectin-1/Syk complex engages CARD9, promoting pro-inflammatory cytokine production and subsequently inducing the differentiation of T cells into IL-17-producing T cells [57]. AR-CARD9 deficiency in humans was recently reported in a large multiplex Iranian kindred with CMC and invasive candidiasis, possibly due to the lack of CARD9 expression on macrophages and DCs [30]. In addition, Dectin-1 deficiency was reported in a family, where four women with either recurrent vulvovaginal candidiasis or onychomycosis [29]. Although with the allele prevalence in the healthy population of 3-8%, Dectin-1 deficiency has been characterized as a polymorphism and a risk factor rather than a PID. Cytokines induced IL-17 production was impaired in both families since the affected genes disrupted the Dectin-1/Syk-CARD9 signaling pathway.

1.3.3 CMC – IL-17F and IL-17RA mutations

Important "proof of concept" confirmation of the crucial role of IL-17 in protection against mucocutaneous candidiasis was provided by the demonstration that mutations of the IL-17 receptor (IL-17RA) and cytokine IL-17F (IL-17F) genes were associated with CMC [58]. In a consanguineous family, a child with CMC was found to display AR complete IL-17RA deficiency. His leukocytes and fibroblasts did not respond to IL-17A or IL-17F homodimers, or to IL-17A/F heterodimers. Four patients from another family were shown to harbour dominate-negative mutations in the IL-17F gene. Mutated IL-17F-containing homodimers and heterodimers were secreted in normal amounts but were not biologically active, as they were unable to bind to the IL-17 receptor. Morbid mutations in IL17RA and IL17F demonstrated that CMC could be directly caused by inborn errors of IL-17 immunity.

1.3.4. CMC – IL-12RB1 mutations

Some patients with deficiency of the IL-12/IL-23 signaling pathway are susceptible to mycobacteria (MSMD). A recent large survey of 141 MSMD patients found that 23% of patients had associated mild CMC, usually manifesting as recurrent oral thrush [59]. These patients have an underlying IL-12β1 deficiency (the most common form of MSMD) affecting the β1 chain for the common IL-12/IL-23 receptor. Mutations in IL-12β1 result in impaired IL-23 signaling and a low proportion of IL-17A-producing T cells in the circulation, which is likely the explanation of their susceptibility to CMC [60].

1.3.5 APECED/APS1 – AIRE mutations

APECED/APS1 is a rare autosomal recessive syndrome characterized by multiple autoimmune polyendocrinopathies, such as hypoparathyroidism and adrenal failure. Intriguingly, up to 90% of APECED patients develop early-onset CMC. The genetic etiology of APECED was identified with mutations in the autoimmune regulator (AIRE)-encoding gene [61]. AIRE governs a T-cell tolerance pathway, by inducing the production, in the thymus and peripheral lymphoid organs, of transcripts encoding

proteins normally present in various peripheral tissues, this triggers the deletion of autoreactive T cells. Human AIRE deficiency therefore results in organ-specific autoimmunity disease. The etiology of the chronic candidiasis seen in these patients was baffling, until Puel *et al*. and Kisand *et al*. demonstrated high titers of neutralizing anticytokine autoantibodies, against IL-17A, IL-17F and IL-22. This provided an explanation for their susceptibility to CMC and a link to the underlying autoimmunity [62, 63].

1.3.6 CMC – MST1/STK4 mutations

Another PID associated with CMC is deficiency of the MST1/serine threonine kinase 4 (MST1/STK4) gene controlling human cell growth and apoptosis. The affected individuals also suffered from recurrent bacterial and viral infections, cutaneous warts and skin abscesses [64, 65]. The underlying mechanism of MST1/STK4 mutations leading to CMC is unclear.

1.3.7 CMC – ACT1 mutations

Mutations in the adaptor molecule ACT1 have been very recently reported in two siblings with CMC [66]. This mutation impairs the homotypic interaction of ACT1 with IL-17 receptors abolishing the response to IL-17A and IL-17F in fibroblasts and to IL-17E in leukocytes. The selectively abolished IL-17 responses are likely responsible for the susceptibility to CMC.

1.3.8 CMC – Gain-of-function-STAT1 mutations

In 14 patients from five families with AD-CMC, Van de Veerdonk FL *et al.* firstly revealed heterozygous mutations in the coiled-coil domain (CCD) of STAT1 [67]. Liu *et al.* [68] and Smeekens *et al.* [69] subsequently elucidated the molecular mechanisms manifesting as gain-of-function (GOF), as opposed to the previously reported loss-of-function (LOF) mutations underlying susceptibility to mycobacterial and/or viral diseases [70]. Takezaki *et al.* recently identified the first GOF mutation in DNA-binding domain (DBD) of STAT1 in patients presenting with CMC [71]. Up to date, numbers of GOF-STAT1 mutations have been found in over half of CMC patients [67-69, 71-74].

IL-17-producing T cell development is impaired in these patients [68, 71, 75], probably due to enhanced STAT1-dependent cellular responses to Th-17 cells repressors, such as IFN-γ, IFN-α/β and IL-27 [68]. However, the underlying mechanisms of GOF-STAT1 mutations associated with impaired IL-17 production in the largest group of CMC have not yet been fully understood.

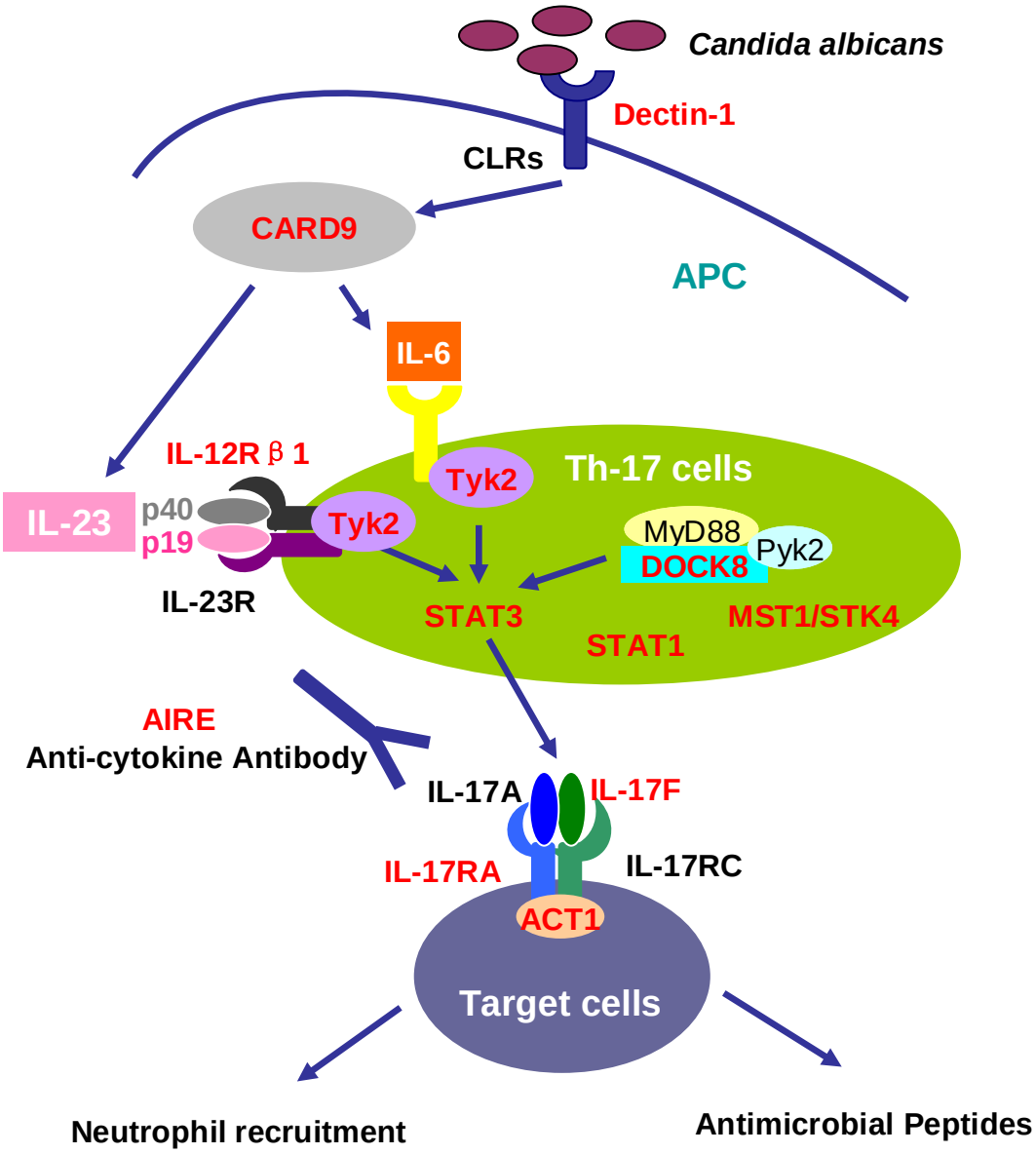

Figure 1.2 Genetic defects associated with Chronic Mucocutaneous Candidiasis. Known deficiencies associated with CMC are shown in red, including Dectin-1, CARD9 (caspase recruitment domain-containing protein 9), IL-12Rβ1 (IL-12 receptor β1), Tyk2 (tyrosine kinase 2), DOCK8 (dedicator of cytokinesis 8), STAT3 (signal transducer and activator of transcription 3), IL-17F, IL-17RA (IL-17 receptor A), AIRE (autoimmune regulator gene), ACT1, MST1 (also known as the serine threonine kinase 4 (STK4)) and gain-of-function (GOF)-STAT1.

1.4 Signal transducer and activator of transcription signaling

The heterozygous negative mutations of STAT3 and the GOF-STAT1 mutations mentioned above responsible for CMC are both affecting the latent cytoplasmic transcription factors – STAT proteins. Therefore, understanding the STAT signalling activation and function may provide better insight of the disease-causing mechanisms of CMC.

Seven members of the STAT family have been identified including STAT1, STAT2, STAT3, STAT4, STAT5a, STAT5b, and STAT6. Transduction signals for STAT proteins (Fig 1.3a) originate from cytokines or growth factors binding to their cognate receptors on the cell surface, which initiate a series of tyrosine phosphorylation events carried out by members of the Janus kinases (JAKs). Following tyrosine phosphorylation, different STAT proteins homodimerize or heterodimerize, this alters the conformation of the STAT molecules and provides them with new properties. The activated STAT dimers gain the ability to bind import carriers that mediate their transport into the nucleus, where they bind to specific DNA sequences in gene promoters and lead to the induction of cytokine-responsive genes [76, 77]. After termination of the signal, STATs are dephosphorylated by phosphatases and translocated back to the cytoplasm from the nucleus. Typically, cytokine-induced transcription is a transient process, lasting only minutes to hours. STATs have been shown to play a role in cell growth and differentiation, proliferation, cell survival and apoptosis [78], however, genetic deficiency studies in humans have highlighted STATs specific functions in the control of various immune responses [79].

1.4.1 STAT structure, function and regulation

STAT structure: All STAT proteins share a similar structural arrangement of functional motifs (Fig 1.3b), including the amino-terminal domain (NTD), the coiled-coil domain (CCD), the central DNA binding domain (DBD), the linker domain (LD) and the Src homology 2 (SH2) domain [78]. In contrast, the carboxy-terminal including the tail segment (TS) and transactivation domain (TAD) is quite divergent and associated with STAT specificity.

Structure associated function: The function of various domains of STATs has been extensively studied. NTD is involved in dimerization and tetramerization [80]. The CCD has considerable potential for involvement in protein-protein interactions and plays a key role in the dimerization of unphosphorylated STAT proteins and binding of nuclear phosphatases leading to STAT dephosphorylation [73, 81]. DBD defines the DNA-binding specificity and mediation of distinct signals for specific ligands. SH2 has been reported to mediate specific interaction between STAT-receptor, STAT-JAK and STAT-STAT [82]. Tyrosine residue in TS and serine residues in TAD are the two phosphorylation sites of STAT proteins.

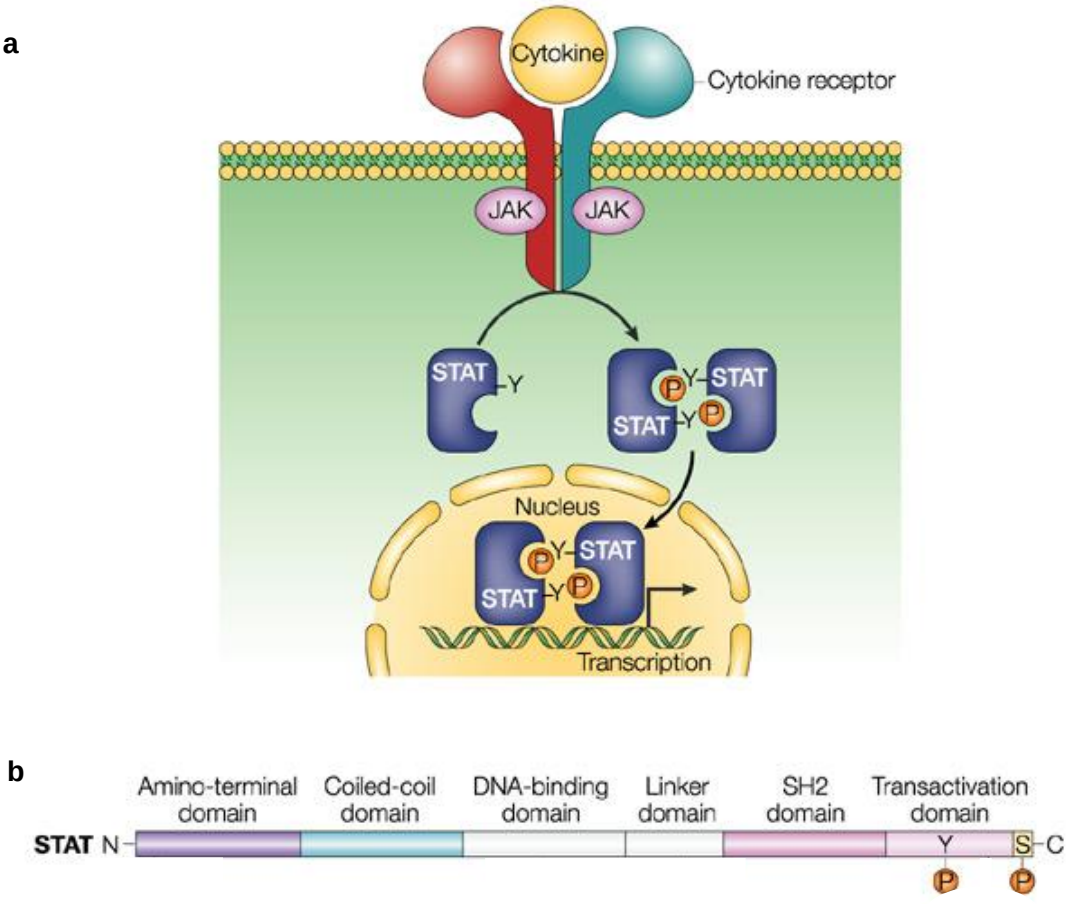

Figure 1.3 STAT signaling and structure [83]**.**
a. In response to cytokine stimulation, STAT proteins become rapidly tyrosine phosphorylated, which allows them to dimerize, translocate to nucleus, where phosphorylated-STATs bind to DNA at their specific promoter sites thus regulating gene expression.
b. Structure of STAT proteins, including amino-terminal domain (NTD), coiled-coil domain (CCD), DNA binding domain (DBD), Linker domain (LD), Src homology 2 (SH2) and transactivation domains (TAD).

Regulation of STAT: The duration and magnitude of STAT activation is critically regulated by a number of different mechanisms at the cytoplasmic and nuclear levels, which together ensure that STAT proteins function in a strictly controlled manner in normal cells. These include the cytoplasmic and/or nuclear protein tyrosine phosphatases (PTP), protein inhibitors of activated STAT proteins (PIAS) and suppressor of cytokine-signaling proteins (SOCS) [80]. In the past several years, significant progress has been made in understanding of STAT acetylation and its role in modulating STAT activities, which relies heavily on the balance between histone deacetylases (HDACs) and histone acetyltransferases (HATs) [84].

1.4.2 STAT1 signaling and IFNs production

STAT1 is the founder member of seven mammalian STATs which plays an essential role in IFN-mediated biological responses [78]. IFNs are cytokines that are crucial in host defense against mycobacterial and viral pathogens [79]. Mammalian type I IFNs (IFN-α/β) are produced by many cell types and confer antiviral activities on them, while type II IFN (IFN-γ) is produced mainly by T lymphocytes and natural killer cells and elicits broad effects, particularly on cells of the immune system. The transmission of both type I IFNs and IFN-γ signals are dependent on the activation of STAT1. It has been well recognized that IFN-α/β signals through STAT1/STAT2 heterodimers, while IFN-γ signals through STAT1 homodimers [85]. In the nucleus, the STAT1 homodimers dissociate from the import carrier and bind to specific DNA target sites such as IFN-γ-activation site (GAS) which is present in the promoters of certain IFN-stimulated genes (ISGs). STAT1/2 heterodimers, however, combine with IFN response factor (IRF)9 to form IFN stimulated gene factor (ISGF)3 which binds to the IFN-stimulated response element (ISRE) and induces responsive gene transcription including IRF1 and CXC-motif chemokine ligand (CXCL)10 genes. Although mechanism of activation and transcriptional regulation of STAT1 have been established, post-transcriptional regulation of STAT1 expression in not fully understood.

1.4.3 STAT3 signaling and IL-17 production

Cytokines that promote IL-17 production include IL-1, TGF-β, IL-6, IL-21 and IL-23

[86]. The last three cytokines transduce their signals through activation of STAT3. Although STAT3 is activated by a large number of cytokines and has crucial functions in various tissues, T cell-specific deletion of STAT3 mainly affects the expression of IL-17 and IL-22 [87]. Conversely, increased STAT3 activation, through the deletion of its negative regulator SOCS3, results in increased numbers of Th-17 cells [88]. The requirement for STAT3 in human IL-17 production was unraveled in patients with HIES (as described above). The impairment of STAT3 signaling and consequently attenuated Th-17 generation may explain these patients' inability to clear bacterial and fungal infections. Chromatin immunoprecipitation-sequencing (ChIP-Seq) and transcriptional profiling have identified multiple genes that are direct targets of STAT3 in T cells including IL-17 and IL-22 genes [86], These two genes are crucial for Th-17 cell-mediated homeostasis and epithelial barrier function [89]. Furthermore, STAT3 directly binds to and regulates expression of several major transcription factors that drive Th-17 cell differentiation, including the gene encoding RORγt (RORc in humans) [86]. In addition, STAT3 regulates the effect of IL-23 as well as IL-6 mediated downstream signaling of these cytokine receptor complex [90].

1.5 Hypothesis and Aim

1.5.1 Hypothesis

As described above, mutations in PID patients with CMC mapped out the fungal immunity pathway, confirming the importance of the STAT3/Th-17 cytokine axis in host defense against *Candida* infections (Fig 1.2). However, the GOF-STAT1 mutations are not themselves on the fungal immune pathway according to current understanding. STAT1 and STAT3 are thought to play opposite roles in most cell types, although the underlying mechanisms are still a matter of speculation and presumably includes altered nuclear transport, competition for common receptor docking sites and/or formation of STAT1/STAT3 heterodimers [91]. As Th-17 cytokine production is highly dependent on STAT3 signaling, it is likely that GOF-STAT1 mutations interfere with this pathway thus reducing downstream IL-17 production which impairs fungal immunity leading to CMC.

1.5.2 Aims

The present study was carried out to investigate how GOF-STAT1 mutations affect the STAT3 signaling pathway by assessing STAT3 activation/phosphorylation, nuclear translocation, DNA-binding, gene expression, cytokine production and whether IL-17 signaling defects in CMC can be epigenetically modified.

Therefore the scope of this thesis:

- How do GOF-STAT1 mutations affect STAT1 activation and gene transcription? (see Chapter 3)

- How do GOF-STAT1 mutations interfere with STAT3 activation and gene transcription? (see Chapter 4)

- Does inhibition of STAT1 modify gene transcription and improve low Th-17-mediated cytokine production in cells bearing GOF-STAT1 mutations? (see Chapter 5)

- Can modification of acetylation modulate gene transcription and rescue low Th-17-related cytokine production in cells with GOF-STAT1 mutations? (see Chapter 6)

CHAPTER 2 SUBJECTS, MATERIALS AND METHODS

2.1 Subjects

2.1.1 Ethical considerations and informed consent

All of the work described in this thesis which involved samples obtained from CMC patients harbouring GOF-STAT1 mutations and healthy volunteers had been approved by Newcastle and North Tyneside Local Research Ethics Committee (Reference No: NAIRB-DL-01 and Great North Biobank – R&D Reference No: 5458/10/H0906/22). Patient-identifiable data were coded and kept securely in a locked office and locked filing cabinet. Signed informed consent from patients and volunteers was obtained following distribution of information sheets prior to clinic visit and verbal explanations prior to signing.

2.1.2 CMC patients with GOF-STAT1 mutations

AD-CMC patients involved in this study all had confirmed GOF-STAT1 mutations affecting the CCD (Appendix Table 8.1). Mutations were identified by using an array-based sequence-capture assay, followed by next-generation sequencing carried out in Radboud University, Nijmegen or in the Human Genetics Laboratory of the Centre for Life, Newcastle University.

2.1.3 Healthy volunteers

Healthy volunteers, all of whom gave informed consent, were recruited from the Musculoskeletal Research Group, Newcastle University. Additionally, healthy blood donor buffy-coat cones were collected from the National Blood Service, following separation of red blood cells for transfusion purposes.

2.2 Materials

Chemicals and biochemicals used for this study are commercially available grade reagents and listed in Appendix Tables 8.2 and 8.3. In addition, details of the antibodies, cytokines, oligonucleotides, primers and small interfering RNAs (siRNA) used for the

research are listed in Tables 8.4 - 8.8 as shown in Appendix.

2.3 Methods

2.3.1 Cell culture and treatment

For the purposes of this research, human peripheral blood mononuclear cells (PBMCs) and immortalized (Epstein-Barr virus – EBV transformed) B cell lines (because of limited availability of patient blood samples) from CMC patients with GOF-STAT1 mutations and healthy volunteers were used. Cells were stimulated *ex-vivo* by incubation with multiple cytokines or treated in addition of chemical drugs.

***PBMC or CD4$^+$ T cell isolation and cytokine stimulation*:** PBMCs or CD4$^+$ T cells were isolated from either fresh peripheral blood samples or buffy-coat cones by use of Lymphoprep density gradient centrifugation. Whole blood was diluted 1:2 with HBSS (Lonza), buffy-coat cone was diluted within 50 ml HBSS, then layered onto Lymphoprep (Axis-Shield Diag) with 3:1 dilution and centrifuged at 800 x g for 20 minutes at room temperature. RosetteSep human CD4$^+$ T cell enrichment cocktail (StemCell Tech) was mixed with diluted cone buffy-coat (75 µl per ml) before being layered for density centrifugation. PBMCs or CD4$^+$ T cells were collected from the interface. Cells were washed twice with HBSS containing 2% FCS (Lonza) 600 x g for 7 minutes at 4^{o}C then 250 x g for 7 minutes at 4^{o}C to remove platelets. Cells were counted using a Burker-Turk haemocytometer and cultured in RPMI-1640 medium (Sigma) containing 2 mM L-glutamine (Sigma), 100 IU/ml penicillin and 100 µg/ml streptomycin (Sigma), at 37^{o}C in a humidified 5% CO_2 incubator.

Cytokine stimulation was performed in 24-well plates with serum-free RPMI-1640 medium. Cells ($3x10^6$/ml, 1 ml per well) were stimulated with multiple cytokines (Appendix Table 8.5). Cytokine stimulation time and doses were described in Table 2.1. For IL-23 and IL-12 stimulation, cells were initially cultured with PHA (Sigma) and IL-2 (Novartis) in IMDM (Sigma) containing 10% serum replacement (Gibco) for 3 days followed by incubation with IL-23 or IL-12 as indicated time periods. Stimulation was stopped by adding ice-cold 1x PBS.

Table 2.1 Cytokines stimulation time and doses.

Cytokine	Final Concentration	Stimulation Time (for WB)	Stimulation Time (for PCR)
IFN-γ	$1x10^3$ IU/m	30 minutes	
IFN-α	$1x10^3$ IU/m	30 minutes	4 hours
IL-27	50 ng/ml	30 minutes	4 hours
IL-21	50 ng/ml	15 minutes	4 hours
IL-6	50 ng/ml	15 minutes	
IL-23	100 ng/ml	30 minutes	4 hours
IL-12	20 ng/ml	20 minutes	4 hours
PHA	2 μg/ml	3 days	3 days
IL-2	40 IU/ml	3 days	3 days

***EBV immortalization and cytokine stimulation*:** PBMCs (5-$10x10^6$ cells pellet) was infected with 1 ml EBV supernatant (previously produced by culturing an EBV infected marmoset B95-8 cell line (kind gift of Professor John Kirby, Newcastle University, and stored at -80°C) in a 7 ml falcon round bottom tube with cap and incubated in beaker with warm water for 1 hour at 37°C, 5% CO_2. After this, cyclosporine-A (CysA) (Sandoz) was added at a final concentration of 1 μg/ml to prevent generation of EBV-specific T suppressor cells (10 μl of an oil-based CysA was very slowly aspirated and transferred into 490 μl absolute alcohol in a bijou, then added to 4.5 ml of RPMI-1640 without FBS; 10 μl of this solution was then added to the 1 ml EBV supernatant and cell pellet). PBMCs with EBV supernatant were incubated for a further 24 hours at 37°C, 5% CO_2 and transferred into a well in a 24-well plate containing 1 ml RPMI-1640 with 10% FCS and 10 μl CysA (final concentration 1 μg/ml) prepared previously. EBV transformation was monitored daily over a couple of weeks.

Before stimulation, EBV transformed cells were starved in serum-free RPMI-1640 medium for 4 hours. Cells ($5x10^6$/ml, 1 ml per well) were then stimulated in 24-well plates as described in Table 2.1. The stimulation was stopped by adding ice-cold 1xPBS.

***Chemical treatment*:** Trichostatin A (TSA; Sigma), an HDAC inhibitor, was used at 100

ng/ml and added to cell medium together with cytokines, whereas Fludarabine (a STAT1 inhibitor, Selleckchem) was added into cell culture 1 hour before stimulation at a final concentration 100 μg/ml. Staurosporine, a phospho-kinase inhibitor, was used to prevent phosphorylation of STAT proteins which was assessed by stimulating EBV transformed cells with $1x10^3$ IU/ml or $0.5x10^3$ IU/ml IFN-α for 30 minutes and adding Staurosporine (Calbiochem) at 1 μM in RPMI-1640 for a further 15, 30, 60 minutes. Pervanadate, a phosphatase inhibitor, was used to inhibit dephosphorylation of STAT proteins, mimicking the gain-of-function mutation. It was prepared by mixing orthovanadate (Sigma) with H_2O_2 for 15 minutes at 22°C. Cells were treated with Pervanadate (0.8 mM orthovanadate and 0.2 mM H_2O_2) 5 minutes before stimulation. Cells were then stimulated with IFN-α for 30 minutes. The stimulation was stopped by adding ice-cold 1x PBS.

***Candida albican stimulation*:** Freeze-dried *Candida albicans* (ATCC, 18804) were rehydrated by adding 6 ml sterile distilled water. The suspension was shook vigorously to dissolve and left at room temperature overnight without disturbing. Rehydrated *C. alibcans* were frozen down as 200 μl aliquots at -20°C. When required, *C. alibcans* were thawed and cultured with Yeast Nitrogen Base (YNB, BD) liquid medium containing 0.5% w/v D-Glucose (Sigma) and 10% FCS in a 37°C, 5% CO_2 incubator overnight, followed by centrifuging at 800 x g for 10 minutes. The *C. alibcans* pellet was then collected and diluted ($1:15x10^3$) for cell stimulation in the presence of Amphotericin B (final concentration 2.5 μg/ml, Sigma) for 5 days. Supernatant was collected and stored at -20°C before being used for cytokine production measurements.

***Cell Viability Assays*:** CellTiter 96® AQueous Non-Radioactive Cell Proliferation Assay (Promega) was used in this study as a colorimetric method for determining cell viability. The method is based on in vivo reduction by metabolically active cells of a tetrazolium compound
(MTS=3-(4,5-dimethylthiazol-2-yl)-5-(3-carboxymethoxyphenyl)-2-(4-sulfophenyl)-2H -tetrazolium) to a coloured formazan, with maximal absorbance at 490 nm, that is released into culture medium. Assays were performed by adding a small amount of the

solution directly to culture wells (1:4), incubating for 3 hours and then recording the absorbance at 490 nm with a 96-well plate reader. The quantity of formazan product, as measured by the absorbance at 490 nm, is directly proportional to the number of living cells in culture.

2.3.2 Western Blotting

Western blotting (WB, also called immunoblotting because an antibody is used to specifically detect its antigen) is a routine technique for protein analysis. It uses gel electrophoresis to separate native proteins by 3-D structure or denatured proteins by the length of the polypeptide. The proteins are then transferred to a polyvinylidene fluoride (PVDF) membrane, where they are recognized with antibodies specific to target protein. WB was performed in this study for the assessment of STAT proteins phosphorylation, subcellular localization and siRNA-mediated gene silencing efficiency.

***Extraction of cellular fraction proteins*:** Cytoplasmic and nuclear proteins were extracted by using NE-PER Nuclear and Cytoplasmic Extraction Kits (Thermo Scientific) according to manufacturer's instructions. Briefly, addition of the first two reagents to a cell pellet causes cell membrane disruption and release of cytoplasmic contents. After recovering the intact nuclei from the cytoplasmic extract by centrifugation, the proteins are extracted out of the nuclei with the third reagent. Cellular fraction proteins were snap-frozen on dry ice and stored at -80^{o}C.

***Extraction of whole cell lysate*:** Following cytokine or chemical treatment, cells were collected and washed once in ice-cold 1x PBS and pelleted at 13,000 x g for 1 minute at 4^{o}C, to remove any residual phenol red from the medium. Following careful removal of PBS to leave a dry cell pellet, 30 µl of whole cell lysis buffer (Appendix Table 8.9) per million cells was added to the cell pellet and incubated on ice for 30 minutes. The cells were then pelleted at 13,000 x g for 8 minutes at 4˚C. Lysates were then carefully removed from the pellet and transferred to pre-cooled eppendorfs and stored at -80˚C.

***Bradford assay for protein quantification*:** To measure the protein concentration in an

extract, the dye-binding assay Bradford (Bradford Assay) was performed. A standard curve was generated by diluting Bovine Serum Albumin (BSA) stock solution (2 mg/ml BSA protein standards (Thermo Scientific)) in the lysis buffer used for extraction. Extracted proteins were diluted in lysis buffer and 300 µl of Bradford Ultra (Expedeon) was added to each sample. Following 5 minutes incubation, protein absorbance was read at 595 nm using a Tecan sunrise microplate absorbance reader. A standard curve was plotted and used to determine the protein concentration of test samples.

***Immunoblotting*:** For immunoblotting, equal amounts of protein (1:5 dilution with 5x Sample buffer) were subjected to Sodium Dodecyl Sulfate – Polyacrylamide Gel Electrophoresis (SDS-PAGE) using 10% polyacrylamide gels (consist of a lower 10% acrylamide separating gel and a upper stacking gel) at a constant voltage of 100 V in the running buffer. After SDS-PAGE, proteins were transferred to a polyvinylidene fluoride (PVDF) membrane by using the iBlot^{TM} Gel Transfer Device (Invitrogen) with iBlot® Transfer Stack, PVDF Regular package (Invitrogen). The membrane was then blocked with 5% (w/v) milk powder in Tris-Buffered Saline-Tween (TBS/T) buffer for 1 hour at room temperature followed by incubation overnight at 4^{o}C with antibodies (Appendix Table 8.4). The blots were then washed three times with TBS/T and incubated with HRP-conjugated goat anti-rabbit (Dako) at a dilution of 1:2,000 in 5% (w/v) milk powder in TBS/T for 1 hour at room temperature. After washing the blots three times with TBS/T, the blots where developed with ECL according to the manufacturer's instructions (GE Healthcare). All the buffers used for WB were described in Appendix Table 8.9.

2.3.3 Electrophoretic mobility shift assay

STAT protein DNA-binding was evaluated using electrophoretic mobility shift assay (EMSA). EMSA is based on the observation that complexes of protein and DNA migrate through a nondenaturing polyacrylamide gel more slowly than free double-stranded oligonucleotides. This gel shift assay is performed by incubating proteins with end-labeled double-stranded DNA oligonucleotides containing the putative binding site and nonspecific DNA competitor, usually a polyanion polymer

such as poly (dI-dC). The specificity of an observed DNA-binding reaction can be evaluated using competition assays in which an excess of unlabeled probe is added together with the labeled probe. In addition to a labeled probe, specific antibodies can be added to the gel shift reaction. If the protein that forms the complex is recognized by the antibody, the antibody can either block complex formation, or it can form an antibody-protein-DNA complex, resulting in a further reduction in the mobility of the protein-DNA complex (supershift).

***Nuclear protein extraction*:** A two-step process was used to obtain crude nuclear extract with homemade buffers (described in Appendix Table 8.10). Low salt detergent hypotonic buffer was used to perforate the plasma membrane and release cytoplasmic contents, leaving nuclear membranes intact. High salt solution was then used to leach out the nuclear proteins. Cells were treated as described then collected and washed once in ice-cold 1x PBS and pelleted at 13,000 x g for 1 minute at 4^{o}C. Cell pellet (20x10^{6} cells) was resuspended in 1 ml of hypotonic buffer and incubated on ice for 15 minutes. Cells were pelleted as before and the supernatant containing cytosolic protein was discarded. The pellet was resuspended in ice-cold hypotonic buffer supplemented with 0.25 M sucrose (in order to fractionate the nuclei). Cells were centrifuged and the pellet was resuspended in 80 µl high salt buffer. Following a 30 minutes incubation on ice, cells were centrifuged for the final time at 10,000 x g for 2 minutes at 4^{o}C and the supernatant containing nuclear protein was snap-frozen on dry ice and stored at -80^{o}C.

***Protein-DNA binding reaction and electrophoresis*:** Labelled or unlabelled DNA oligonucleotides (Appendix Table 8.6) were resuspended in dH_2O (Sigma) to a concentration of 100 pmol/µl. Oligonucleotides were heated to 95^{o}C for 5 minutes in annealing buffer at the final concentration of 10 pmol/µl and then allowed to cool to room temperature for 4 hours to enable annealing of probes. The native acrylamide gel was prepared the day before the EMSA reaction and left to set at 4^{o}C overnight. The gel was pre-run for 30 minutes in running buffer prior to the loading of samples in order to remove any traces of Ammonium Persulphate (APS; Sigma), to equilibrate ions within the running buffer and to ensure constant gel temperature. The binding conditions were

prepared for STAT proteins and incubated at room temperature for 20 minutes in the dark. When using unlabelled competitor oligonucleotides or antibodies (Appendix Table 8.4) to confirm the binding of candidates, these were added 15 minutes prior to the addition of fluorescently labelled oligonucleotide. Orange G loading dye (from EMSA kit, LiCor Bioscience) was then added (1x final concentration) and samples were loaded onto the gel. Electrophoresis was performed at 100 V at 4^{o}C in the dark for approximately 4 hours, or until the dye front has reached the end of the gel. Visualisation was carried out using the LiCor Odyssey Infrared Imager (LiCor Bioscience). All the buffers and binding conditions used for EMSA were described in Appendix Table 8.10.

2.3.4 Flow cytometry - phosflow cell signaling

Flow cytometry measures the optical properties of single cells as they pass through the functional core of the instrument. When cells are stained with fluorescence markers, it can be used to measure the expression level of multiple surface and intracellular proteins of individual cells in a population. BD Phosflow technology was performed in this study to reveal intracellular staining of STAT1 phosphorylation events.

Following cytokine stimulation, EBV cells were fixed immediately by adding 10x volumes of pre-warmed 1x Lyse/Fix Buffer (BD). Following incubation at 37^{o}C for 10 minutes, cells were pelleted by centrifugation at 600 x g for 8 minutes at room temperature. Pellet was resuspended by vortexing, followed by permeabilization with 1 ml (per 1-10x10^{6} cells) of Phosflow Perm buffer III (BD) and incubated at -80^{o}C in the dark overnight. Cells were then washed twice in staining buffer (PBS containing 2% FCS) at 600 x g for 8 minutes at 4^{o}C. Pellet was resuspended in 100 µl staining buffer and 10 µl of Alexa Fluor® 647 STAT1 (pY701) antibody (BD) for 1 hour incubation at room temperature in the dark. Prior to flow cytometric analysis, cells were washed once in staining buffer and then resuspended in 300 µl staining buffer.

2.3.5 Quantitative real time-polymerase chain reaction

Gene expression analysis was determined using a *Taqman* primer-probe based approach of quantitative real time-polymerase chain reaction (qRT-PCR). The probe is

constructed containing a reporter fluorescent dye on the 5' end and a quencher dye on the 3' end. During DNA amplification, the reporter dye is released from the quencher and emits fluorescence to enable the detection of specific PCR product when the polymerase enzyme cleaves the probe from DNA.

***RNA isolation*:** Total RNA was extracted from cells using TRI Reagent (Sigma). Cells ($2\text{-}5x10^6$) following cytokines treatment were collected and pelleted. Each sample was homogenised in 1 ml TRI Reagent. The homogenate was then incubated at room temperature for 5 minutes to ensure complete dissociation of nucleoprotein complexes. Chloroform (0.2 ml) was added and the components mixed. After 3 minutes incubation at room temperature, samples were centrifuged at 13,000 x g for 15 minutes at 4^oC. The aqueous phase containing the RNA was collected. RNA was then precipitated with 0.5 ml of isopropanol by incubating the mixture for 10 minutes at room temperature. RNA was pelleted by centrifugation at 13,000 x g for 10 minutes at 4^oC, and washed with 75% ethanol (7500 x g for 5 minutes at 4^oC). Finally, the RNA was resuspended in 20 µl RNase- and DNase-free H_2O (Sigma) and stored at -80^oC.

***Complementary DNA reverse transcription*:** For reverse transcription, 0.5 µg RNA sample was mixed with 2 µg Random hexamer pd $(N)_6$ (GE Healthcare) and H_2O (Sigma) up to 9 µl. Samples were incubated at 70^oC for 10 minutes. Following this, pre-prepared buffer containing 0.5 µl of 10 mM dNTPs (Bioline), 4 µl of 5x first stand buffer, 2 µl of 0.1 M Dithiothreitol (DTT), 0.5 µl (100 units) of Superscript II (Invitrogen) and 0.5 µl of H_2O was added to each tube and incubated at 42^oC for 1 hour. The stable complementary DNA (cDNA) was then stored at -20^oC for further use.

***Gene expression analysis by qRT-PCR*:** Gene expression analysis was performed with *TaqMan* Gene Expression Assays (Applied Biosystems, ABI) which consists of a pair of unlabeled PCR primers and a *TaqMan* probe with a FAM dye label on the 5' end and a nonfluorescent quencher on the 3' end (listed in Appendix Table 8.7). PCR reactions (10 µl) were prepared containing 1x gene expression assay (primer and probe mix), 1x *TaqMan* Gene Expression Master mixture (Life Technologies) and cDNA (diluted 1:5

for RORc, IL-22, IL-17, diluted 1:10000 for 18S, and diluted 1:10 for all other genes). The Prism 7900HT sequence detection system (ABI) was used for PCR cycling (50^{o}C for 2 minutes, 95^{o}C for 10 minutes and 40 cycles of 95^{o}C for 15 seconds and 60^{o}C for 1 minute) and detection. For analysis, gene expression was normalised to the house keeping gene 18S rRNA. Data were expressed in the $2^{-\Delta Ct}$ format, where ΔCt = Ct (target) – Ct (18s).

2.3.6 siRNA-mediated gene silencing

Short/small interfering RNA (siRNA) is a widely used approach to effectively knock down gene expression and to study protein function in a wide range of cell types. In order to assess the roles of certain transcription factors in the regulation of STAT-induced gene expression, gene expression was silenced using siRNA Accell SMARTpool (Thermo Scientific) targeting of HDAC1, HDAC2 or HDAC3, or a non-targeting sequence as a negative control in PBMCs or EBV cells. Gene silencing was performed in 24-well plates, cells ($3x10^6$/ml for PBMCs, $5x10^6$/ml for EBV cells) were incubated with 1 μM final concentration of Accell siRNA (Appendix Table 8.8) in Accell delivery medium (Thermo Scientific) for 72 hours at 37^{o}C in 5% CO_2 incubator without serum replacement for the first 48 hours, after which 2.5% serum replacement was added into PBMC cultures but not EBV cells. For IL-23 stimulation, PHA and IL-2 were added into the cell culture at the same time as cell transfection was performed. Cytokine stimulation was carried out after 72 hours transfection. To evaluate gene knockdown efficiency, longer incubation (96 hours transfection) was required for HDAC1, HDAC2 and HDAC3 protein expression assessment.

2.3.7 Chromatin immunoprecipitation assay

Chromatin immunoprecipitation (ChIP) assay was performed in this study to evaluate STAT3 DNA binding *in vivo* in cells from CMC patients with GOF-STAT1 mutations. ChIP assay is a powerful technique which can identify links between the genome and the proteome by monitoring transcription regulation through histone modification or transcription factor−DNA binding interactions. The strength of ChIP assays is their ability to capture a snapshot of specific protein-DNA interactions occurring *in vivo*.

Additionally, ChIP allows for measurement of relative changes in protein-DNA interaction levels using quantitative polymerase chain reaction (qPCR).

***Cross-linking*:** EBV cells were stimulated with IFN-α as described before. Formaldehyde (Sigma) was added to crosslink cells (～$50x10^6$ cells) at a final concentration of 1% and incubated at room temperature for 10 minutes. Glycine (Sigma) was added at a final concentration of 0.125 M to quench un-reacted formaldehyde. Cells were pelleted in a 15 ml falcon at 1300 x g at 4^oC for 5 minutes.

***Lysis and sonication*:** After discarding the supernatant, the cell pellet was resuspended in 800 µl SDS cell lysis buffer (prepared as described in Appendix Table 8.11) containing 1x protease inhibitor cocktail II (Millipore) and incubated on ice for 30 minutes. Sonication was carried out using a probe sonicator (Soniprep 150, MSE, UK), on ice, at 10 minutes for 10x 15 second intervals with 15 second rest periods. Sonicated lysates were then centrifuged at 1300 x g at 4^oC for 5 minutes.

***Immunoprecipitation*:** Chromatin (100 µg) was diluted (1:10) with ChIP dilution buffer containing 1x protease inhibitor cocktail II and 30 µg of blocked *Staphylococcus aureus* (Staph A) membranes (Zysorbin from Invitrogen) and incubated with rotation at 4^oC for 30 minutes. The blocked Staph A membranes facilitate the antibody being coupled to a solid substrate. Following this incubation, samples were centrifuged at 2500 x g at 4^oC for 5 minutes. Supernatant was removed and split into 2 tubes. Antibody (3 µg) either irrelevant or target-specific was used for each immunoprecipitation. Samples were then incubated overnight at 4^oC with rotation. The following day, 50 µl Staph A was added into each sample and incubated for 60 minutes at 4^oC, followed by 30 minutes at room temperature. Supernatant was removed by centrifugation at 6000 x g for 5 minutes, and the pellet then washed in low salt immune complex wash, high salt immune complex wash, lithium chloride complex wash and finally buffer TE, each for 5 minutes with rotation and the supernatant discarded. The pellet was resuspended in 500 µl ChIP elution buffer for further 20 minutes incubation with rotation at room temperature. All the buffers mentioned above were prepared as described in Appendix Table 8.11.

Following the final wash, supernatant was collected and 20 µl 5 M NaCl was added to each 500 µl samples. After an incubation at 65^{o}C for 4 hours, 10 µl of 0.5 M EDTA, 2 µl of 1 M Tris-HCl (pH6.5) and 2 µg of proteinase K (Sigma) was added to each sample and incubated at 45^{o}C for 1 hour. Following reversal of cross-linking, eluate was mixed with an equal amount of phenol and centrifuged at 13000 x g for 5 minutes. DNA purification was carried out using spin columns provided in the Gel Extraction kit (Qiagen) according to the manufacturer's instructions.

***Polymerase chain reaction*:** DNA was amplified by PCR using human c-Fos promoters (F: 5'-CCACGCTTTGCACTGAATTA-3'; R: 5'-GAGAACATTCGCACCTGGTT-3') located in the STAT3 region. Real time-PCR analysis was performed on an ABI 7500HT sequence detection system. In brief, qPCRs comprised of 3 µl of immunoprecipitated DNA template, 0.5 µM forward and reverse primers, 6.5 µl of Jumpstart SYBR green master mixture (Sigma) in a total reaction volume of 13 µl. PCR was performed in triplicate. After the initial 5 seconds incubation at 95^{o}C, qPCRs were carried out by 40 cycles of 95^{o}C for 5 seconds, annealing at 57^{o}C for 30 seconds, and extension at 72^{o}C for 30 seconds and a final step of 95^{o}C for 5 seconds. After each run, a dissociation curve was performed to ensure that no primer-dimers contaminated the quantification and that the product had the expected melting temperature. A signal intensity value for each sample was calculated from the average of the experiments. Average values of eluates were normalized to average values of inputs after subtracting the background control, and differences between samples calculated using the following equation: [1/(2, *A*)]x100.

2.3.8 Enzyme-linked immunosorbent assay

Enzyme-linked immunosorbent assay (ELISA) is a biochemistry assay that uses a solid-phase enzyme immunoassay to detect the presence of a substance, usually an antigen, in a liquid or wet sample. It was employed in this study to evaluate STAT3 DNA-binding and cytokine production in cell culture medium.

***TransAM STAT3 DNA binding*:** STAT3 DNA binding was evaluated by TransAM

STAT3 kit (Active Motif) according to manufacturer's instructions. TransAM STAT3 is an ELISA-based kit, containing immobilized oligonucleotide (hSIE) containing a STAT consensus binding site (5'-TTCCCGGAA-3'). The activated STAT3 contained in nuclear extracts binds to this oligonucleotide. The primary antibody used to detect STAT recognizes an epitope on STAT3 that is accessible only when STAT3 is activated and bound to its target DNA. An HRP-conjugated secondary antibody provides a sensitive colorimetric readout that is easily quantified by spectrophotometry at 450 nm using a Tecan sunrise microplate absorbance reader.

***Cytokine production*:** Production of IL-17 and IL-22 cytokines in cell culture supernatant was measured by ELISA kit (eBioscience) according to manufacturer's instruction using in-house ELISA buffers and microtiter plates.

Production of IL-10 cytokine was detected in cell culture supernatant with buffers described in Appendix Table 8.12. IL-10 capture antibody (2 μg/ml; BD) was coated on to microtiter plates overnight at 4^{o}C. After 1 hour blocking with blocking buffer, 50 μl of appropriately diluted samples in diluent buffer was added and incubated overnight at 4^{o}C. Standards (duplicates) and blanks were run with samples to ensure accuracy. After three washes with washing buffer, 50 μl of detection antibody (1 μg/ml, BD) was added to each well and incubated at room temperature for 1 hour. Following four washes, 50 μl of ExtrAvidin-Peroxidase (Sigma) conjugate (1:1000 dilution) was added to each well and incubated for 30 minutes at room temperature. Substrate (50 μl) was added after five washes and incubated at room temperature until color developed. The reaction was stopped by adding 50 μl 3 M H_2SO_4 and the absorbance read at 490 nm using a Tecan sunrise microplate absorbance reader.

2.3.9 Transfection of cell lines

To evaluate transcriptional activity of STAT3 in CMC patients with gain-of-function STAT1 mutations, STAT3 Luciferase Assay (Cignal Reporter Assay, Qiagen) was performed in EBV transformed cells. Cell transfection efficiency was evaluated by comparing EBV cell line to SW1353 (SW) cell line (human chondrocytes, ATCC, HTB-94) with the positive control (40:1:1 mixture of constitutively expressing GPF,

constitutively expressing firefly luciferase, and constitutively expressing Renilla luciferase) from the Cignal Report Assay kit. SW cells were seeded at a density of $7x10^4$/ml, 100 µl per well in a 96-well plate and serum-starved in DMEM (containing high glucose, 2 mM L-glutamine, 100 IU/ml penicillin, 100 µg/ml streptomycin) for 24 hours prior to transfection. EBV cells were cultured at a density of $5x10^6$/ml, 100 µl per well in a 96-well plate in RPMI-1640 serum-free medium. Optimization of cell transfection was performed with indicated amount of GFP (Cignal Reporter Assay, Qiagen) and Attractene Reagent (Qiagen) mixture for 48 hours transfection according to manufacturer's instructions (Table 2.2). Transfection efficiency was observed by using Zeiss Inverted Microscope (Zeiss, Germany).

Table 2.2 Pipetting scheme for optimizing cell transfection in a 96-well plate.

Amount of DNA (µg)	0.1	0.1	0.1
Volume of Attractene Reagent (µl)	0.25	0.375	0.75
Final volume of diluted DNA (µl)	50	50	50
Amount of DNA (µg)	0.2	0.2	0.2
Volume of Attractene Reagent (µl)	0.5	0.75	1.5
Final volume of diluted DNA (µl)	50	50	50
Amount of DNA (µg)	0.3	0.3	0.3
Volume of Attractene Reagent (µl)	0.75	1.125	2.25
Final volume of diluted DNA (µl)	50	50	50

2.3.10 Statistical analysis

Two statistical analyses were performed in this study.

Mann Whitney (nonparametric) *t* test was used to compare groups between healthy controls and CMC patients in responses to different treatments (cytokines, fludarabine or TSA). Statistical analysis and plotting of data was performed using Prism 5.0 software (GraphPad Software, USA). P values less than or equal to 0.05 were considered significant (*), $P \leq 0.01$ highly significant (**).

Estimation of the effects between different treatments was analyzed employing analysis of variance techniques using Version 21 of the SPSS statistical software system. Type

III sums of squares were used to adjust for imbalances in the number of experiments performed in each of the groups. Maximum likelihood estimates and 95% confidence intervals (CI) were calculated using a pooled estimate of the variability weighted by the number of observations in each group [92]. A generalized linear model allowed comparison of healthy controls and CMC patients, and estimation of the effects of fludarabine and TSA together with their interactions. Pairwise comparisons were performed using the somewhat conservative Bonferroni adjustment for multiplicity. Statistically significant differences between the treatment groups were presented as $P \leq 0.05$ significant (*), $P \leq 0.01$ highly significant (**).

CHAPTER 3 GOF-STAT1 MUTATIONS ENHANCE STAT1 ACTIVATION AND GENE TRANSCRIPTION

3.1 Rationale

Mutations underlying susceptibility to *Candida* infections in a large subgroup of AD-CMC patients has recently been identified in the STAT1 gene affecting CCD and DBD [67]. Mutations in STAT1 gene have previously been described albeit in other domains resulting in primary immune deficiencies of different clinical phenotypes. The heterozygous STAT1 loss-of-function mutant alleles with an AD inheritance confer susceptibility to mycobacterial disease [93]. The homozygous loss-of-function STAT1 mutant alleles with an AR inheritance confer susceptibility to a broad range of bacterial and viral infections [94]. Between them, the recessive hypomorphic STAT1 (homozygous and compound heterozygous) loss-of-function mutant alleles confer susceptibility to milder intramacrophagic bacterial and viral diseases [95].

In contrast, the STAT1 mutant alleles identified in AD-CMC are gain-of-function and lead to increased STAT1-dependent cellular responses [68]. It is not known how the enhanced STAT1 activation in AD-CMC leads to impaired Th-17 immunity and confers susceptibility to fungal infections which is the hallmark of this PID. In the present chapter, I present results confirming the enhanced STAT1 activation as a result of the gain-of-function mutations and investigate downstream effects on STAT1 function, specifically STAT1-dependent gene induction.

3.2 Aims

In the presence of GOF-STAT1 mutations:

- Confirm enhanced STAT1 activation/phosphorylation
- Investigate kinetics and mechanisms of STAT1 phosphorylation and dephosphorylation
- Evaluate the effect on STAT1 DNA-binding activity
- Determine downstream effect on STAT1-dependent gene induction

3.3 Results

3.3.1 GOF-STAT1 mutations result in enhanced STAT1 phosphorylation

To evaluate STAT1 activation, I compared STAT1 phosphorylation in AD-CMC patients to healthy controls. Upon stimulation with IFN-γ, IFN-α or IL-27, GOF-STAT1 mutants showed higher levels of STAT1 phosphorylation both in PBMCs and EBV transformed cells. Total STAT1 was expressed at equal levels, as shown by WB (Fig 3.1).

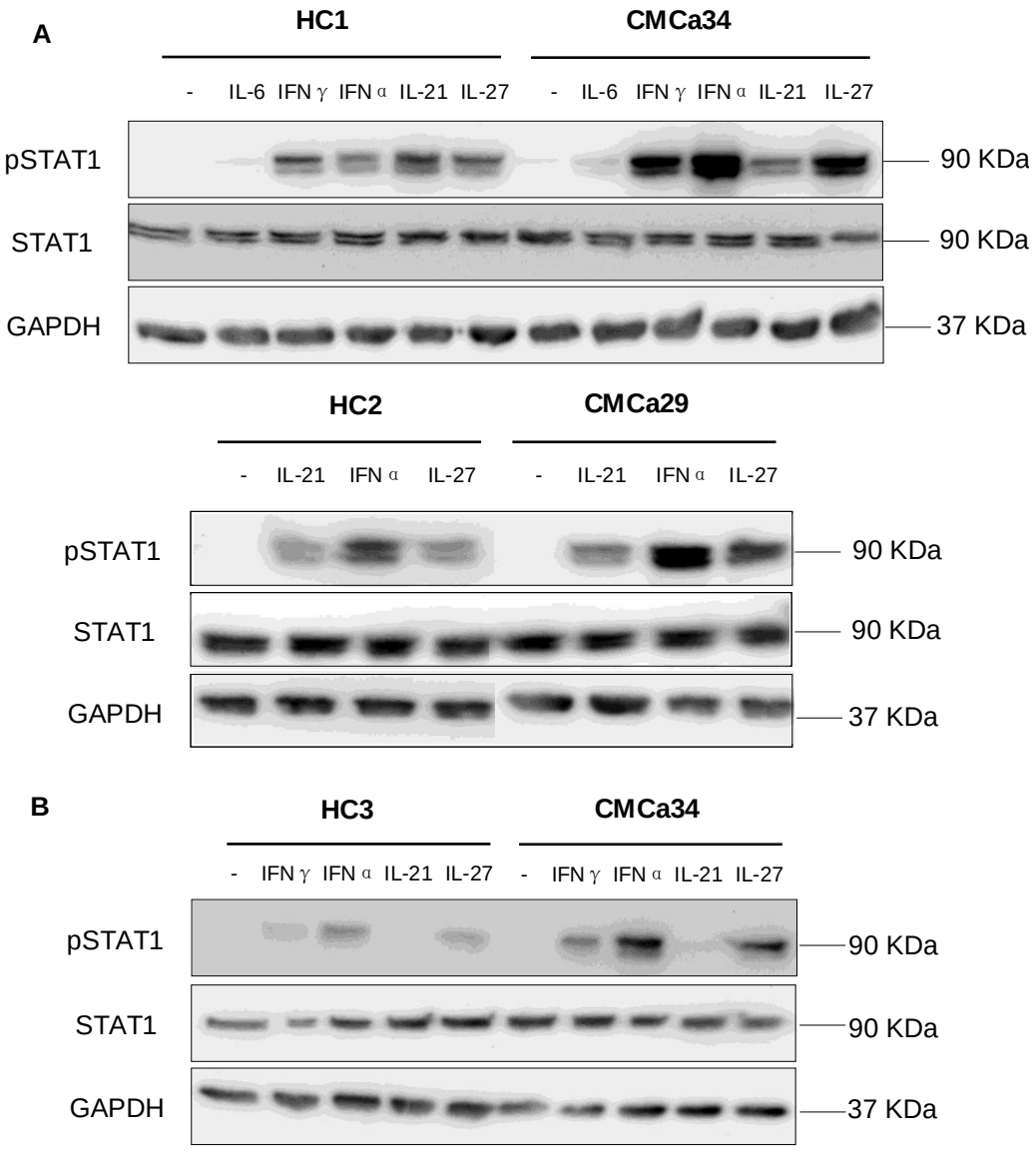

Figure 3.1 Increased STAT1 phosphorylation in cells of AD-CMC patients.
Western blotting was performed on whole cell lysates of EBV transformed cells (A) and PBMCs (B) from 3 healthy controls (HC) and 2 CMC patients (CMC). Prior to lysing, cells were stimulated for 15 minutes with 50 ng/ml IL-6, IL-21, or 30 minutes with $1x10^3$ IU/ml IFN-γ, IFN-α and 50 ng/ml IL-27. GAPDH was used as a loading control. Data shown are representative of at least 3 independent experiments.

3.3.2 Enhanced initial phosphorylation and impaired dephosphorylation of STAT1 accounting for gain-of-function

To understand the underlying mechanism involved in gain of function STAT1 activation, I assessed STAT1 dephosphorylation following IFN-α treatment. These mutations led to a delayed STAT1 dephosphorylation for up to 90 minutes, a time at which STAT1 phosphorylation in healthy subjects had almost returned to baseline levels as shown by WB (Fig 3.2). Flow cytometry confirmed the delayed dephosphorylation of the mutant STAT1 by intracellular staining (Fig 3.3).

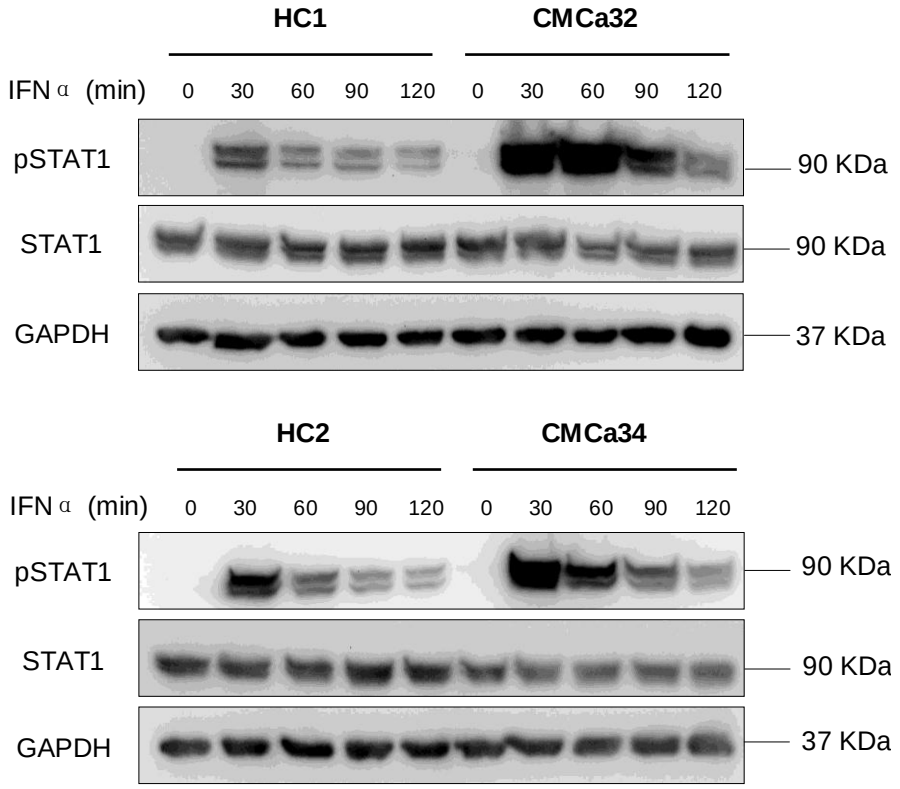

Figure 3.2 STAT1 mutants lead to impaired dephosphorylation.
Dephosphorylation in EBV transformed cells from CMC patients (CMC) and healthy controls (HC) stimulated or not with IFN-α ($1x10^3$ IU/ml) for the indicated time periods. GAPDH was used as a loading control. Data shown are representative of 2 independent experiments.

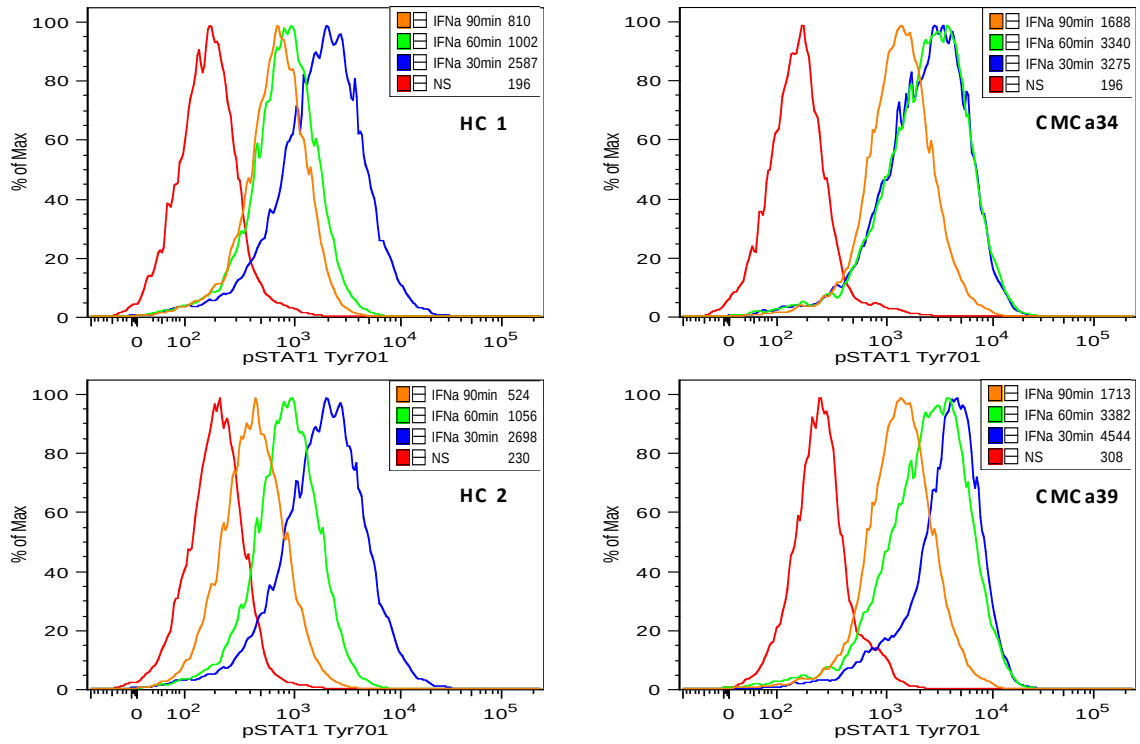

Figure 3.3 STAT1 mutants result in delayed dephosphorylation.
Dephosphorylation measured by means of flow cytometry in EBV transformed cells from CMC patients (CMC) and healthy controls (HC) stimulated with or without IFN-α ($1x10^3$ IU/ml) for the indicated time periods. Results are representative of 2 independent experiments as mean fluorescence intensity (NS, non-stimulated).

Hyper-phosphorylation of STAT1 could be mimicked in control cells by addition of pervanadate, a phosphatase inhibitor that prevents dephosphorylation and nuclear exit. Fig 3.4 demonstrated that addition of pervanadate increased STAT1 phosphorylation in control cells to levels seen in cells with the GOF-STAT1 mutations.

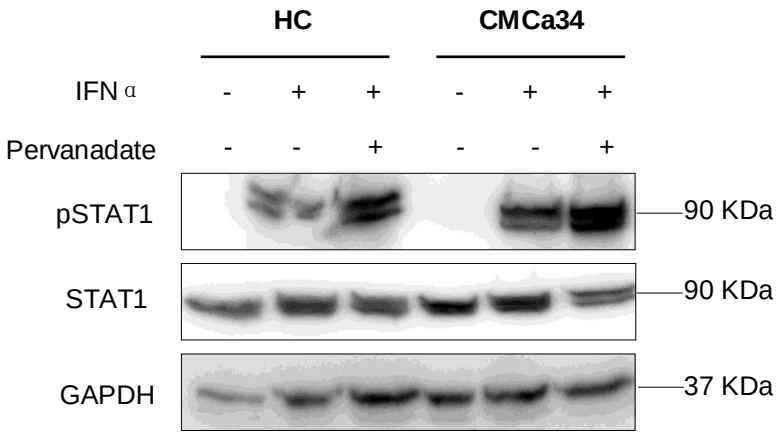

Figure 3.4 Blocking dephosphorylation mimics hyper-phosphorylation.
WB of whole cell lysates extracted from EBV cells derived from a healthy control (HC) and an AD-CMC patient (CMC), in the absence or presence of the phosphatase inhibitor pervanadate for 5 minutes and then treated or not with IFN-α ($1x10^3$ IU/ml) for 30 minutes. GAPDH was used as a loading control. Data shown are representative of 2 independent experiments.

Conversely, addition of staurosporine, a tyrosine kinase inhibitor reduced the initial level of phosphorylation for the GOF-STAT1, allowing the subsequent dephosphorylation to occur with similar kinetics to normal cells (Fig 3.5). A similar effect was achieved with suboptimal stimulation of cells with GOF-STAT1 mutations (Fig 3.6), which also led to lower levels of phosphorylation and normalization of dephosphorylation. These data demonstrated that STAT1 mutations resulted in a gain of STAT1 phosphorylation due to an impaired dephosphorylation as well as enhanced initial phosphorylation.

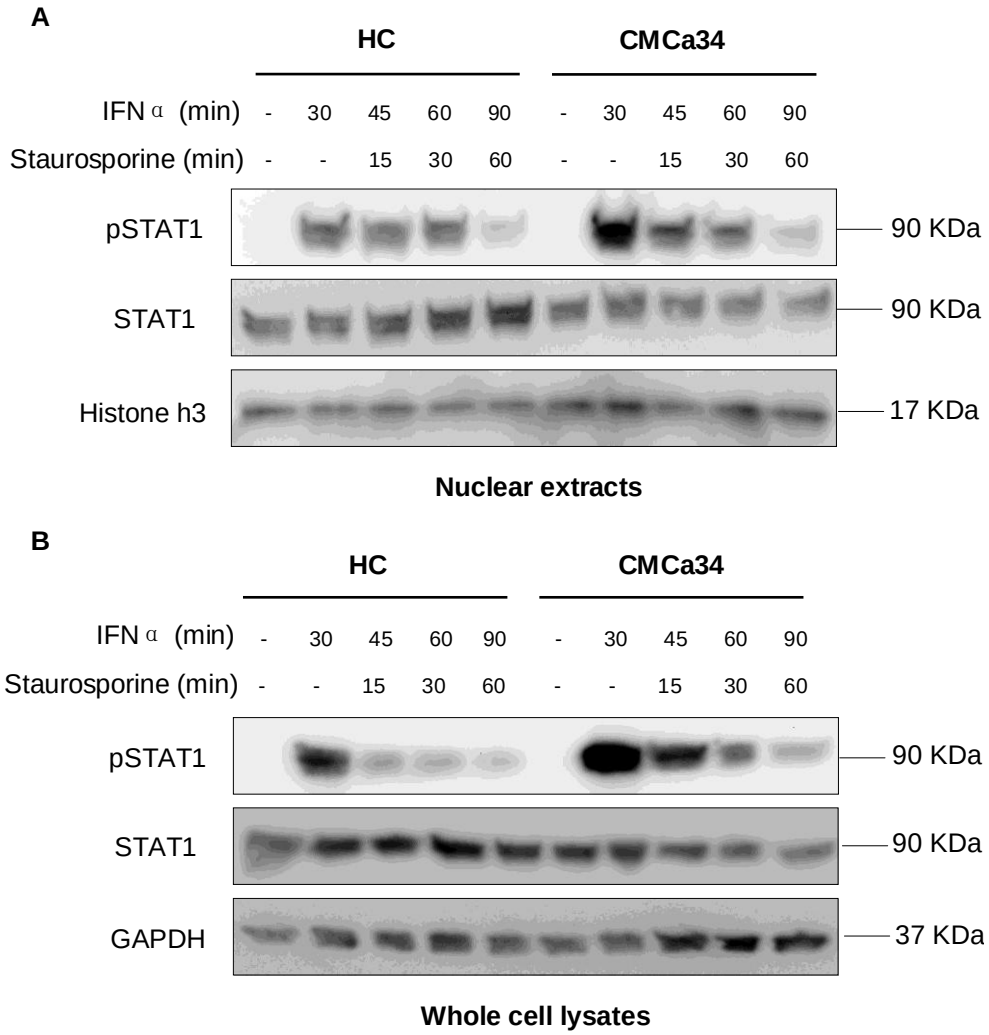

Figure 3.5 Limiting initial phosphorylation normalize dephosphorylation kinetics in cells with GOF-STAT1 mutations.

GOF-STAT1 dephosphorylation of nuclear extracts (A) or whole cell lysates (B) was tested by WB in EBV cells from a healthy control (HC) and an AD-CMC patient (CMC). Cells were left unstimulated or stimulated with IFN-α ($1x10^3$ IU/ml) for 30 minutes, then incubated with or without 1 μM of the tyrosine kinase inhibitor staurosporine for 15, 30, or 60 minutes. Histone H3 and GAPDH antibodies were used as the loading control for nuclear and whole cell extracts respectively.

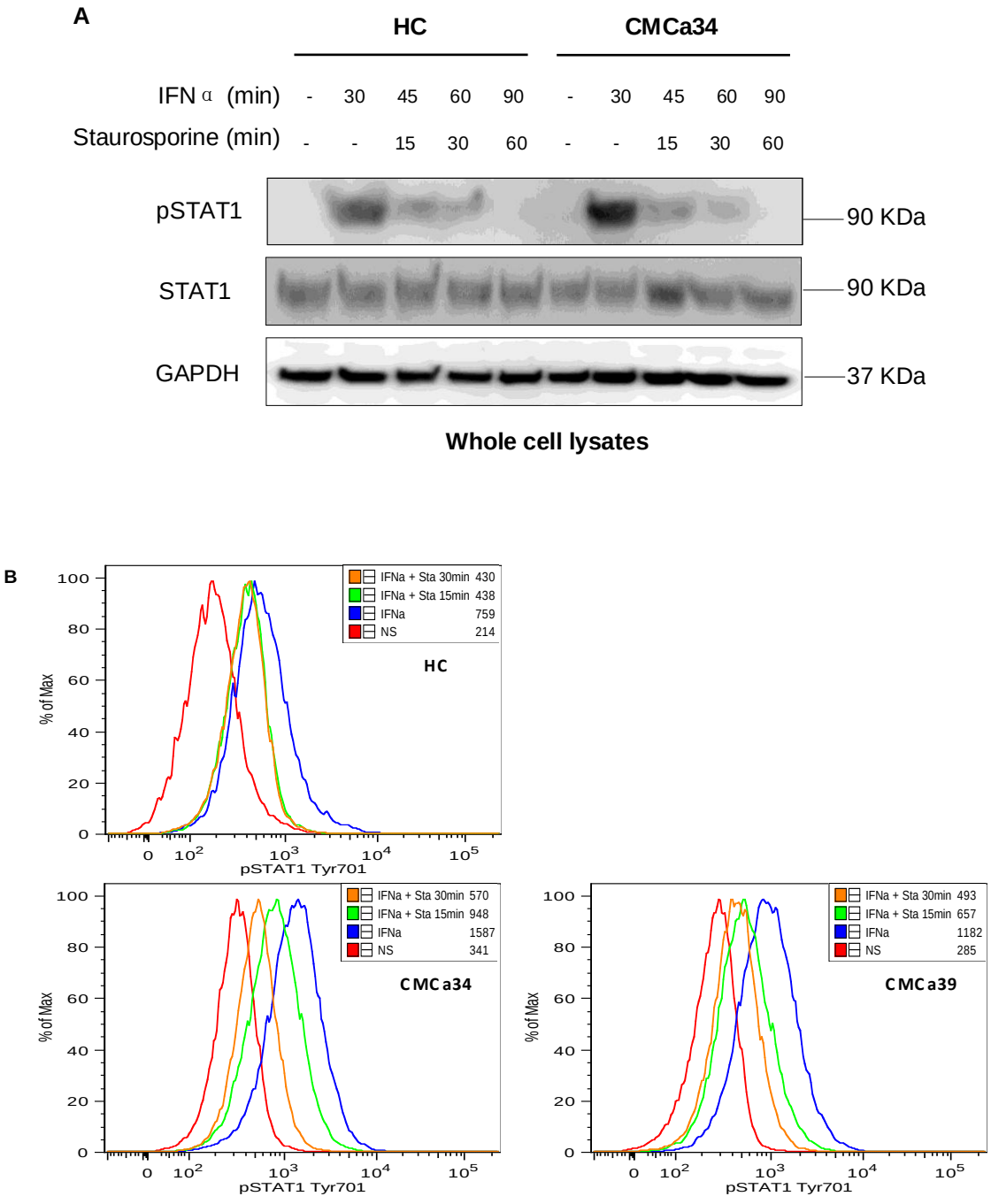

Figure 3.6 Suboptimal stimulation and limiting phosphorylation normalize dephosphorylation kinetics in cells with GOF-STAT1.

A. STAT1 dephosphorylation of whole cell lysates was tested by WB in EBV cells from a healthy control (HC) and an AD-CMC patient (CMC). Cells were left unstimulated or stimulated with IFN-α ($0.5x10^3$ IU/ml) for 30 minutes, then incubated with or without 1 μM of the tyrosine kinase inhibitor staurosporine for 15, 30, or 60 minutes. GAPDH was used as a loading control. B. Kinetics of STAT1 dephosphorylation were studied by intracellular phospho-tyrosine 701 STAT1 staining in EBV cells from a healthy control (HC) and 2 AD-CMC patients (CMC) treated with IFN-α and staurosporine as described above. Results are presented as mean fluorescence intensity (NS, non-stimulated).

3.3.3 GOF-STAT1 mutations result in enhanced STAT1 DNA binding

To determine STAT1 DNA binding in EBV transformed cells following IL-6, IL-21, IL-27, IFN-α or IFN-γ stimulation, I incubated nuclear extracts with a mutant human *sis*-inducible element (hSIE) probe (a STAT-consensus binding site element) and tested binding in EMSA. IFN-γ-, IFN-α- and IL-27-induced STAT1 homodimers, whilst IFN-α-induced STAT1/STAT3 heterodimers DNA-binding to the hSIE was stronger in cells from AD-CMC patients than in those from healthy controls (Fig 3.7). STAT protein DNA-binding specificity was confirmed by using unlabeled competitor or targeted antibodies (Fig 3.8).

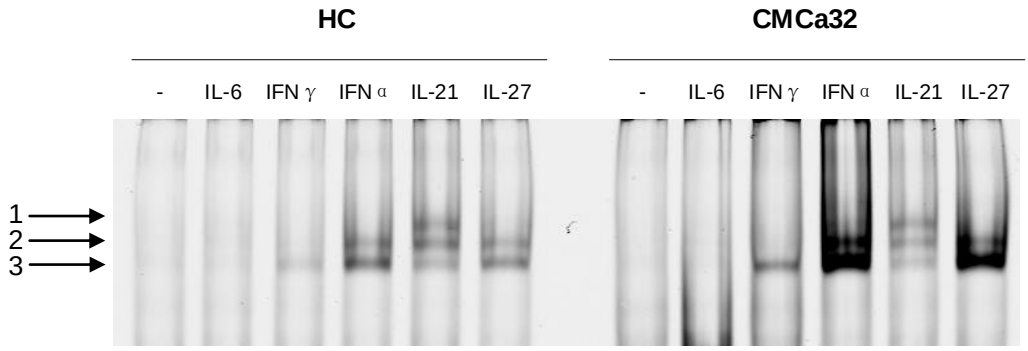

Figure 3.7 GOF- STAT1 mutations lead to enhanced STAT1 DNA-binding.
DNA binding was assessed using the hSIE probe and nuclear extracts from EBV transformed cells derived from a healthy control (HC) and an AD-CMC patient (CMC) following stimulation with IL-6, IL-21 (50 ng/ml) for 15 minutes, or IFN-α, IFN-γ ($1x10^3$ IU/ml), IL-27 (50 ng/ml) for 30 minutes. Arrows indicate STAT1 and STAT3 complexes binding to the probe: 1, STAT3 homodimers; 2, STAT3/STAT1 heterodimers; 3, STAT1 homodimers. Results are representative of at least 3 independent experiments.

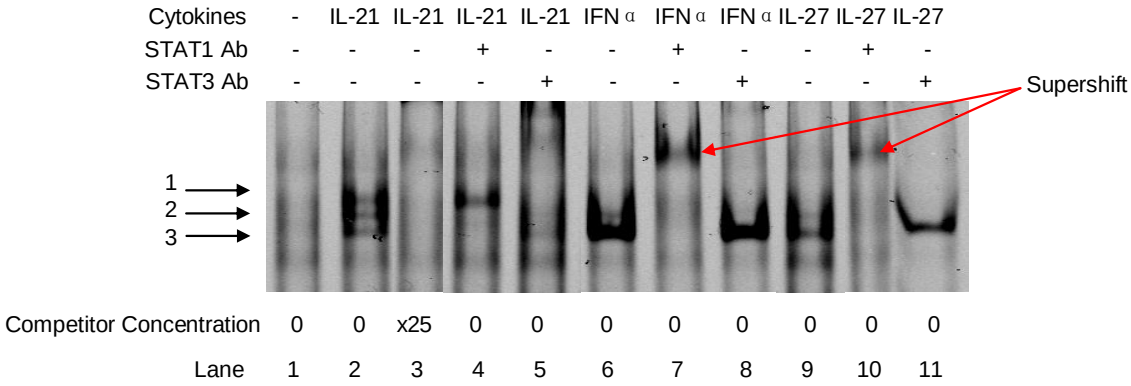

Figure 3.8 EMSA analyses investigating STAT protein binding to the hSIE probe. The EMSA reaction contained the labeled hSIE probe and nuclear extracts from normal EBV cells following stimulation with IL-21 (50 ng/ml) for 15 minutes, IFN-α ($1x10^3$ IU/ml) or IL-27 (50 ng/ml) for 30 minutes. Lane 3 contains unlabeled hSIE probe as competitor; Lanes 4, 7, 10 contain a STAT1 antibody, Lanes 5, 8, 11 contain a STAT3 antibody. Left arrows indicate STAT1 and STAT3 complexes binding to the probe: 1, STAT3/3 homodimers; 2, STAT3/STAT1 heterodimers; 3, STAT1/1 homodimers. Red arrows indicate the supershift with STAT3 antibody.

3.3.4 GOF-STAT1 mutations lead to increased STAT1 transcriptional activity

I next examined the effects of GOF-STAT1 mutations on STAT1-induced gene transcription. The expression of IFN-α- or IL-27-induced genes CXCL10 and IRF1 in mutant cells was markedly enhanced compared with control subjects. Conversely, in line with the comparable levels of STAT1 phosphorylation shown by WB (Fig 3.1), IL-21-induced STAT1-dependent gene expression was not different compared to healthy controls (Figure 3.9).

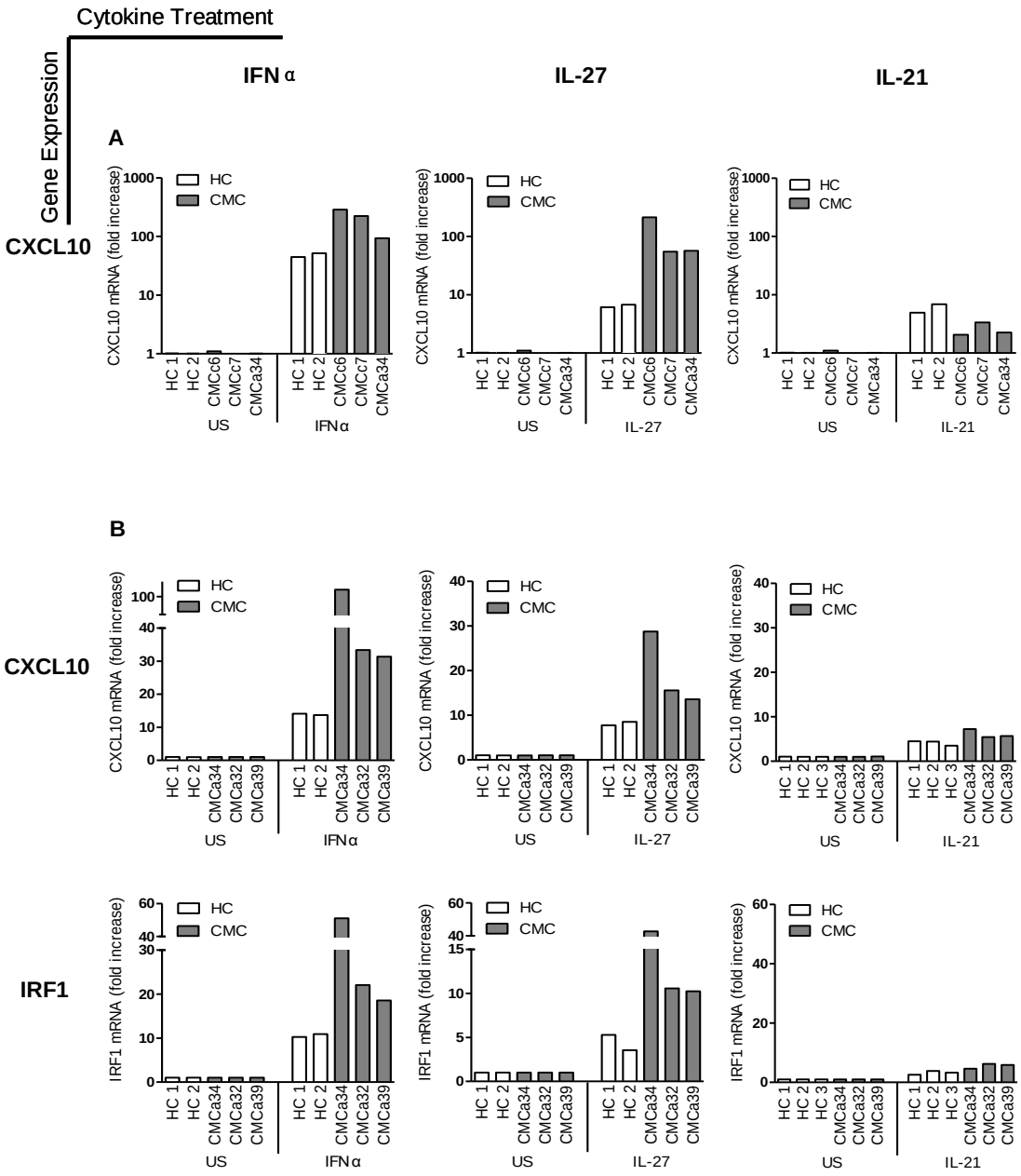

Figure 3.9 GOF-STAT1 mutations increase transcription of STAT1-dependent gene.

Expression of CXCL10 and IRF1 genes in PBMCs (A) or EBV transformed cells (B) was assessed in AD-CMC patients (CMC) or healthy controls (HC) by qRT-PCR. Cells were stimulated with IFN-α ($1x10^3$ IU/ml), IL-27, IL-21 (50 ng/ml) or unstimulated (US) for 4 hours. Two independent experiments were performed.

3.4 Summary

In the present chapter, I confirmed GOF-STAT1 mutations in AD-CMC patients led to increased STAT1 phosphorylation, DNA-binding activity to hSIE probe and STAT1 target gene (CXCL10 and IRF1) induction. These mutations affected cellular response to cytokines including IFN-α, IFN-γ and IL-27.

To understand the underlying mechanisms involved in the gain of STAT1 observed in CMC patients, I used pervanadate and staurosporine to interrogate STAT1 dephosphorylation and phosphorylation. My results demonstrated that the impaired dephosphorylation of IFN-α activated mutant STAT1 could be mimicked in healthy controls by adding pervanadate - a phosphatase inhibitor. On the other hand, the delayed dephosphorylation could be normalized by blocking the initial phosphorylation with staurosporine - a tyrosine kinase inhibitor. Furthermore, I showed that suboptimal stimulation of STAT1 combined with limiting initial phosphorylation resulted in lower levels of STAT1 phosphorylation that allowed dephosphorylation kinetics to return to normal. There results indicated that the underlying mechanism involves a gain of STAT1 activation due to the delayed dephosphorylation as well as the enhanced initial phosphorylation of STAT1.

I have demonstrated that GOF-STAT1 mutations lead to hyper-activation of STAT1 with enhanced and prolonged responses to STAT1-dependent cytokines. However, how this mutation interferes with Th-17 immunity leading to fungal infection remains unclear. Recent studies strongly implicated that STAT3 activation triggers transcription of IL-17 which is crucial for mounting protective immune responses against fungi. The following chapter investigates how GOF-STAT1 mutations interfere with STAT3 activation and function.

CHAPTER 4 GOF-STAT1 MUTATIONS DECREASE STAT3 GENE TRANSCRIPTION

4.1 Rationale

The importance of Th-17 cytokines for fungal immunity in humans was only recently reported [96], when the critical role of STAT3 signaling for production of Th-17 cytokines [45, 60] was identified in PID patients with the HIES, who have CMC as part of their clinical phenotype. Subsequent reports of additional mutations (CARD9, Dectin-1, TYK2, IL-17F, IL-17RA, IL-12Rβ1, ACT1 and AIRE) in PID patients with CMC mapped out the fungal immunity pathway [97], confirming the importance of the STAT3/Th-17 cytokine axis. However, the GOF-STAT1 mutations were not themselves on the Th-17 signaling immune pathway according to currently understanding. This raises the question of how GOF-STAT1 mutations interfere with STAT3 signaling and consequently reduce Th-17 related cytokine production.

STAT1 and STAT3 are thought to play opposite roles in most cell types, although the underlying mechanisms are still not fully understood. STAT1 enhances inflammation and innate and adaptive immunity, triggering anti-proliferation and pro-apoptotic responses, while STAT3 promotes cell survival/proliferation, motility and immune tolerance. There is an intriguing convergence of distinct cytokine and growth factor receptor signaling on overlapping sets of STATs, particularly on STAT1 and STAT3 [98]. STAT1 is a central mediator of all types IFNs (I, II & III) by binding to GAS or ISRE that regulates expression of genes involved in cell cycle arrest and apoptosis [99], as well as IL-27 (a member of the IL-12 family) to induce STAT1-dependent inflammatory target gene expression [100]. STAT3 is mainly activated by IL-6, IL-23 and IL-21 and is essential for differentiation of Th-17 cells, recently shown to be crucial for protection against fungal infections, whilst mediating cell proliferation and survival. However, type II IFNs can in addition activate STAT3 [85, 101]. Activated STAT1 and STAT3 can bind to the same DNA sequences as either homodimers or STAT1/3 heterodimers [102], but trigger the transcription of a different set of genes [103].

The regulation of STAT activity is dependent on initial phosphorylation in the

cytoplasm, translocation to the nucleus, subsequent DNA binding at cytokine-inducible promoter regions and activation of gene transcription. To investigate how enhanced STAT1 activation interferes with STAT3-dependent IL-17 production, in this chapter, I present results investigating STAT3 phosphorylation, nuclear translocation, DNA-binding and gene transcription in CMC patients harbouring GOF-STAT1 mutations.

4.2 Aims

In the presence of GOF-STAT1 mutations:

- Investigate the effect on STAT3 activation/phosphorylation
- Assess nuclear translocation of phosphorylated STAT3
- Evaluate the effect on STAT3 DNA-binding activity
- Determine downstream effect on STAT3-dependent gene induction

4.3 Results

4.3.1 STAT3 phosphorylation in the presence of GOF-STAT1 mutations is not reduced

To evaluate STAT3 activation, I stimulated PBMCs with IL-23 as an improtant cytokine for Th-17 cells proliferation and expansion. Optimization of IL-23-induced STAT3 phosphorylation was shown in Fig 4.1, where phytohemagglutinin (PHA) was used as a mitogen to trigger T cell division, whilst IL-2 was used to activate T cell proliferation and differentiation. I found that in normal PBMCs, IL-23-induced STAT3 phosphorylation could be detected in the presence of PHA and IL-2 for 3 days before exposing to IL-23 stimulation. Follow this culture condition, the results showed that IL-23-induced STAT3 phosphorylation/activation in the presence of GOF-STAT1 mutations was not reduced (Fig 4.2A). In addition, I compared STAT3 phosphorylation in CMC patients to healthy controls upon stimulation with other STAT1/STAT3-activating cytokines (IL-6, IFN-α, IL-21 and IL-27) in both PBMCs and EBV transformed cells. Consistent with IL-23 stimulation data, STAT3 phosphorylation in GOF-STAT1 mutations was not reduced as was expected, but was similar or even increased compared to control EBV cells (Fig 4.2B and C).

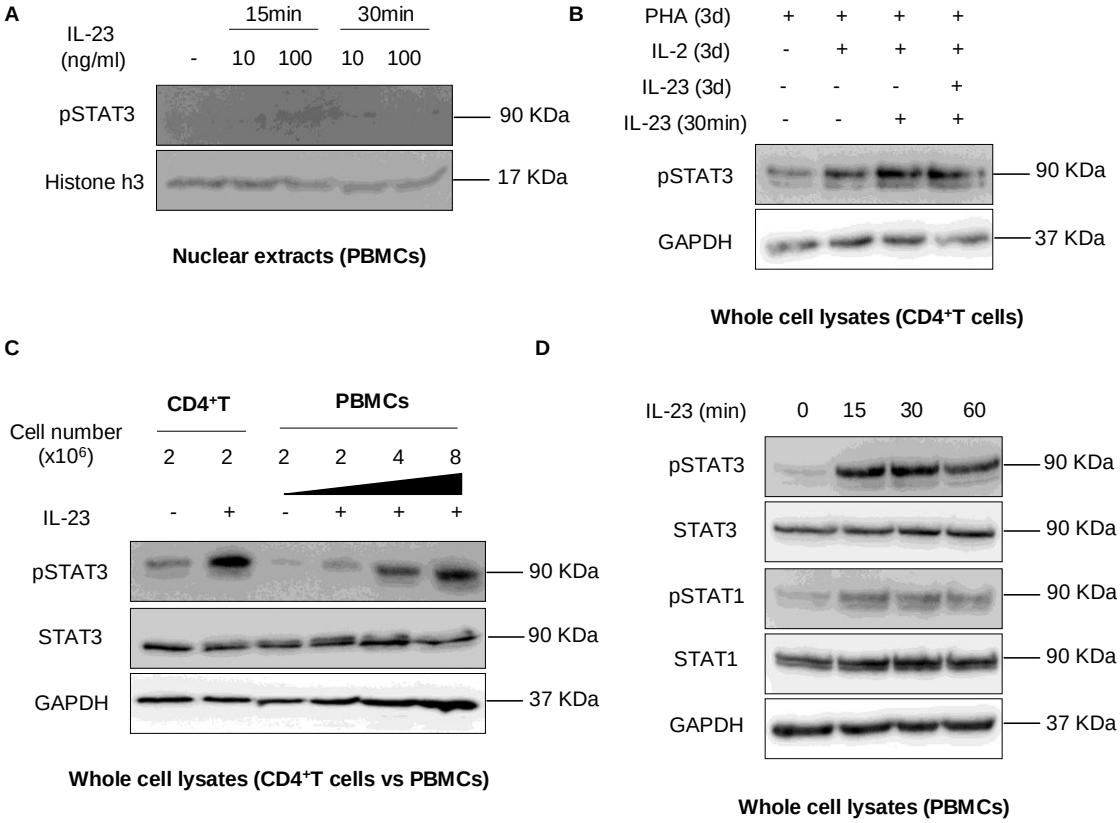

Figure 4.1 Optimization of IL-23-induced STAT3 phosphorylation.

A. Western blotting was performed on nuclear extracts from IL-23-stimulated PBMCs with indicated doses and time periods. B. WB of whole cell lysates from $CD4^+$T cells pre-cultured with PHA (2 μg/ml) and IL-2 (40 IU/ml) for 3 days with or without addition of IL-23 (10 ng/ml), followed by IL-23 (100 ng/ml) stimulation for 30 minutes. C. Optimization of cell number for whole cell lysates extraction by comparing IL-23-induced STAT3 phosphorylation in $CD4^+$T cells and PBMCs with PHA and IL-2 pre-treatment. D. Kinetics of IL-23-induced STAT3 phosphorylation was studied by WB on whole cell lysates extracted from PBMCs ($3x10^6$) with PHA and IL-2 pre-treatment. Anti-GAPDH and anti-Histone H3 antibodies were used as cytoplasmic and nuclear markers, respectively.

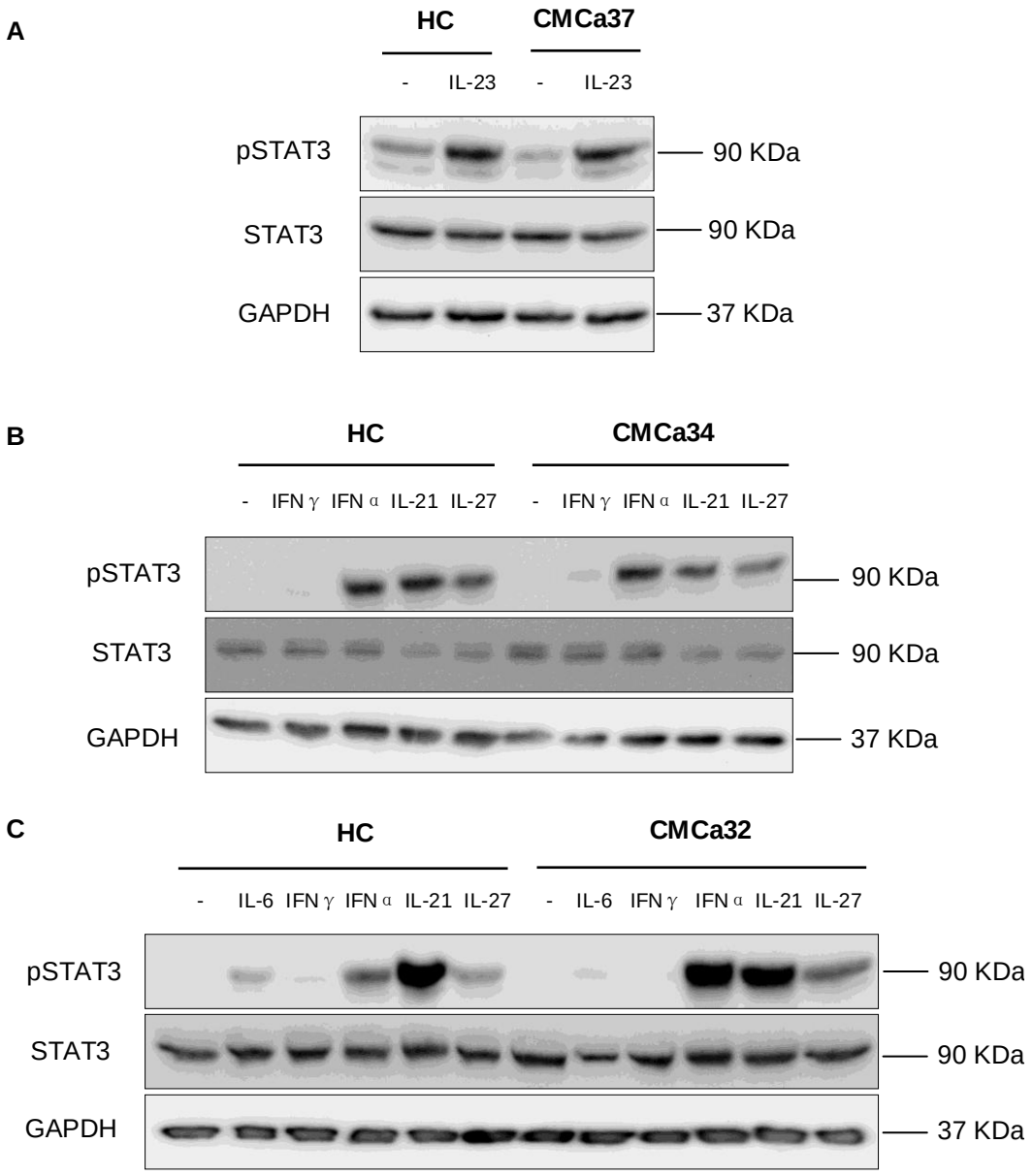

Figure 4.2 STAT3 phosphorylation in the presence of GOF-STAT1 mutations is not reduced.

Western blotting was performed on whole cell lysates from healthy controls (HC) and CMC patients (CMC) with GOF-STAT1 mutations. (A) IL-23-induced STAT3 phosphorylation in PBMCs. Cells were pre-cultured with PHA (2 μg/ml) and IL-2 (40 IU/ml) for 3 days and stimulated with IL-23 (100 ng/ml) for 30 minutes before lysing. Various cytokines induced STAT3 phosphorylation in PBMCs (B) or EBV transformed cells (C). Prior to lysing, cells were stimulated for 15 minutes with 50 ng/ml IL-6, IL-21, 30 minutes with $1x10^3$ IU/ml IFN-γ, IFN-α or 50 ng/ml IL-27. Data shown are representative of at least 3 independent experiments.

4.3.2 Phosphorylated STAT3 translocates to the nucleus in cells with GOF-STAT1 mutations

I next hypothesized that the decreased IL-17 production in CMC patients with GOF-STAT1 mutations could be due to impaired STAT3 nuclear translocation. To evaluate this possibility, I prepared nuclear, cytoplasmic and total cell extracts from IL-23-stimulated PBMCs or IFN-α-stimulated EBV cell lines and checked for the presence of phosphorylated STAT3. As shown in Fig 4.3, both IL-23 and IFN-α stimulation led to a comparable accumulation of phospho-STAT3 in the nuclei of cells from CMC patients and healthy controls.

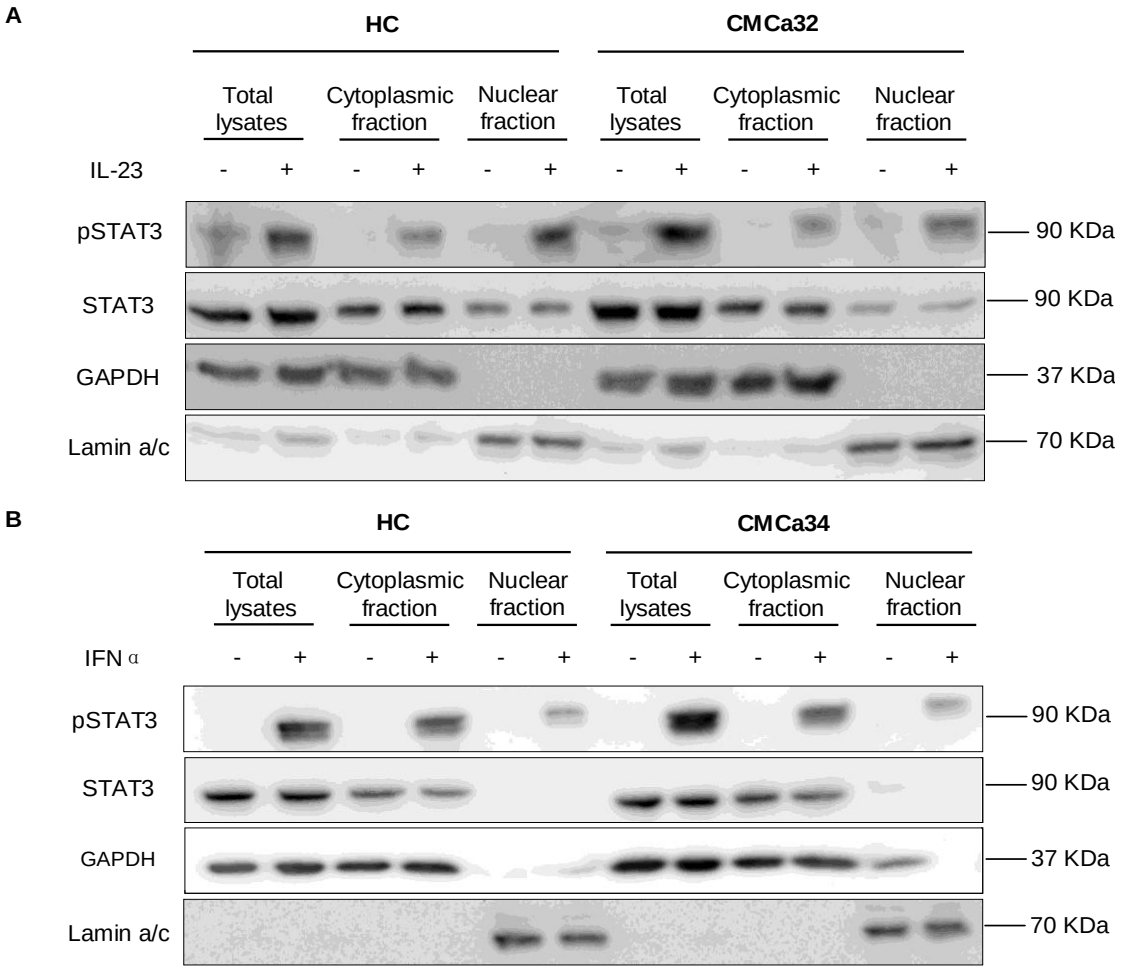

Figure 4.3 Nuclear translocation of STAT3 upon IL-23 or IFN-α stimulation in cells with GOF-STAT1 mutations.

PBMCs were pre-cultured with PHA and IL-2 and stimulated with IL-23 (A) or EBV cells were stimulated with IFN-α (B) as described above. Nuclear, cytoplasmic and total cell extracts were prepared from same number of cells. Extracts were then blotted and membranes were probed with anti-phospho-STAT3 (Tyr705) and anti-STAT3 antibodies. Anti-GAPDH and anti-Lamin A/C antibodies were used as cytoplasmic and nuclear markers, respectively. Results are representative of 2 independent experiments.

4.3.3 STAT3 DNA-binding is maintained in cells with GOF- STAT1 mutations

To investigate whether low STAT3-dependent IL-17 production in patients with GOF-STAT1 mutations was due to impaired STAT3 DNA-binding, I assessed STAT3 binding to a STAT-consensus binding site element (hSIE) in EMSA as well as in an ELISA-based hSIE-binding kit (TransAM STAT3 Kit). My EMSA results showed that IL-21-induced STAT3 homodimers binding to hSIE probe was comparable in cells from CMC patients to those from healthy controls, whilst IFN-α- and IL-27-induced STAT1/3 heterodimers DNA-binding to hSIE was mildly increased in cells from CMC patients to those from healthy controls (Fig 4.4). Additionally, similar levels of STAT3 binding in CMC patients and controls were observed in the TransAM hSIE-binding assay (Fig 4.5).

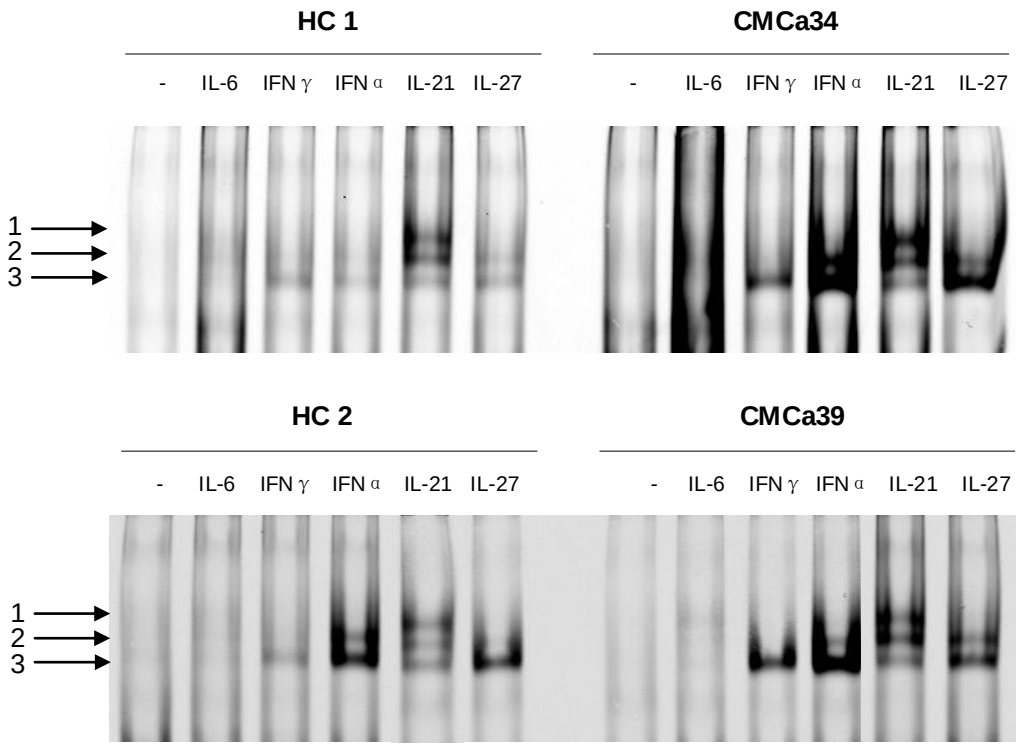

Figure 4.4 Comparable levels of STAT3 binding to the hSIE probe in STAT1 mutant cells and controls evaluated in EMSA.
DNA binding was assessed using the hSIE probe and nuclear extracts from EBV transformed cells derived from healthy controls (HC) and CMC patients (CMC) following stimulation with IL-6, IL-21 (50 ng/ml) for 15 minutes, or IFN-α, IFN-γ ($1x10^3$ IU/ml), IL-27 (50 ng/ml) for 30 minutes. Arrows indicate STAT1 and STAT3 complexes binding to the probe: 1, STAT3/3 homodimers; 2, STAT1/STAT3 heterodimers; 3, STAT1/1 homodimers. Results are representative of at least 3 independent experiments.

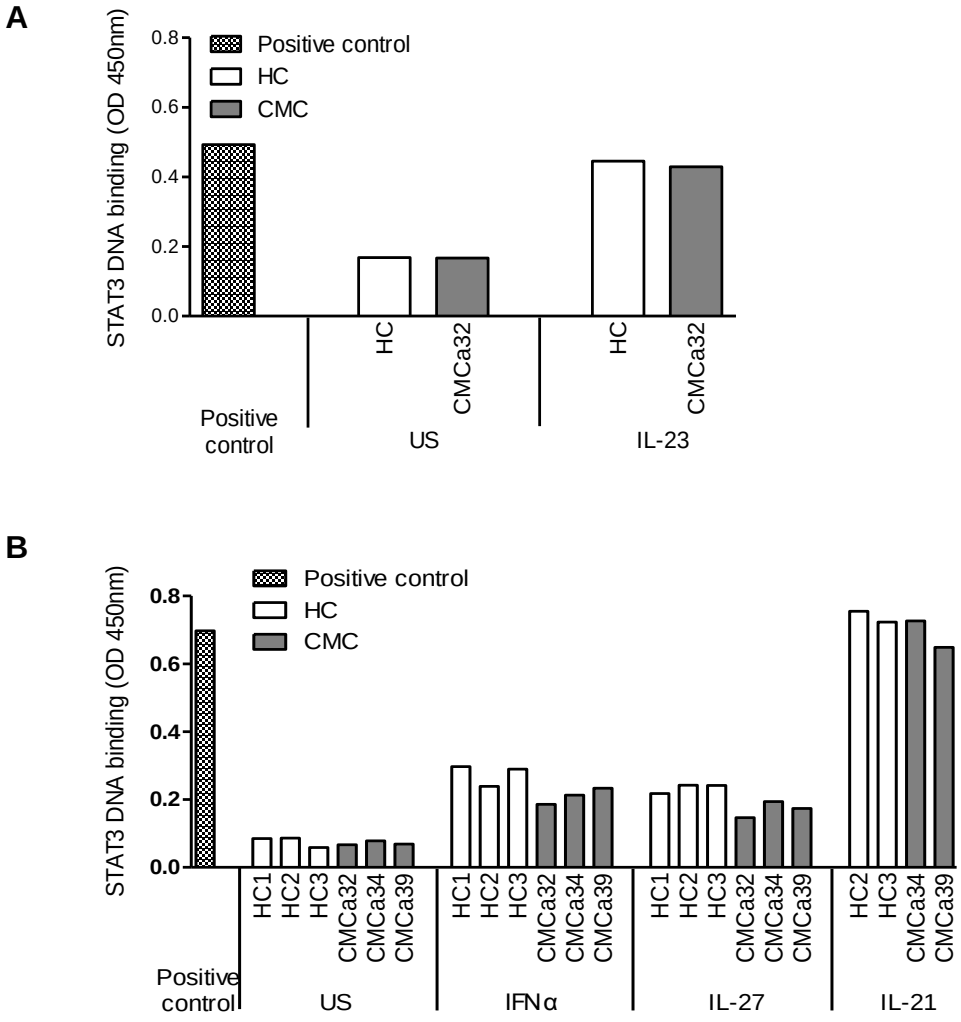

Figure 4.5 Comparable levels of STAT3 binding to the hSIE in STAT1 mutant cells and controls evaluated in the TransAM ELISA-based assay.
Nuclear extracts from unstimulated (US) and IL-23-stimulated PBMCs (A) or IFN-α-, IL-27- and IL-21-stimulated EBV cells derived from healthy controls (HC) and CMC patients (CMC) were incubated with immobilized hSIE and bound STAT3 was detected using a STAT3 antibody according to the TransAM Kit instructions. Nuclear extracts of IL-6-stimulated Hep G2 cells (supplied in the TransAM kit) were used as a positive control. Results are representative of 2 independent experiments.

To further confirm STAT3 DNA-binding in GOF-STAT1 mutations was maintained, I investigated the occupancy of STAT3 at the c-Fos promoter by ChIP assay. Results showed that IFN-α stimulation induced the recruitment and binding of STAT3 at its endogenous c-Fos promoter in a CMC patient was decreased compared to a control (Fig 4.6).

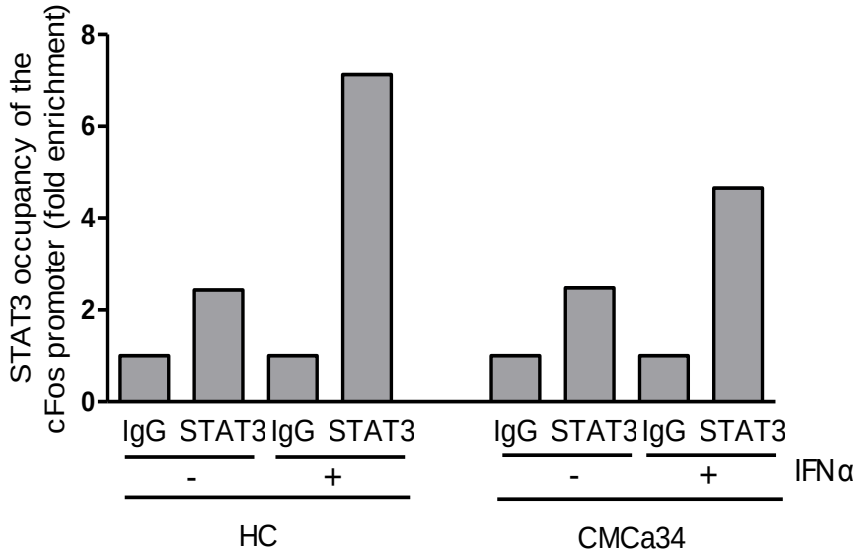

Figure 4.6 Occupancy at the c-Fos promoter by STAT3 is maintained in the presence of GOF-STAT1 mutations.

ChIP assay was carried out using 25 μg cross-linked chromatin prepared from IFN-α ($1x10^3$ IU/ml, 30 minutes) stimulated EBV transformed cell lines derived from a healthy control and a CMC patient with GOF-STAT1. Antibodies used for immunoprecipitation were both rabbit polyclonal raised against STAT3 or a control antibody Immunoglobulin G (IgG). Three micrograms of STAT3 antibody or IgG were used in each ChIP reaction. Immunoprecipitated DNA was subjected to qRT-PCR using c-Fos primers. Each PCR reaction was performed in triplicate. A signal intensity value for each sample was calculated from the average of the experiments. Average values of eluates were normalized to average values of control antibody sample and expressed as fold enrichment above background (i.e. IgG).

4.3.4 GOF- STAT1mutations lead to decreased STAT3 transcriptional activity

The above results suggested the disruption of STAT3-dependent IL-17 production in the presence of GOF-STAT1 mutations may occur at the level of gene transcription. To address this, the following experiments aimed to investigate whether GOF-STAT1 mutations have an effect on transcription of STAT3-induced genes. I stimulated PBMCs with IL-23 and measured transcription of the Th-17 related transcription factors: RORc, IL-17A and IL-22 as well as a non-Th-17 related but STAT3-dependent gene IL-10. The results demonstrated that GOF-STAT1 mutations decreased the transcription of both Th-17 and non-Th-17 related but STAT3-induced genes (Fig 4.7). In addition, I investigated other STAT3-induced gene transcription following stimulation with various STAT1/STAT3-activating cytokines in both PBMCs and EBV cell lines. Consistently,

results showed that all these STAT3-dependent genes (c-Fos, SOCS3, c-Myc) were down-regulated in cells with GOF-mutations of STAT1 (Figs 4.8 and 4.9). This broad effect of GOF-STAT1 on decreasing STAT3-dependent gene transcription might explain the reduced IL-17 levels in CMC patients with STAT1 mutations.

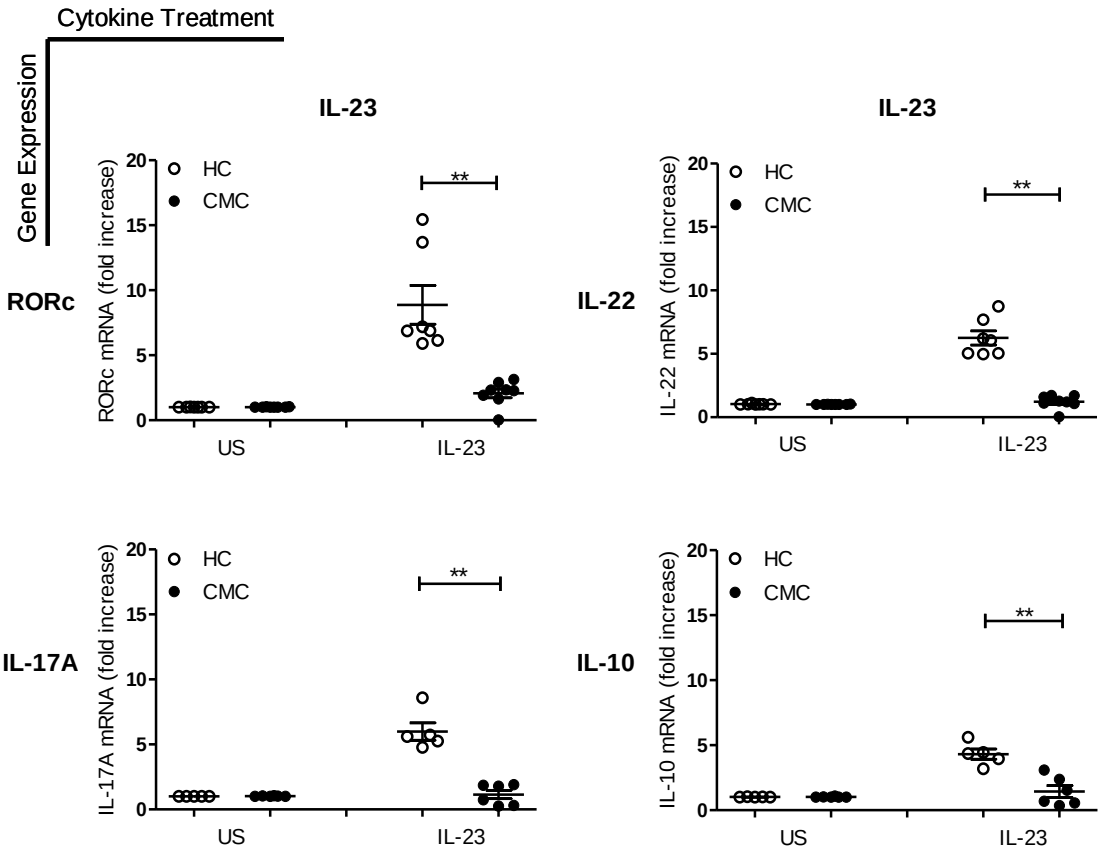

Figure 4.7 Decreased transcription of STAT3-induced genes in the presence of GOF-STAT1 mutations in IL-23-stimulated PBMCs.

Expression of RORc, IL-17A, IL-22 and IL-10 genes in PBMCs was assessed in CMC patients with GOF-STAT1 mutations (CMC) and healthy controls (HC) by qRT-PCR (Mean $\pm$ SEM). PBMCs were pre-cultured with PHA (2 μg/ml) and IL-2 (40 IU/ml) for 3 days and then stimulated with IL-23 (100 ng/ml) or were left unstimulated (US) for 4 hours (** $P \leq 0.01$).

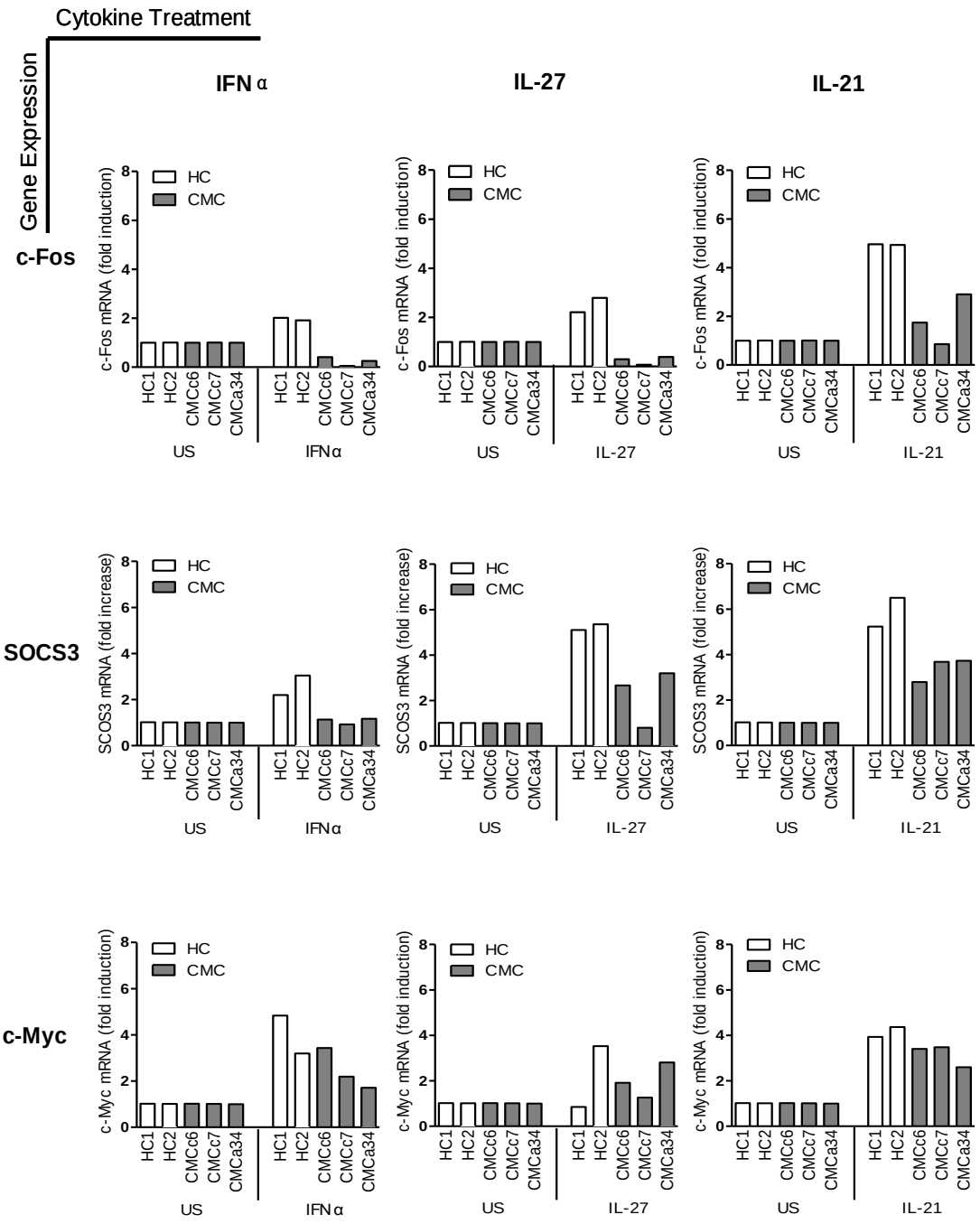

Figure 4.8 Decreased transcription of STAT3-induced genes in the presence of GOF-STAT1 mutations in PBMCs stimulated with IFN-α, IL-27 or IL-21.
Expression of c-Fos, SOCS3 and c-Myc genes in PBMCs was assessed in CMC patients with GOF-STAT1 mutations (CMC) and healthy controls (HC) by qRT-PCR. Cells were stimulated with IFN-α ($1x10^3$ IU/ml), IL-27 and IL-21 (50 ng/ml) or left unstimulated (US) for 4 hours.

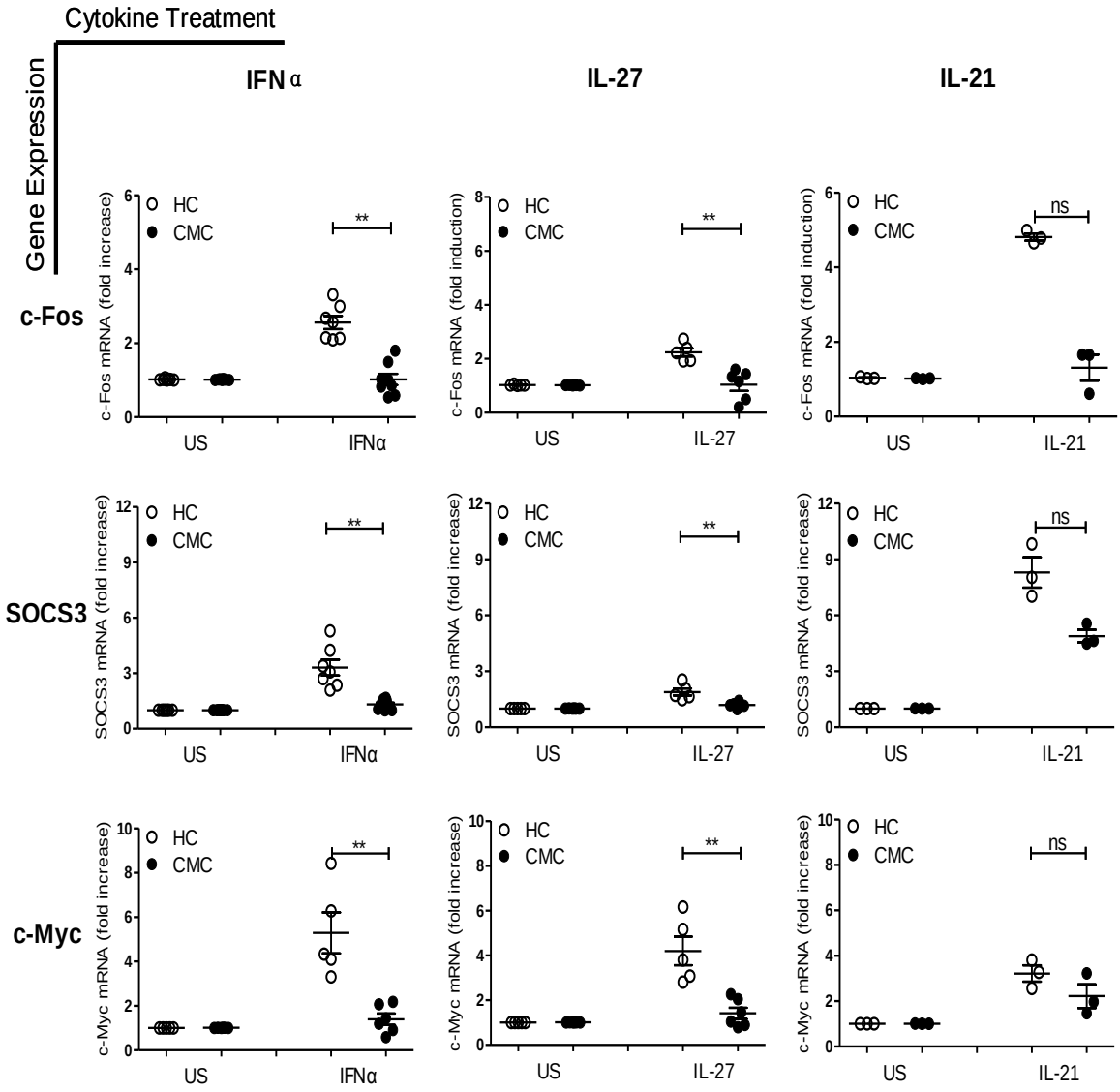

Figure 4.9 Decreased transcription of STAT3-dependent genes in presence of GOF-STAT1 mutations in EBV transformed cells stimulated with IFN-α, IL-27 or IL-21.

Expression of c-Fos, SOCS3 and c-Myc genes in EBV transformed cells was assessed in CMC patients with GOF-STAT1 mutations (CMC) or healthy controls (HC) by qRT-PCR (Mean±SEM). Cells were stimulated with IFN-α ($1x10^3$ IU/ml), IL-27 and IL-21 (50 ng/ml) or left unstimulated (US) for 4 hours (** $P \leq 0.01$, ns=not significant).

To evaluate the transcriptional activity of STAT3 in cells with GOF-mutations of STAT1, I intended to perform STAT3 Luciferase Assay (Cignal Report Assay, Qiagen) in EBV transformed cells from both CMC patients and healthy controls. STAT3 reporter assays can provide a quantitative assessment of STAT3 signal transduction activation by measuring the activities of downstream transcription factors. However, this reporter assay is established on a stable and successful cell transfection, which could be assessed by monitoring GFP expression (supplied in the assay as a positive control). My results revealed that the transfection efficiency of EBV cells was very low, as it is well known that primary human cells are difficult to transfect. Conversely, the transfection efficiency of an adherent human chondrocyte cell line (SW cells) was far better (Fig 4.10). These results suggested that EBV cell lines are difficult to transfect and not suitable for performing STAT3 Reporter Assays.

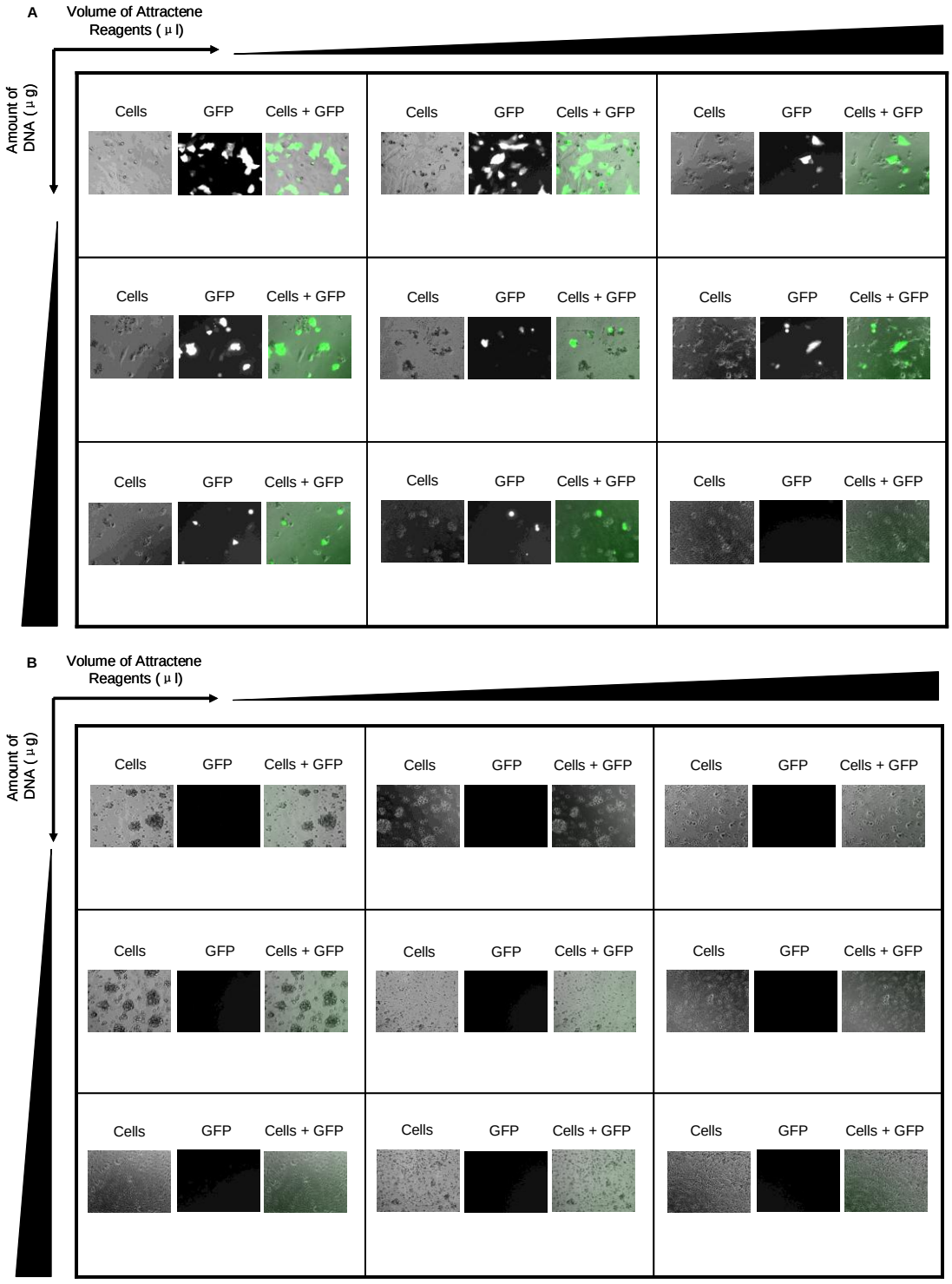

Figure 4.10 Comparison of cell transfection efficiency in EBV cells and SW cells. Cell transfection was carried out in SW cells (A) and EBV transformed cells (B) with GFP tagged positive control for 48 hours transfection. The amount of DNA and Attractene Reagent is given in Table 2.2. GFP positive control was used from the Cignal Report Assay kit (40:1:1 mixture of constitutively expressing GPF, firefly luciferase and Renilla luciferase constructs).

4.4 Summary

It has been suggested that STAT1 and STAT3 oppose each other in many biological processes [104]. In the present chapter, I investigated how enhanced STAT1 activation interferes with STAT3 activation and signaling in CMC patients. My results showed that STAT3 phosphorylation in the presence of GOF-STAT1 mutations was not reduced following stimulation of PBMCs with a selective STAT3-activating cytokine (IL-23) and STAT1/STAT3-activating cytokines (IFN-α, IL-21 and IL-27). The unimpaired phosphorylation of STAT3 was also confirmed in EBV transformed cells with GOF-STAT1 mutations following stimulation with IFN-α, IL-21 and IL-27. Both IL-23 and IFN-α induced phosphorylated STAT3 could translocate into nuclei of cells with GOF-mutations of STAT1. Cytokine (IL-23, IFN-α, IL-21 and IL-27) activated STAT3 binding to hSIE was maintained in cells bearing GOF-STAT1 mutations. However, the recruitment of activated STAT3 to its endogenous target gene promoter (c-Fos) was decreased in EBV cells with GOF-mutations of STAT1. Furthermore, in contrast with healthy controls, the transcription of STAT3-dependent genes induced by cytokine (IL-23, IFN-α, IL-27 and IL-21) stimulation was markedly reduced. Impaired STAT3-inducible gene transcription included both Th-17 (RORc, IL-17, IL-22) and non-Th-17 (IL-10, c-Fos, SOCS3, c-Myc) related genes in cells with GOF-STAT1 mutations. The broad defective transcription of STAT3-dependent gene might explain the reduced IL-17 levels and other clinical phenotypes in CMC patients harbouring GOF-STAT1 mutations.

I have demonstrated the GOF-STAT1 mutations lead to decreased transcription of STAT3-induced gene, which might be the mechanism underlying reduced Th-17 related cytokine levels in CMC patients. In the following chapter I investigate whether inhibition of enhanced STAT1 signaling improves STAT3 function in these CMC patients.

CHAPTER 5 INHIBITION OF STAT1 ENHANCES STAT3 GENE TRANSCRIPTION IN CMC

5.1 Rationale

Fludarabine is a chemotherapy drug known as an antimetabolite. It is used in the treatment of hematological malignancies (cancers of blood cells such as leukemias and lymphomas). Fludarabine can prevent cells from making DNA and RNA, which stops cell growth and causes cell death. It has been shown that fludarabine can also induce significant reduction of STAT1 phosphorylation without affecting other STAT proteins [105, 106]. It is therefore recognized as a STAT1 activation inhibitor.

STAT1 mutations identified in AD-CMC patients are gain-of-function. In the previous chapter I have shown that the enhanced STAT1 activation interferes with STAT3 signaling at the gene transcription level, where GOF-STAT1 decreases STAT3-induced transcription of both Th-17 and non-Th-17 related genes. This is likely the underlying mechanism of low IL-17 production in CMC patients with these mutations. In this chapter, I present results demonstrating how inhibition by fludarabine of the STAT1 hyper-phosphorylation/activation caused by the GOF-STAT1 mutations in CMC patients influences STAT3-induced gene transcription and IL-17 production.

5.2 Aims

In the presence of fludarabine in GOF-STAT1 mutant cells:

- Investigate STAT1 and STAT3 phosphorylation
- Evaluate the effect on STAT1- and STAT3-induced gene transcription
- Assess the effect on *Candida albicans*-induced cytokine production

5.3 Results

5.3.1 Fludarabine inhibits STAT1 phosphorylation without affecting phosphorylation of STAT3

To evaluate the effect of fludarabine on cytokine-induced STAT1 and STAT3 activation, I assessed EBV transformed cells from a healthy donor and either left them untreated or exposed them to fludarabine, then stimulated them with IL-21 (a cytokine which strongly activates both STAT1 and STAT3 signaling in EBV cells). Results showed that fludarabine led to a dose-dependent inhibition of STAT1 activation after IL-21 treatment of EBV cells (Fig 5.1). In contrast, phosphorylation of STAT3 induced by IL-21 was only minimally affected by fludarabine treatment (Fig 5.1). Thus, fludarabine induced a specific defect in STAT1 activation following cytokine stimulation. No effect of fludarabine on cell viability was confirmed by cell proliferation assay (Promega) (Fig 5.2).

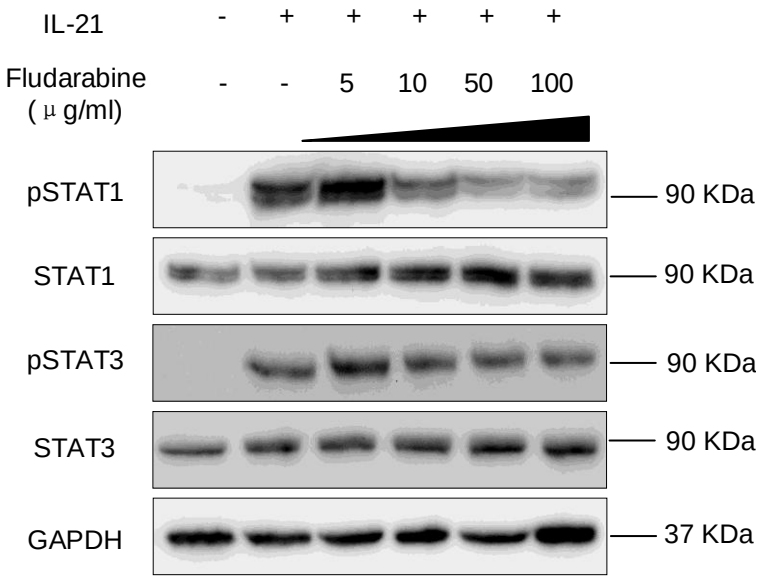

Figure 5.1 Fludarabine inhibits STAT1 phosphorylation without affecting phosphorylation of STAT3.
Western blotting was performed on whole cell lysates of EBV transformed cells derived from a healthy subject. Prior to lysing, cells were left untreated or exposed to fludarabine at the indicated doses for 1 hour, then stimulated with IL-21 (50 ng/ml) for 15 minutes.

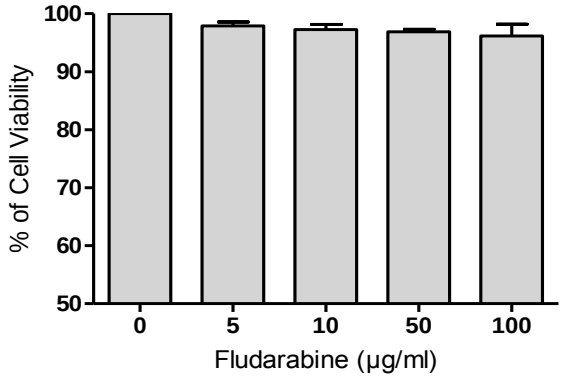

Figure 5.2 Effect of fludarabine doses on cell viability in short time culture.
After four hours in the presence of fludarabine (at the indicated doses), cell viability was assessed by measuring the activity of mitochondrial reductase enzymes on formazan production. Mean optical density from triplicate wells of treated cells was compared to untreated cells (expressed as 100%).

5.3.2 Fludarabine improves STAT3-induced gene transcription in cells with GOF-STAT1 mutations

Given that fludarabine induced specific inhibition of STAT1 phosphorylation, I next assessed its effect on downstream STAT1- and STAT3-induced gene transcription. Results showed that fludarabine led to substantial inhibition of IFN-α- and IL-27-induced STAT1-dependnet gene (CXCL10 and IRF1) transcription in EBV cells from both healthy controls and CMC patients (Fig 5.3). Interestingly, transient inhibition of STAT1 activation improved transcription of IL-23-activated Th-17 related genes (RORc, IL-17A and IL-22) in cells from CMC patients, which approached levels seen in healthy controls (Fig 5.4). This improved STAT3-dependent gene transcription was also observed in IFN-α-, IL-27- and IL-21-induced c-Fos and SOCS3 gene expression in EBV cell lines from CMC patients with GOF-STAT1 mutations (Fig 5.5). However, no obvious difference was seen for IL-10 and c-Myc gene transcription (Fig 5.5).

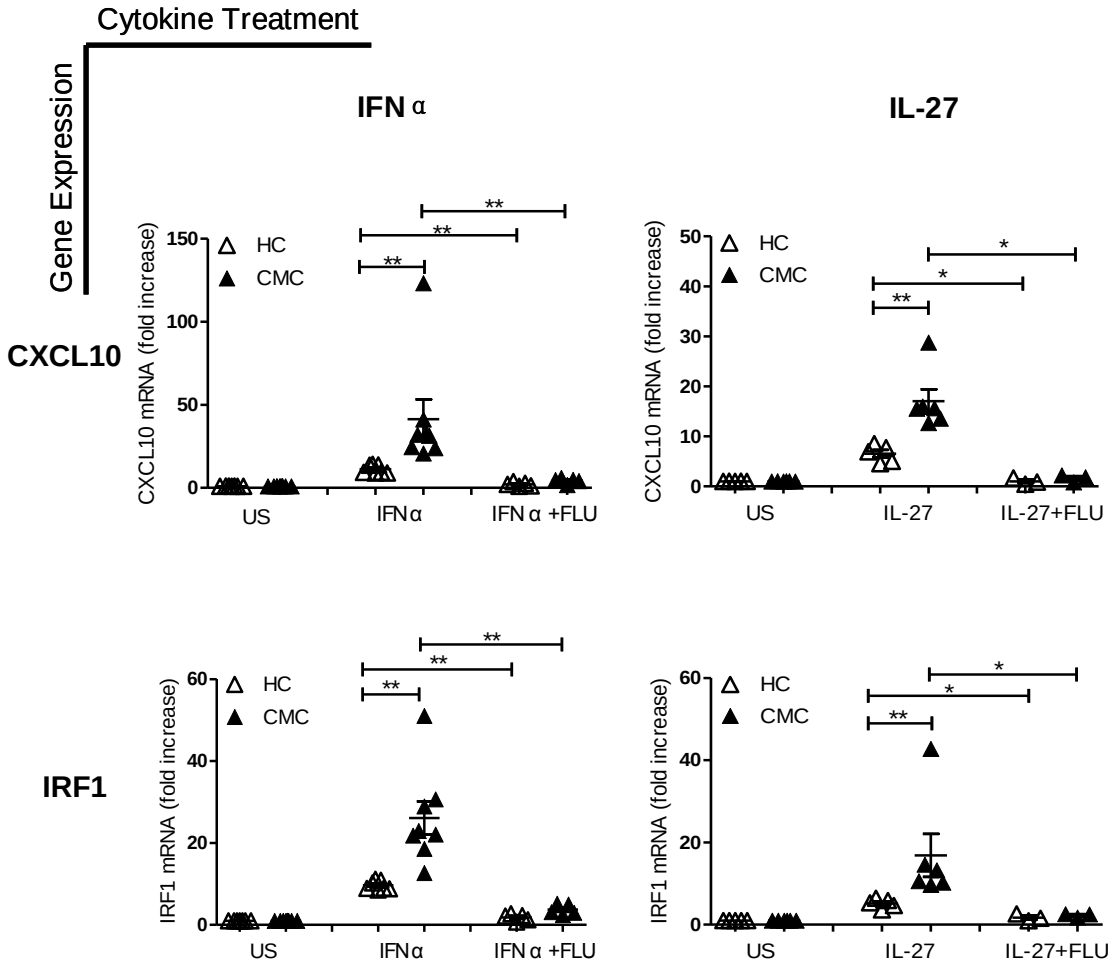

Figure 5.3 Fludarabine reduces previously high GOF-STAT1-dependent gene transcription.

Expression of CXCL10 and IRF1 genes in EBV transformed cells was assessed in CMC patients with GOF-STAT1 mutations (CMC) or healthy controls (HC) by qRT-PCR (Mean±SEM). Cells were stimulated with IFN-α ($1x10^3$ IU/ml) and IL-27 (50 ng/ml) or left unstimulated (US) for 4 hours, fludarabine (FLU) 100 μg/ml was added 1 hour before cytokine stimulation (* $P \leq 0.05$, ** $P \leq 0.01$).

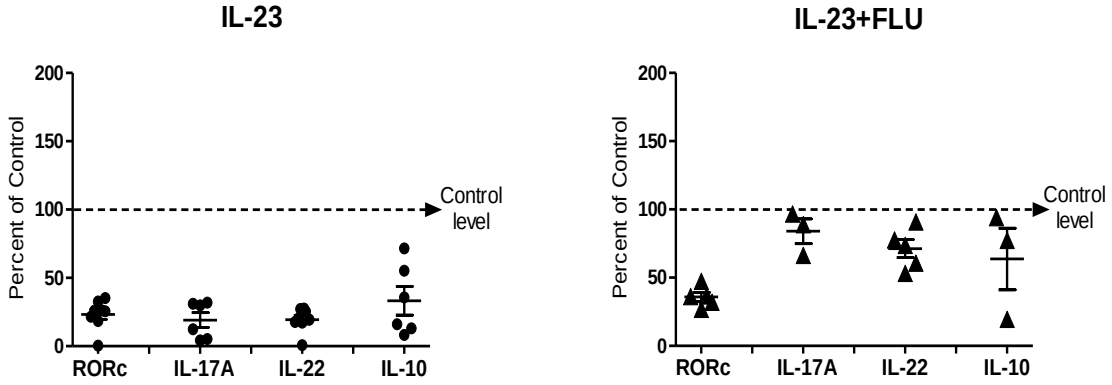

Figure 5.4 Fludarabine improves low STAT3-induced gene transcription in PBMCs with GOF-STAT1 mutations.

Expression of RORc, IL-17A, IL-22 and IL-10 genes in PBMCs was assessed in CMC patients or healthy controls by qRT-PCR. Cells were stimulated with IL-23 (100 ng/ml) for 4 hours, fludarabine (FLU) 100 μg/ml was added 1 hour before cytokine stimulation. Relative effect of fludarabine on IL-23 stimulated STAT3-denpendent gene expression in CMC patients is shown as a percentage of the levels in healthy controls which are presented as 100% (dotted line) (Mean±SEM).

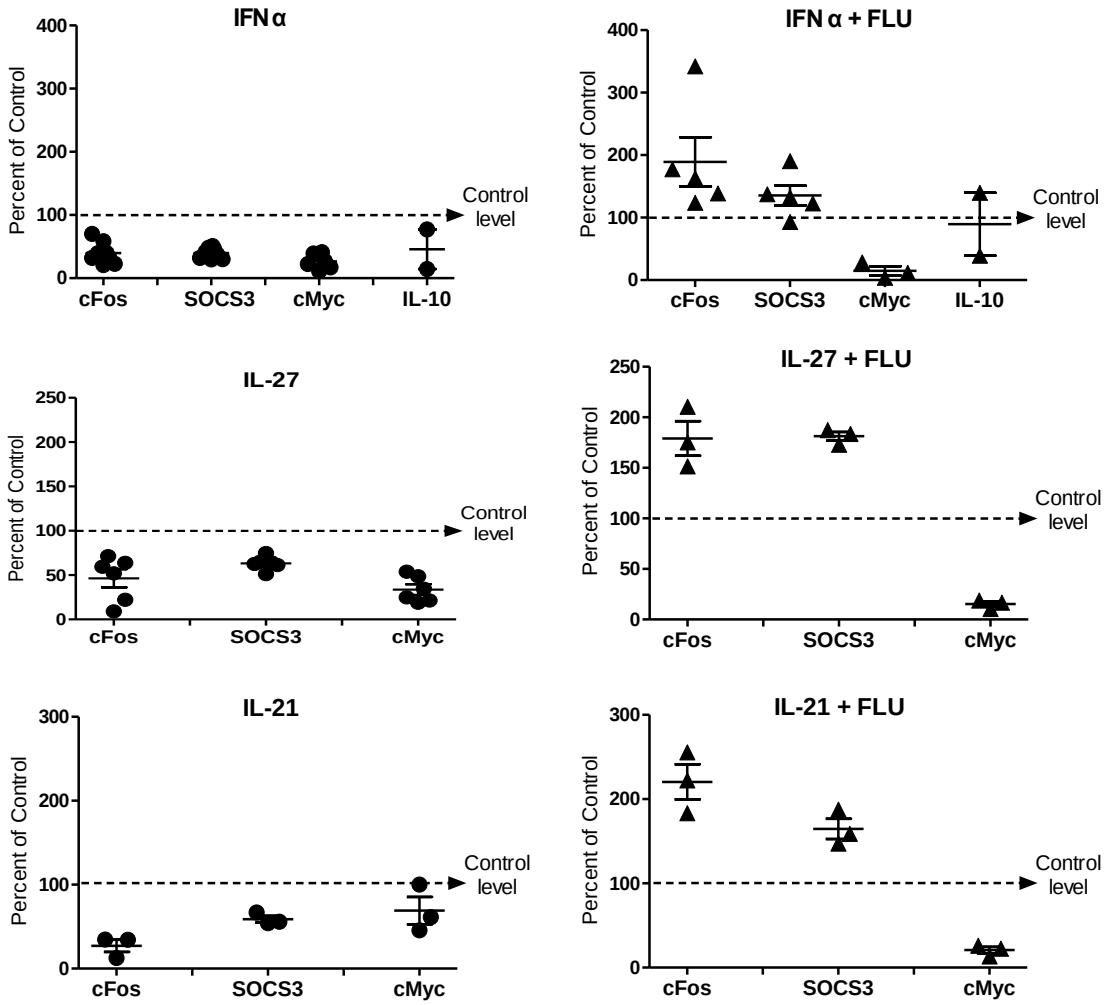

Figure 5.5 Fludarabine improves low STAT3-induced gene transcription in EBV cells with GOF-STAT1 mutations.

Expression of c-Fos, SOCS3, c-Myc and IL-10 genes in EBV cells was assessed in CMC patients or healthy controls by qRT-PCR. Cells were stimulated with IFN-α ($1x10^3$ IU/ml), IL-27 or IL-21 (50 ng/ml) for 4 hours, fludarabine (FLU) 100 μg/ml was added 1 hour before cytokine stimulation. Relative effect of fludarabine on cytokine-induced STAT3 gene expression in CMC patients is shown as a percentage of the levels in healthy controls which are presented as 100% (dotted line) (Mean±SEM).

5.3.3 Fludarabine cannot rescue low IL-17 production in CMC patients with GOF-STAT1 mutations

The above results suggested that transient inhibition of STAT1 in CMC patients with GOF-STAT1 mutations might improve low STAT3-indcued gene transcription. The next experiments aimed to investigate whether low IL-17 production could indeed be restored in CMC patients in the presence of fludarabine. To address this, I assessed PBMCs collected from CMC patients with GOF-STAT1 mutations and healthy controls

and either left them untreated or exposed them to *Candida albicans* with the addition of fludarabine for 5 days. Cytokine production in cell culture supernatant was measured by ELISA. My results confirmed the previous findings of low IL-17 and IL-22 production in CMC patient cells exposed to *Candida albicans*. IL-10 production is also lower in CMC patients than healthy subjects. However, upon addition of fludarabine to cell cultures of either healthy controls or CMC patients, hardly any cytokine production was seen (Fig 5.6), suggesting that the presence of fludarabine in long-term cultures was unable to restore low IL-17 or IL-22 production in cells with GOF-STAT1 mutations.

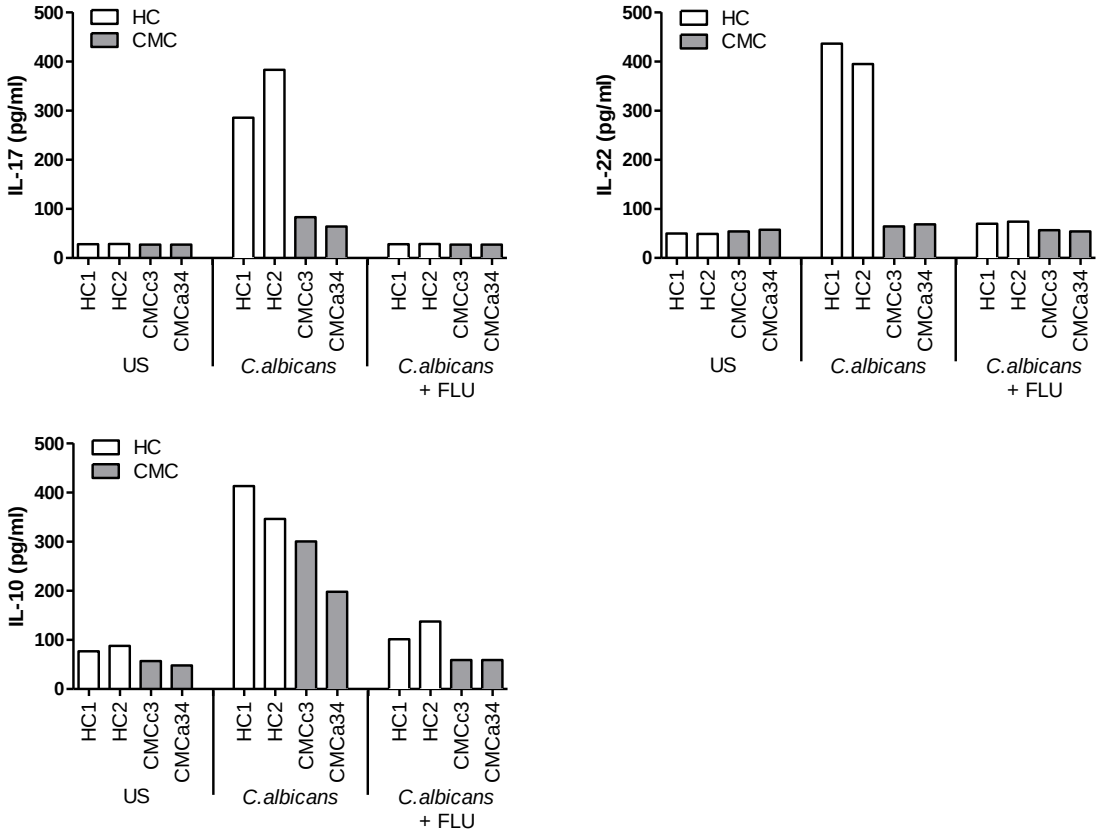

Figure 5.6 Cytokine production of *Candida albicans*-stimulated PBMCs in the presence of fludarabine.

Cytokine production of IL-17, IL-22 and IL-10 in *Candida albicans*-stimulated PBMCs was assessed in 2 CMC patients with GOF-STAT1 mutations (CMC) and 2 healthy controls (HC) by ELISA. Cells were left unstimulated (US) or stimulated with *Candida albicans* (1:15x10^3 dilution) with or without fludarabine (FLU) 100 μg/ml for 5 days. Amphotericin B (2.5 μg/ml) was added at day 0 and day 3 to prevent *Candida albicans* overgrowth.

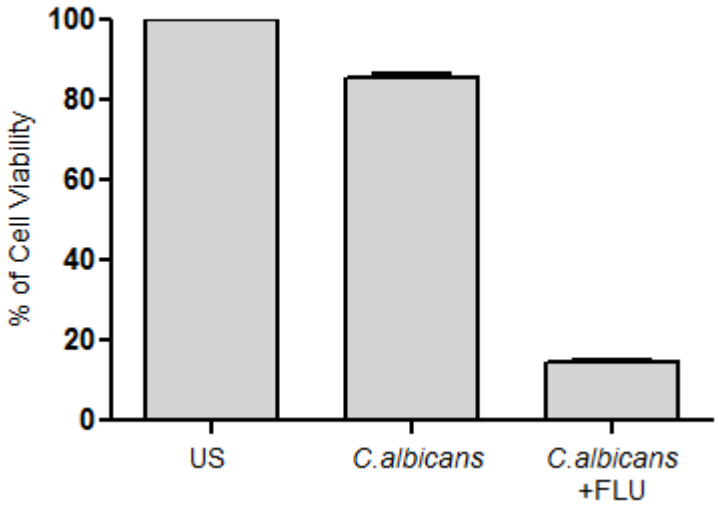

Figure 5.7 Effect of fludarabine on cell viability in lone-term culture.
PBMCs from healthy control were left unstimulated (US) or stimulated with *Candida albicans* (1:15x10^3 dilution) with or without fludarabine (FLU) 100 μg/ml for 5 days. Amphotericin B (2.5 μg/ml) was added at day 0 and day 3 to prevent *Candida albicans* overgrowth. Cell viability was assessed on day 5 by measuring the activity of mitochondrial reductase enzymes on formazan production. Mean optical density from triplicate wells of treated cells was compared to untreated cells (expressed as 100%).

5.4 Summary

The low STAT3-induced gene transcription caused by STAT1 hyper-activation in CMC patients bearing GOF-STAT1 mutations may be the cause of low IL-17 production seen in these patients and their consequent susceptibility to *Candida* infections. In the present chapter, I used a STAT1 inhibitor (fludarabine) to inhibit STAT1 activation and investigated its effects on STAT3 phosphorylation and transcription. I confirmed the specificity of fludarabine for inhibition of STAT1 activation and by demonstrating a dose-dependent inhibition of STAT1 phosphorylation without affecting STAT3. In line with this, fludarabine significantly inhibited downstream STAT1-dependent gene (CXCL10 and IRF1) transcription in both healthy controls and CMC patients. Moreover, fludarabine treatment improved low transcription of Th-17 related genes (RORc, IL-17A and IL-22) expression in IL-23-stimulated PBMCs and other STAT3-dependent gene (c-Fos and SOCS3) in IFN-α-, IL-27- and IL-21-stimulated EBV cells from CMC patients with GOF-STAT1 mutations. Although transient inhibition of STAT1 improved STAT3-dependent gene transcription, long-term exposure to fludarabine in *Candida albicans*-stimulated PBMCs cultures could not restore low IL-17 and IL-22 production in CMC patients, due to the long-term culture with a high dose (100 μg/ml) of fludarabine could cause cell death.

The above results demonstrate that fludarabine treatment can transiently improve low STAT3-induced gene transcription in CMC patients but still cannot restore low Th-17 cytokine production. As recent data strongly implicate epigenetic regulation of gene transcription by acetylation, in the following chapter I investigate whether the disrupted STAT3 function in CMC patients with GOF-STAT1 mutations could be modified by regulating acetylation.

CHAPTER 6 MODIFICATION OF ACETYLATION ALTERS STAT3 FUNCTION

6.1 Rationale

Unlike phosphorylation/dephosphorylation, which mainly acts as an on/off switch for STAT activity, post-translational covalent modification of histones like acetylation and methylation have recently been shown to critically modify STAT-dependent intracellular signaling [84]. The extent of histone acetylation is determined by the activities of the enzymes, HDACs and HATs [107]. Various chemically and structurally diverse agents have been discovered which specifically inhibit HDAC activity. These include the natural product trichostatin A (TSA) which has a broad spectrum of epigenetic activities and has been investigated as a potential anti-cancer drug [108].

The enhanced STAT1 activation and function caused by GOF-mutations identified in CMC decreases STAT3-induced transcription of both Th-17 and non-Th-17 related genes. Although inhibition of STAT1 by fludarabine can transiently improve low STAT3-induced gene transcription, it cannot restore low Th-17 cytokine production in CMC patients as demonstrated in the previous chapter. In this chapter, I investigated whether the disrupted STAT3 function in CMC patients with GOF-STAT1 mutations could be modified by regulating acetylation.

6.2 Aims

In the presence of GOF-STAT1 mutations:

- Investigate the effect of TSA on STAT1 and STAT3 phosphorylation
- Evaluate the effect of TSA on STAT1- and STAT3-induced gene transcription
- Assess the effect of TSA on *Candida albicans*-induced cytokine production
- Identify which HDACs are involved in regulating STAT3-induced gene transcription
- Investigate the combined effect of TSA and fludarabine on STAT3-induced gene transcription

6.3 Results

6.3.1 TSA does not alter phosphorylation of STAT1 and STAT3

To evaluate the effect of TSA on cytokine-induced STAT1 and STAT3 activation, I assessed phosphorylation of STAT1 and STAT3 following stimulation of PBMCs with IL-23 or EBV transformed cells with IFN-α from healthy controls and AD-CMC patients. To avoid cell toxicity, the dose-dependent effect of TSA on cell viability was assessed by cell proliferation assay (Promega). Fig 6.1 showed that there was no significant toxicity at 100 ng/ml of TSA. With the same dose, TSA did not alter IL-23 and IFN-α-induced phosphorylation of STAT1 and STAT3 in either healthy controls or CMC patients (Fig 6.2).

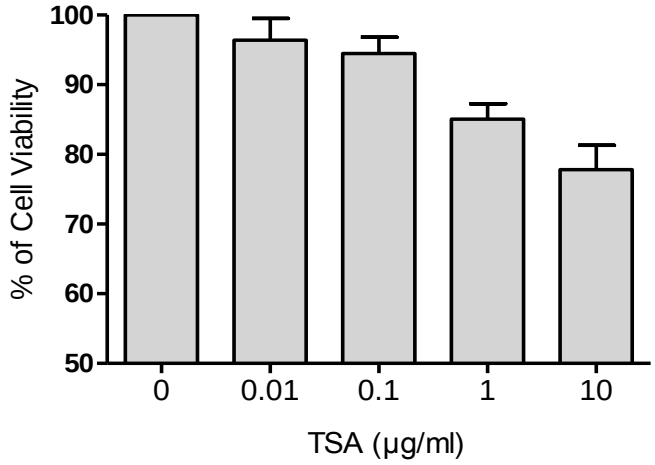

Figure 6.1 Effect of TSA doses on cell viability.
After four hours addition of TSA at the indicated doses, cell viability was assessed by measuring the activity of mitochondrial reductase enzymes on formazan production. Mean optical density from triplicate wells of treated cells was compared to untreated cells (expressed as 100%).

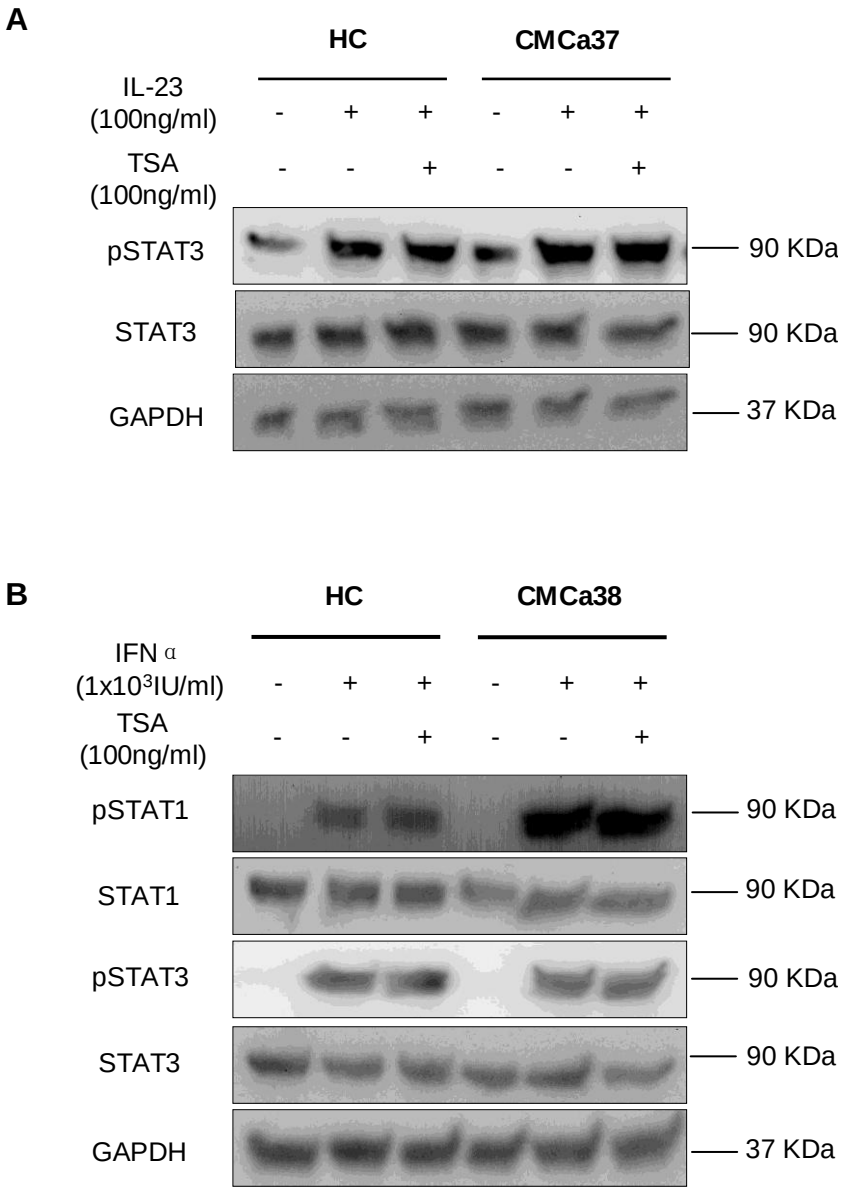

Figure 6.2 TSA does not alter cytokine-induced phosphorylation of STAT1 and STAT3.

Western blotting was performed on whole cell lysates of PBMCs (A) or EBV transformed cells (B) derived from healthy controls (HC) and CMC patients with GOF-STAT1 mutations (CMC). Prior to lysing, cells were left untreated or exposed to TSA (100 ng/ml) together with IL-23 (100 ng/ml) for 30 minutes in PBMC cultures (pre-cultured with 2 μg/ml PHA and 40 IU/ml IL-2 for 3 days) or IFN-α ($1x10^3$ IU/ml) for 15 minutes in cultures of EBV cell lines. GAPDH was used as a loading control.

6.3.2 TSA accelerates prolonged dephosphorylation of STAT1 in cells with GOF-STAT1 mutations

GOF-STAT1 mutations led to a delayed dephosphorylation of STAT1 for up to 90

minutes in CMC patients as previously demonstrated. However, addition of TSA allowed dephosphorylation to take place with similar kinetics as in normal cells (Fig 6.3).

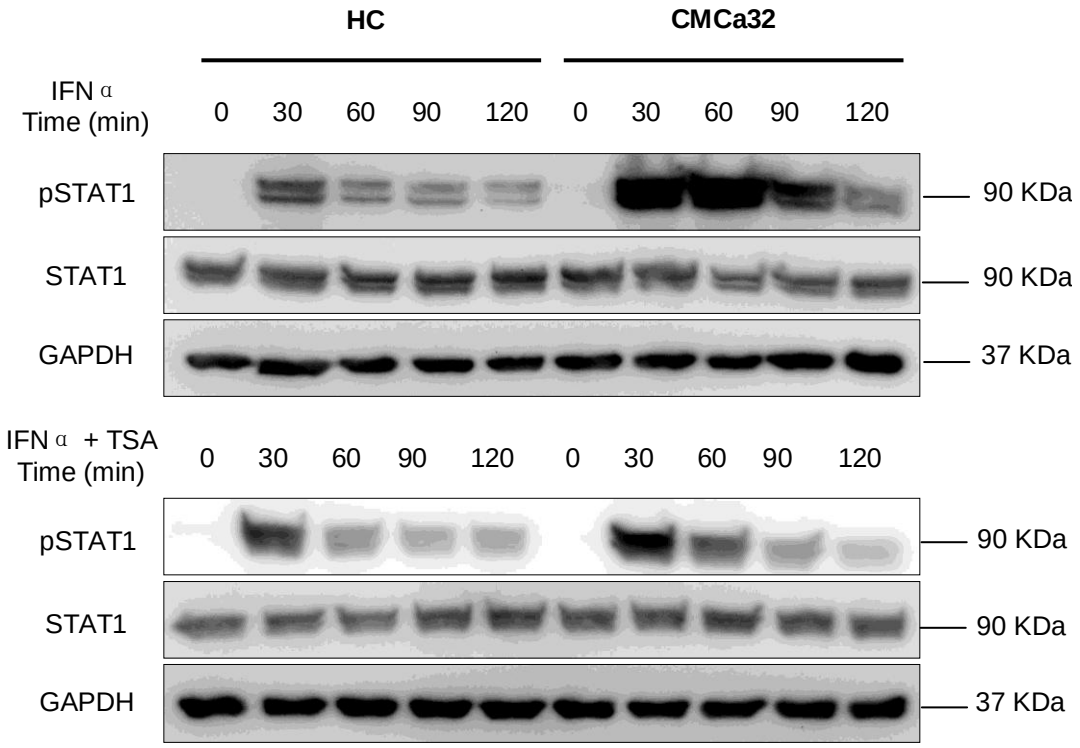

Figure 6.3 TSA accelerates delayed dephosphorylation of STAT1 in cells with GOF-STAT1 mutations.
Dephosphorylation in EBV transformed cells from a CMC patient (CMC) and a healthy control (HC) stimulated with IFN-α ($1x10^3$ IU/ml) with or without TSA (100 ng/ml) for the indicated time periods. GAPDH was used as a loading control.

6.3.3 TSA alters STAT1- and STAT3-induced gene transcription in cells with GOF-STAT1 mutations

I next assessed the effect of TSA on downstream STAT1- and STAT3-induced gene transcription. My results showed that TSA reduced IFN-α, IL-27 and IL-21-induced transcription of STAT1-dependnet genes (CXCL10 and IRF1) in EBV cell lines from CMC patients to levels that were lower than in healthy controls (Fig 6.4). Conversely, in PBMCs from CMC patients, addition of TSA increased low transcription levels of IL-23-activated Th-17 dependent genes (IL-17, IL-22 and marginally RORc) to levels seen in healthy controls (Fig 6.5 A). This was however, not the case for IL-10 gene

transcription (Fig 6.5A). The increased STAT3-dependent gene transcription was also observed in IFN-α-, IL-27- and IL-21-induced c-Fos and SOCS3 gene expression in EBV cells with GOF-STAT1 mutations (Fig 6.5B). However, no obvious difference was seen for IL-10 and c-Myc gene expression (Fig 6.5B).

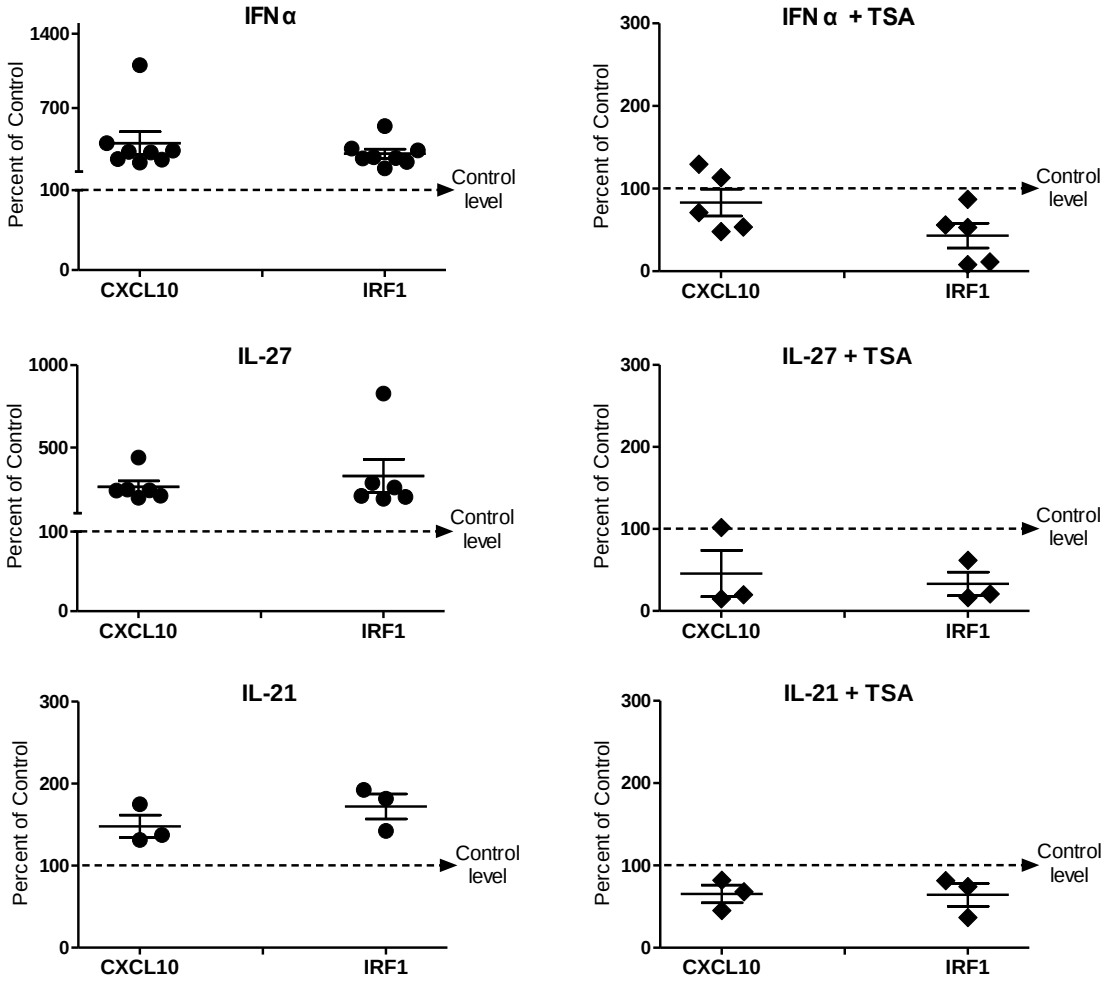

Figure 6.4 TSA decreases STAT1-induced gene transcription in EBV cells with GOF-STAT1 mutations.

Expression of CXCL10 and IRF1 genes in EBV transformed cells was assessed in CMC patients with GOF-STAT1 mutations or healthy controls by qRT-PCR. Cells were stimulated with IFN-α ($1x10^3$ IU/ml), IL-27 or IL-21 (50 ng/ml) with or without TSA (100 ng/ml) for 4 hours. Relative effect of TSA on cytokine-induced STAT1 gene expression in CMC patients is shown as percentage of levels in healthy controls which are presented as 100% (dotted line) (Mean±SEM).

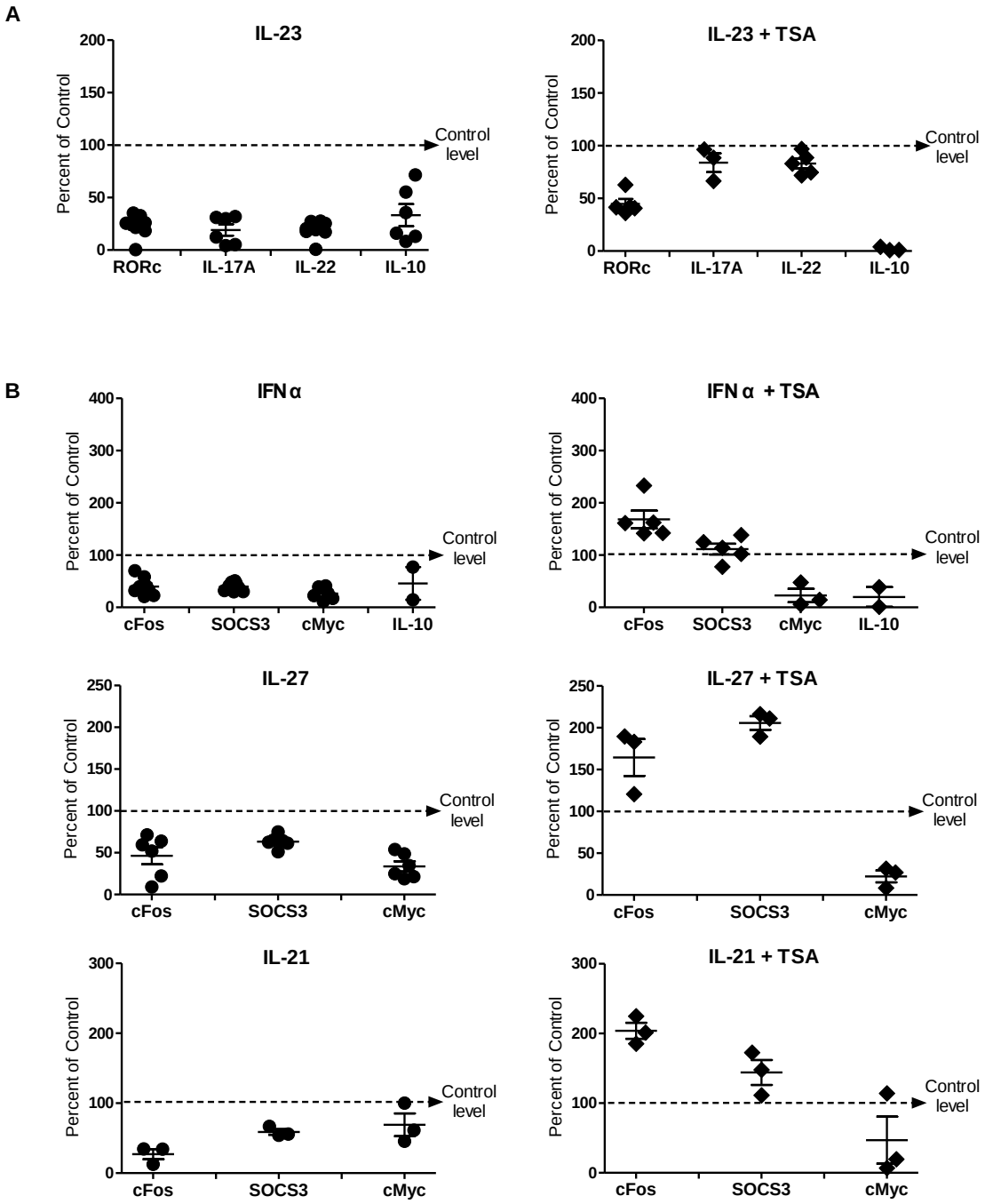

Figure 6.5 TSA increases low STAT3-induced gene transcription in cells with GOF-STAT1 mutations.

Expression of RORc, IL-17, IL-22 and IL-10 genes in PBMCs (A), or c-Fos, SOCS3, c-Myc and IL-10 genes in EBV transformed cells (B) was assessed in CMC patients with GOF-STAT1 mutations or healthy controls by qRT-PCR. Cells were stimulated with IL-23 (100 ng/ml, with PHA and IL-2 pre-treatment), IFN-α ($1x10^3$ IU/ml), IL-27 and IL-21 (50 ng/ml) with or without TSA (100 ng/ml) for 4 hours. Relative effect of TSA on cytokine-induced STAT3 gene expression in CMC patients is shown as percentage of levels in healthy controls which are presented as 100% (dotted line) (Mean±SEM).

6.3.4 TSA increases Candida albicans-induced IL-22 production in cells with GOF-STAT1 mutations

Given that addition of TSA which promotes acetylation in cells with GOF-STAT1 mutations increased low STAT3-induced gene transcription, the next experiments aimed to investigate whether low Th-17 related cytokine production could be restored in CMC patients in the presence of TSA. My results confirmed that *Candida albicans*-induced IL-17 and IL-22 production from CMC patients' cells was barely detectable. Production of IL-17 increased in healthy subjects with addition of TSA but not in CMC patients. Interestingly, production of IL-22 increased in both healthy controls and CMC patients with addition of TSA. In contrast, IL-10 which was produced at comparable levels in healthy controls and CMC patients was reduced upon addition of TSA (Fig 6.6). These findings demonstrated that TSA which promotes acetylation can increase low IL-22 production in cells from CMC patients with GOF-STAT1 mutations.

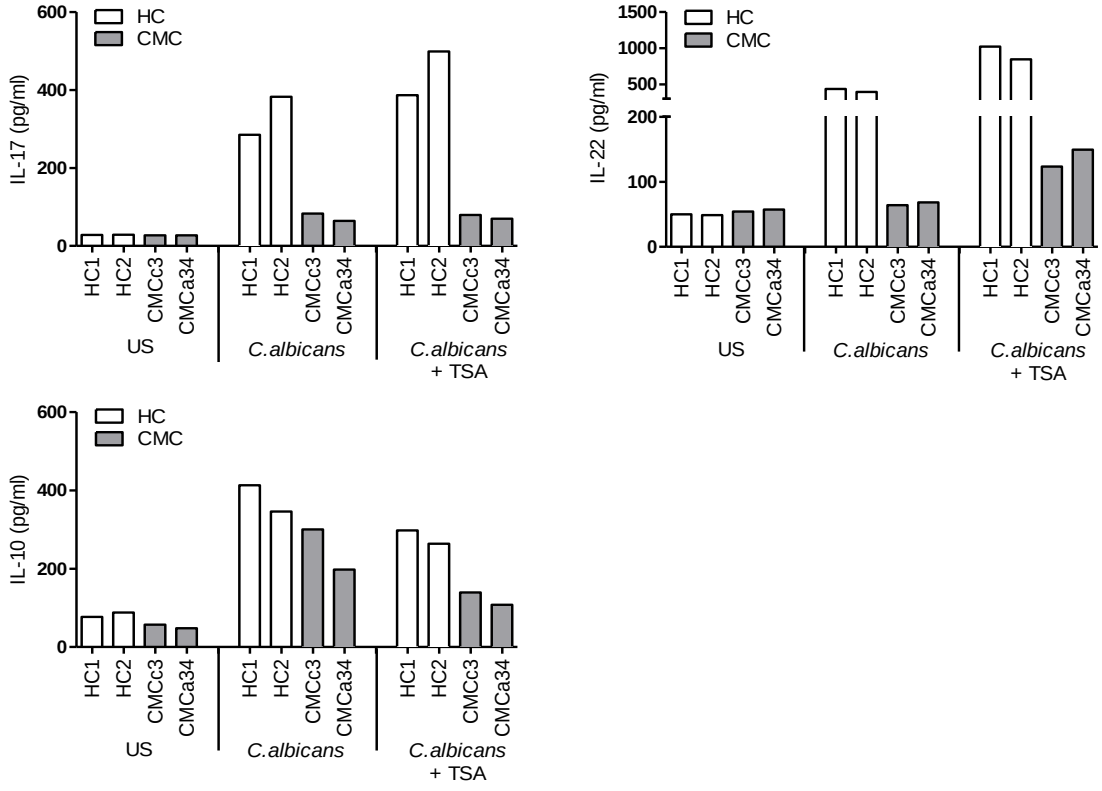

Figure 6.6 Cytokine production of *Candida albicans*-stimulated PBMCs in presence of TSA.

Cytokine production of IL-17, IL-22 and IL-10 in *Candida albicans*-stimulated PBMCs was assessed in 2 CMC patients with GOF-STAT1 mutations (CMC) and 2 healthy controls (HC) by ELISA. Cells were left unstimulated (US) or stimulated with *Candida albicans* (1:15x10^3 dilution) with or without TSA (100 ng/ml) for 5 days. Amphotericin B (2.5 μg/ml) was added at day 0 and day 3 to prevent *Candida albicans* overgrowth.

6.3.5 HDAC1 may be involved in regulating STAT3-induced gene transcription in cells with GOF-STAT1 mutations

Given that TSA, a non-selective HDAC inhibitor, could increase low STAT3-induced gene transcription in cells with GOF-STAT1 mutations, subsequent experiments were carried out to identify which HDACs are involved in modulating STAT3 gene induction. I therefore transfected cells with siRNA targeting HDAC1, HDAC2 and HDAC3 individually or with an irrelevant siRNA (as a negative control) and assessed cytokine-induced STAT3-dependent gene expression. Results showed that silencing HDAC1 increased IL-23-induced RORc, IL-17A and IL-22 gene expression in PBMCs from a healthy control but did not have much effect in CMC patient cells. Silencing HDAC2 had a marginal effect on STAT3-dependent gene expression in patient cells, whilst silencing HDAC3 appeared to have no effect at all (Fig 6.7A). Silencing HDAC1 in EBV transformed cells from two CMC patients' enhanced IFN-α-induced c-Fos and SOCS3 genes transcription (Fig 6.8A). Gene silencing efficiency was confirmed by immunoblotting of total lysates with specific antibodies against HDAC1, HDAC2 and HDAC3 (Figs 6.7B and Fig 6.8B). These results indicate that HDAC1 but not HDAC2 or HDAC3 is likely to be involved in regulating STAT3-induced gene transcription.

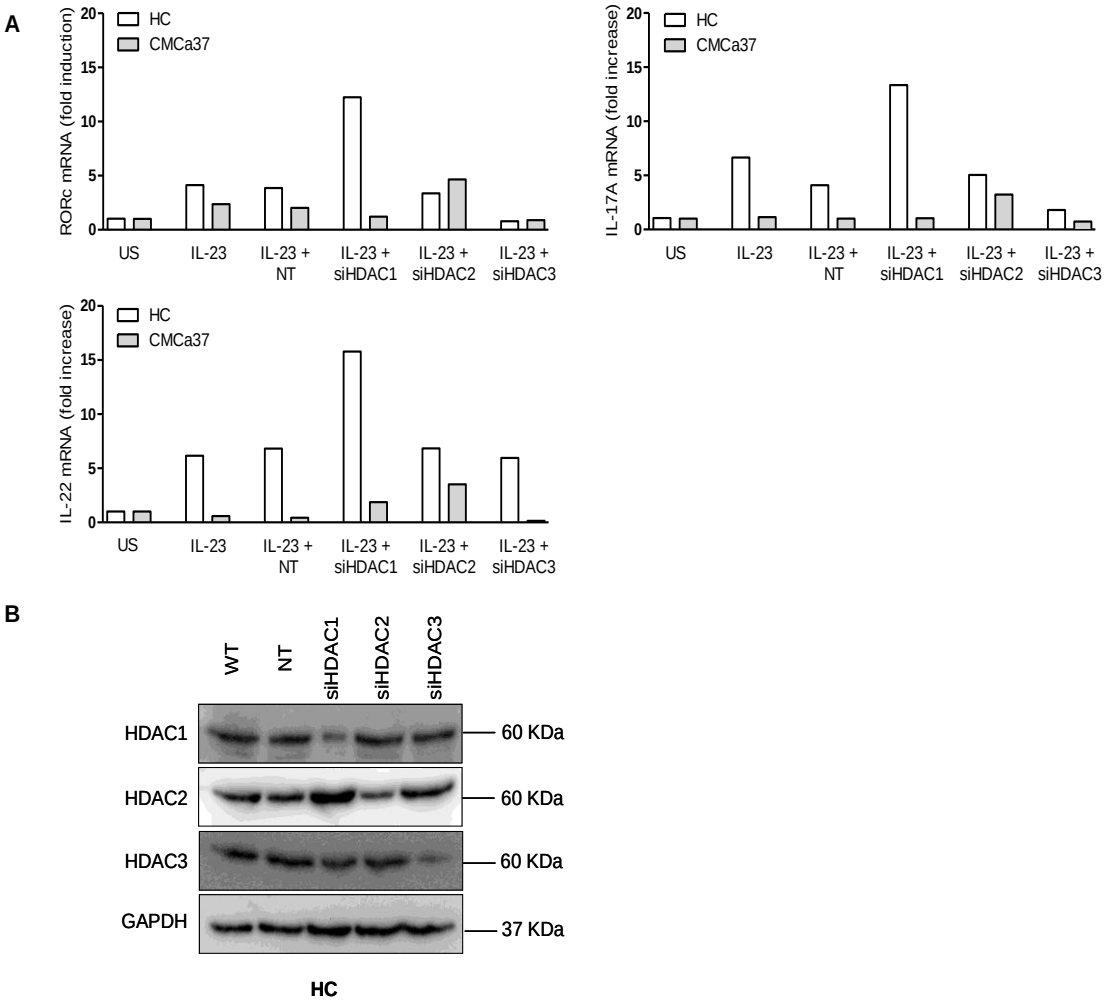

Figure 6.7 HDAC1 but not HDAC2 or HDAC3 regulates STAT3-induced gene transcription in normal PBMCs.

A. Expression of RORc, IL-17A and IL-22 genes was assessed in PBMCs from a CMC patient with GOF-STAT1 mutation and a healthy control by qRT-PCR. Cells were transfected with 1 μM solution of Accell SMARTpool siRNA targeting the HDAC1, HDAC2, HDAC3, and a non-targeting siRNA (NT, negative control) for 72 hours in the presence of PHA (2 μg/ml) and IL-2 (40 IU/ml). After transfection, cells were left unstimulated (US) or stimulated with IL-23 (100 ng/ml) for 4 hours. B. Gene silencing efficiency was assessed by blotting the total cell extracts with anti-HDAC1, anti-HDAC2, anti-HDAC3, and anti-GAPDH antibodies at 96 hours after transfection.

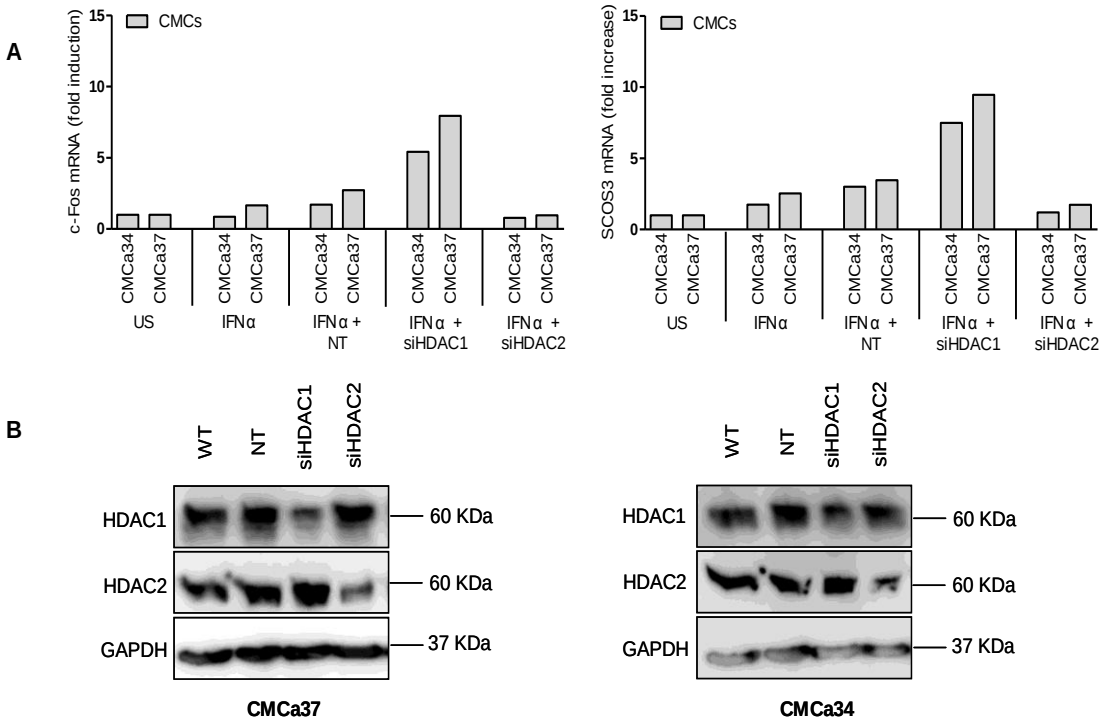

Figure 6.8 HDAC1 but not HDAC2 regulates STAT3-induced gene transcription in EBV cells with GOF-STAT1 mutations.

A. Expression of c-Fos and SOCS3 genes was assessed in EBV transformed cells derived from 2 CMC patients with GOF-STAT1 mutations by qRT-PCR. Cells were transfected with 1 μM solution of Accell SMARTpool siRNA targeting the HDAC1, HDAC2, and a non-targeting siRNA (NT, negative control) for 72 hours. After transfection, cells were left unstimulated (US) or stimulated with IFN-α ($1x10^3$ IU/ml) for 4 hours. B. Gene silencing efficiency was assessed by blotting the total cell extracts with anti-HDAC1, anti-HDAC2, and anti-GAPDH antibodies at 96 hours after transfection.

6.3.6 TSA and fludarabine have a synergistic effect on STAT3-induced gene transcription in cells with GOF-mutations of STAT1

Although restored acetylation can increase low STAT3-induced gene transcription and low IL-22 production, TSA cannot fully restore disrupted STAT3 function in cells with GOF-STAT1 mutations, similar to that observed with fludarabine treatment (chapter 5). I therefore further investigated the combined effect of TSA and fludarabine on STAT3-induced gene transcription in CMC patients. Previous experiments demonstrated significant differences between IL-23-induced STAT3-dependent gene expression in healthy controls and CMC patients with GOF-STAT1 mutations. IL-23 stimulation in the absence or presence of fludarabine or TSA in CMC patients overall showing

reduced STAT3-dependent gene induction relative to healthy subjects, whilst addition of fludarabine or TSA led to a slight increase in gene expression levels. However, when fludarabine and TSA were used together, the effect was far more pronounced, demonstrating the combination of fludarabine and TSA had a synergistic effect on STAT3-induced gene transcription (Figs 6.9 and 6.10).

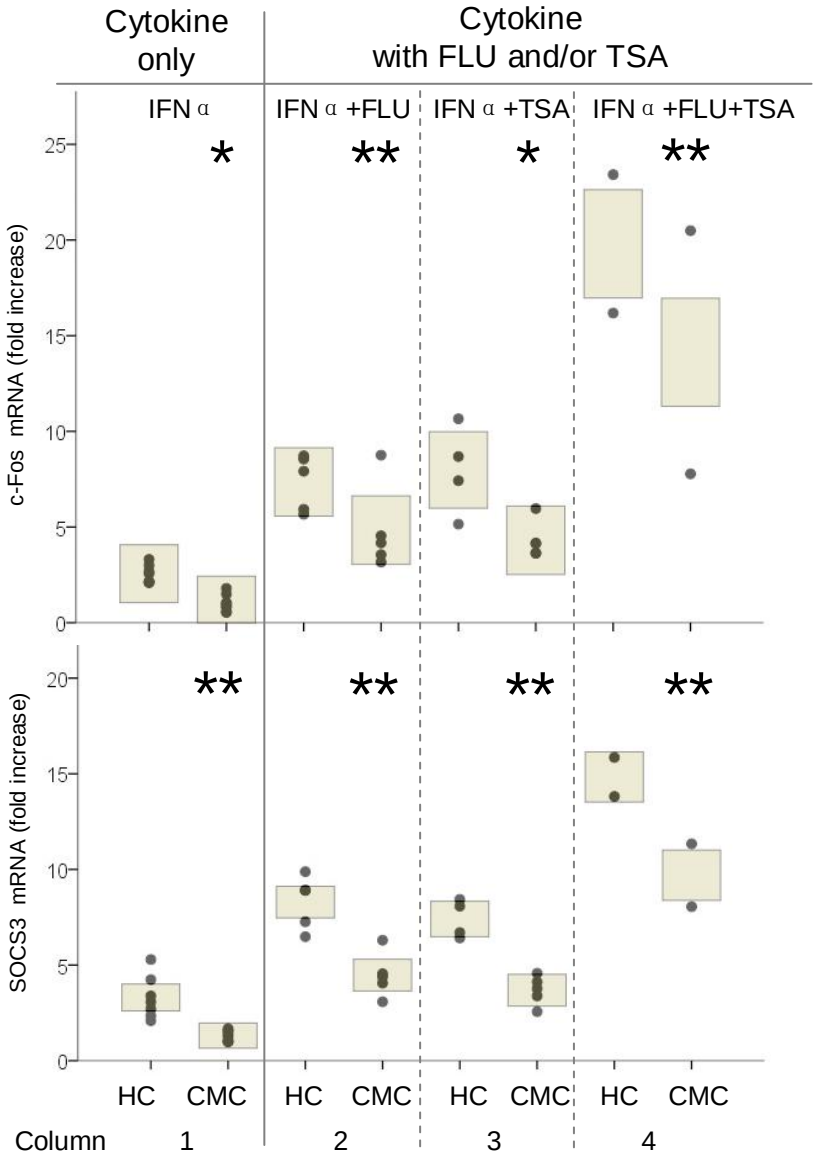

Figure 6.9 Combination of fludarabine and TSA have a synergistic effect on STAT3-induced gene transcription in EBV cell lines.

Expression of c-Fos and SOCS3 genes was assessed in EBV transformed cells derived from GOF-STAT1 mutant cells and controls by qRT-PCR (presented as individual data (plots) with CI value (boxes) using a pooled estimate of the variability). Cells were stimulated with IFN-α ($1x10^3$ IU/ml) in the absence or presence of fludarabine (FLU, 100 μg/ml) and/or TSA (100 ng/ml) for 4 hours. FLU was added 1 hour before cytokine stimulation. Column 1: * $p \leq 0.05$, ** $p \leq 0.01$, CMC vs. HC; Columns 2, 3, 4: * $p \leq 0.05$, ** $p \leq 0.01$, IFN-α vs. FLU/TSA/FLU+TSA in CMC.

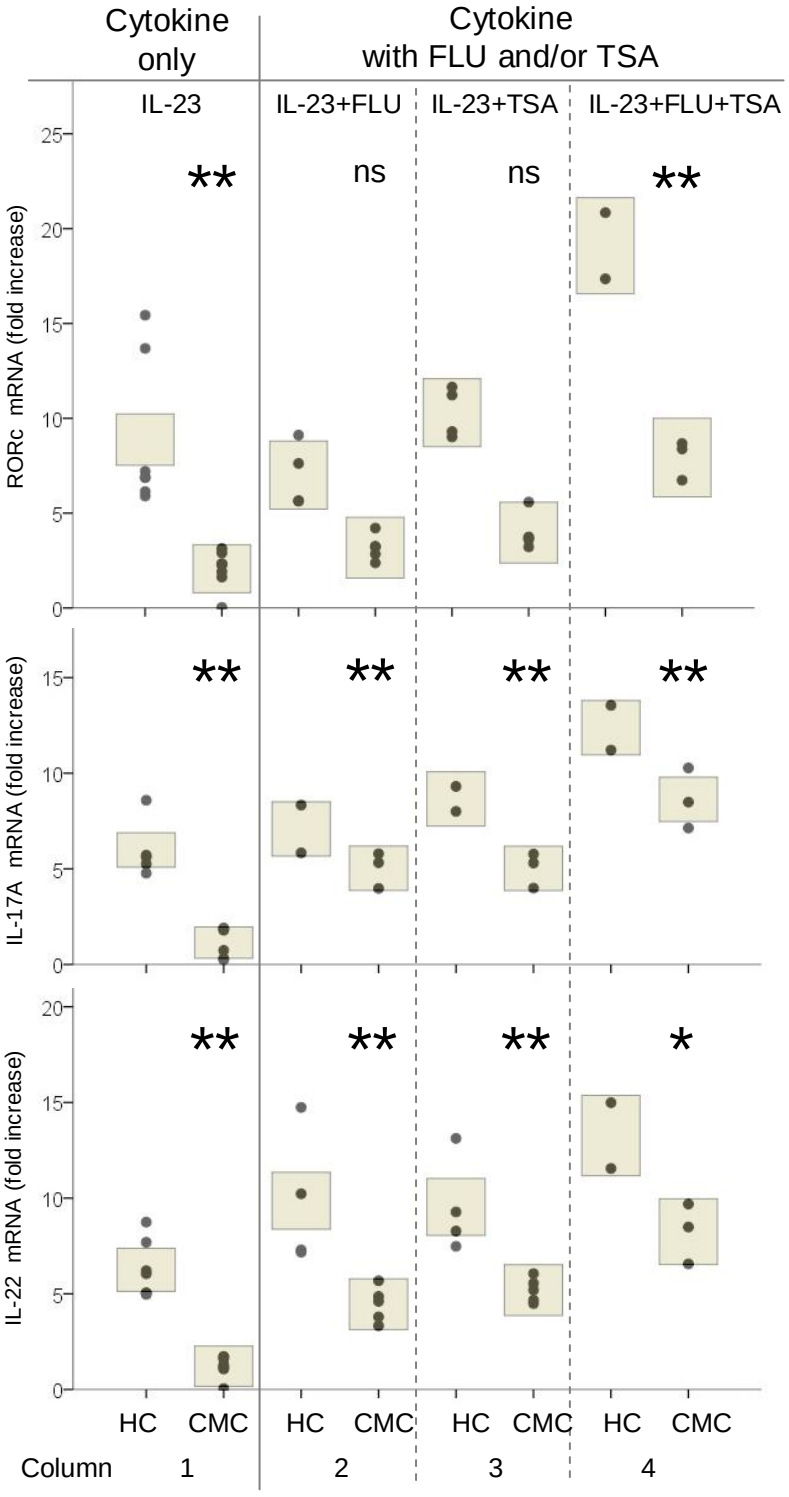

Figure 6.10 Combination of fludarabine and TSA have a synergistic effect on STAT3-induced gene transcription in PBMCs.

Expression of RORc, IL-17, IL-22 and IL-10 genes was assessed in PBMCs from GOF-STAT1 mutant cells and controls by qRT-PCR (presented as individual data (plots) with CI value (boxes) using a pooled estimate of the variability). Cells were stimulated with IL-23 (100 ng/ml) in PHA and IL-2 pre-treated PBMCs with or without Fludarabine (FLU, 100 μg/ml) and/or TSA (100 ng/ml) for 4 hours. FLU was added 1 hour before cytokine stimulation. Column 1: ** $p \leq 0.01$, CMC vs. HC; Columns 2, 3, 4: * $p \leq 0.05$, ** $p \leq 0.01$, IL-23 vs. FLU/TSA/FLU+TSA in CMC; ns=no significant.

6.4 Summary

Recent data strongly implicate epigenetic regulation by acetylation of transcriptional activity of STAT proteins. In the present chapter, I used a non-selective HDAC inhibitor TSA to promote acetylation and investigated its effects on STAT1 and STAT3 activation and function. I found addition of TSA did not alter cytokine (IL-23 and IFN-α)-induced phosphorylation of STAT1 and STAT3 in either healthy subjects or CMC patients. However, TSA was able to normalize the delayed dephosphorylation of STAT1 in cells with GOF-STAT1 mutations. Addition of TSA also decreased the cytokine (IFN-α, IL-27 and IL-21)-induced STAT1-dependent gene (CXCL10 and IRF1) transcription in EBV cells from CMC patients. In contrast, the presence of TSA increased the low levels of Th-17 related gene (IL-17A, IL-22 and marginally RORc) expression in IL-23-stimulated PBMCs as well as other STAT3-dependent gene (c-Fos and SOCS3) in IFN-α-, IL-27- and IL-21-stimulated EBV cells from CMC patients with GOF-STAT1 mutations. Gene silencing of HDAC1 improved STAT3-dependent gene (RORc, IL-17, IL-22, c-Fos and SOCS3) induction in PBMCs or EBV cells either from CMC patients or a healthy subject, suggesting that HDAC1 but not HDAC2 or HDAC3 may be involved in regulating STAT3 gene transcription. More importantly, restoring acetylation by adding TSA could elevate the low levels of the Th-17-related cytokine IL-22 in *Candida albicans*-stimulated PBMCs with GOF-STAT1 mutations. This was not seen for IL-17A production where addition of TSA had no effect in CMC patient cells but boosted IL-17A levels in cells from healthy controls. Interestingly, combining fludarabine and TSA had a synergistic effect on STAT3-induced gene transcription in cells from both CMC patients with GOF-STAT1 mutations and healthy controls, suggesting that inhibition of STAT1 and enhancing acetylation may act through different pathways to regulate STAT3-dependent gene transcription. This effect was not seen in *Candida albicans*-induced cytokine production as fludarabine completely inhibited cytokine production.

The above results demonstrate that the disrupted STAT3 function in cells with GOF-STAT1 mutations could be modified by promoting acetylation, which can restore impaired STAT3 gene transcription and increase the production of IL-22 known to have an important role in fungal immunity.

CHAPTER 7 GENERAL DISCUSSION

CMC is a subtle, non-conventional PID where patients suffer with persistent, recurring infection of the skin, nails and mucosa with the yeast *Candida*. Previous research focused on the 2 largest groups of patients with CMC-those with the APECED and those with isolated AD-CMC. By comparatively studying responses to *Candida* stimulation in these 2 groups, it was found that APECED and AD-CMC patients differed markedly in their ability to produce IL-17 in that IL-17A was normal or increased in APECED patients but markedly reduced in AD-CMC, indicating for the first time that these 2 clinically similar phenotypes have a distinctly different underlying disease mechanisms [75]. Subsequent research of APECED patients elegantly explained the disease-causing mechanism in the context of existing autoantibodies to cytokines IL-17A, IL-17F and IL-22 as well as Type I IFNs [63, 109]. In patients with isolated AD-CMC, GOF-STAT1 mutations were identified until recently. How these mutations lead to low IL-17 production and susceptible to *Candida* infections, however, remains a crucial research question that needs addressing and was the essence of this study.

7.1 GOF-STAT1 mutations enhance STAT1 activation and gene transcription

To date, four types of human mutations in STAT1 have been identified, including (1) AR complete STAT1 deficiency, (2) AR partial STAT1 deficiency, (3) AD STAT1 deficiency, and (4) AD gain of STAT1 activity as shown in Table 7.1 [73]. The two types of AR STAT1 affect the NTD, CCD, SH2 and TS domains of the STAT1 protein. These mutations result in a broad infectious phenotype with susceptibility to mycobacteria and viruses, due to the impairment of IFN-γ-mediated and/or IFN-α/β-mediated immunity [94, 110, 111]. AD STAT1 deficiency affects DBD, SH2 and TS domains of the STAT1 protein and selectively predisposes to mycobacterial disease, due to the impairment of IFN-γ-mediated immunity, since IFN-α/β-mediated immunity is maintained [93, 112-115]. In contrast to these loss-of-function mutations of STAT1, the AD gain of STAT1 which affects the CCD and DBD was identified mainly in the large subgroup of AD-CMC patients with susceptibility to *Candida* infections [67,

71] as well as patients with disseminated dimorphic fungal infections [116] or an IPEX (immunodysregulation polyendocrinopathy enteropathy X-linked syndrome)-like phenotype [117].

Table 7.1 Human STAT1 mutations.

	STAT1 domain affects	Main cellular phenotype	Main clinical phenotype
AR complete STAT1 deficiency	NTD, SH2	No STAT1-dependent response to IFN-γ, IFN-α/β, IFN-λ and IL-27	Lethal intracellular bacteria (mainly mycobacteria) and viral (mainly herpes) diseases
AR partial STAT1 deficiency	NTD, CCD, TS	Impaired STAT1-dependent response to IFN-γ, IFN-α/β, IFN-λ and IL-27	Curable intracellular bacteria (mainly mycobacteria) and viral (mainly herpes) diseases
AD LOF STAT1 deficiency	DBD, SH2, TS	Impaired STAT1-dependent response to IFN-γ and IL-27	Mycobacterial diseases
AD GOF STAT1 disorder	CCD, DBD	Enhanced STAT1-dependent response to IFN-γ, IFN-α/β, IL-27, IL-6 and IL-21. Impaired IL-17 T-cell immunity	CMC, disseminated dimorphic fungal infections and autoimmunity

AR, autosomal recessive; AD, autosomal dominant; LOF, loss-of-function; GOF, gain-of-function; NTD, N-terminal domain; SH2, Src homology 2 domain; CCD, coiled-coil domain; DBD, DNA-binding domain; TS, tail segment domain.

Previous studies have reported the GOF-STAT1 mutations in AD-CMC affected cellular responses to the cytokines including IFN-α/β, IFN-γ and IL-27, which predominantly activate STAT1 signaling [68]. Consistent with this finding, in chapter 3, I showed that cells (PBMCs and EBV transformed cells) with these mutations stimulated with IFN-γ, IFN-α and IL-27, generated reproducibly stronger responses than control cells in terms of STAT1 phosphorylation, hSIE-binding activity, and the induction of target genes (CXCL10 and IRF1). Of note, my results revealed normal IL-21 responses and undetectable IL-6 responses in EBV transformed cells. The lack of response to IL-6 can be explained by the fact that a small proportion of B cells express IL-6 receptors

(IL-6R), which can change dramatically in response to factors such as infection [118]. It is likely that the EBV immortalized B cells used in my study lacked IL-6R as opposed to the transfected STAT1-deficient sarcoma cell lines with GOF-STAT1 mutant alleles used in previous research [68].

Most of these GOF-STAT1 mutations were found in the CCD of STAT1 protein, in a pocket near residues essential for dephosphorylation. My results confirmed that mutations at this site resulted in impaired dephosphorylation of STAT1 as reported previously [68, 74]. I demonstrated this by showing delayed dephosphorylation of STAT1 in IFN-α-stimulated mutant cells or mimicking impaired dephosphorylation with pervanadate in healthy cells. However, the delayed dephosphorylation in AD-CMC patients may be due to the initial hyper-phosphorylation of STAT1, which then requires a longer time to dephosphorylate. I demonstrated that suboptimal stimulation of cells with GOF-STAT1 mutations in the presence of staurosporine resulted in lower levels of initial phosphorylation of STAT1 that allowed dephosphorylation to occur with similar kinetics to normal cells. These results indicated that the initial hyper-phosphorylation and impaired dephosphorylation both contribute to the gain of STAT1 activity caused by these mutations.

7.2 GOF-STAT1 mutations decrease STAT3 gene transcription

Several mutations affecting the STAT3/IL-17 pathway resulting in selective susceptibility to *Candida* infections characteristic of CMC have been reported [97]. As STAT1 and STAT3 negatively regulate one another in most biological progresses, the gain-of-function STAT1 reported in CMC patients may be reducing Th-17 cytokine production by interfering with STAT3 signaling.

In chapter 4, I showed that GOF-STAT1 mutations did not affect STAT3 phosphorylation, nuclear accumulation and DNA-binding to a non-specific STATs consensus binding site element hSIE probe. However, activated STAT3 occupancy at its endogenous target gene promoter was decreased in STAT1 mutant cells. Subsequently, these mutations had a substantial disruption of STAT3 signaling at the gene transcription level, as shown by the markedly decreased gene expression of both Th-17 (RORc, IL-17, IL-22) and non-Th-17 (IL-10, c-Fos, SOCS3) genes. The affected cytokine-induced

gene transcription was demonstrated including a STAT3-selective cytokine IL-23, which has an essential role in differentiation and expansion of Th-17 cells [119], as well as other STAT1 and STAT3 activating cytokines IFN-α, IL-21 and IL-27. The broad defective of STAT3-inducible gene transcription likely underlie decreased IL-17 production and susceptibility to fungal infection in these CMC patients and might also link to the defective dentition and increased incidence of oesophageal and oral cancers seen in CMC patients with GOF-STAT1 mutations.

Two potential mechanisms might explain how STAT1 hyper-activation in CMC patient cells impairs transcription of STAT3-dependent genes: 1) enhanced sequestration of STAT3 by hyper-active STAT1 in poorly functional STAT1/3 heterodimers resulting in reduced formation of transcriptionally active STAT3 homodimers. I showed in semi-quantitative EMSA assays that the STAT3 homodimers and STAT1/3 heterodimers formation was comparable in patient and control cells, suggesting that this may not be the underlying mechanisms involved. However, I was not able to precisely quantify and assess the function of STAT1/3 heterodimers to confirm this; 2) because of the high degree of similarity between STAT3 and STAT1 consensus DNA binding sites, the constitutively activated STAT1 might compete with normal activated STAT3 for DNA binding, thereby preventing STAT3-induced gene transcription. My limited ChIP assay data demonstrated STAT3 occupancy of its endogenous c-Fos promoter was retained but decreased in STAT1 mutant cells, suggesting that hyper-activate STAT1 competing STAT3 DNA-binding may be the underlying mechanisms involved in disruption of STAT3 signaling. However, further work is essential to resolve this issue by using ChIP sequencing and RNA microarrays as the state-of-the-art technologies providing specificity and functional relevance for target gene binding and gene transcription.

The STAT3 Reporter Assay used for determining the transcriptional activity of STAT3 in AD-CMC patients technically did not work due to the difficulties in transfecting EBV cell line. It is recognized that primary lymphocytes and lymphoid tumor cells, as well as cell lines of the lymphoid lineage are difficult to transfect in conventional ways [120]. Reported attempts to transduce B and T lymphocytes using retroviruses [121], diethylaminoethyl dextran, or liposomes [122] have only had limited success. Lentiviral vectors or other approach of cell transfection might be considered to achieve

stable and efficient cell transfection in lymphoid cell lines for future work.

7.3 Inhibition of STAT1 enhances STAT3 gene transcription in CMC

Given that STAT1 hyper-activation is responsible for the low IL-17 production in AD-CMC patients, I addressed the question of whether this could be modified by inhibiting STAT1.

In chapter 5, I demonstrated that fludarabine, a STAT1 inhibitor, led to a selective inhibition of STAT1 activation and STAT1-target gene (CXCL10 and IRF1) transcription without affecting the activation/phosphorylation of STAT3. However, addition of fludarabine did increase low levels of STAT3-dependent gene (RORc, IL-17, IL-22, c-Fos and SOCS3) expression in AD-CMC patient cells. It is likely that abolishing STAT1 activation in CMC patients allows transcriptionally active STAT3 to bind to DNA thus enhancing STAT3 signaling. However, inhibiting STAT1 did not increase transcription of all STAT3 target genes, as there were barely any changes seen with c-Myc and IL-10 gene expression.

Although fludarabine could improve STAT3-dependent gene transcription, it was unable to restore the low levels of *C. albicans*-induced IL-17 or IL-22 production in cells with GOF-STAT1 mutations. Fludarabine is a purine analog, which interferes with DNA synthesis. I showed that fludarabine did not affect cell viability as the doses used in short time cell culture (as is needed for gene expression assessment), however, it indeed cause cell death with long-term culture (as is needed for assessment of cytokine production).

7.4 Modification of acetylation alters STAT3 function in CMC

Although phosphorylation is a crucial post-translational mechanism that regulates the activities of STAT proteins, acetylation is also known to be critical post-transcriptional mechanism regulating transcriptional activities of STAT proteins [84]. Acetylation of histones increases accessibility of nucleosomal DNA to transcription factors and generally leads to elevated gene transcription [123]. The characterization of several HATs, such as the transcription coactivator of p300 and CREB-binding protein (p300/CBP) [124], has provided a potential explanation for the relationship between

histone acetylation and gene transcriptional activities. Conversely, deacetylated histones with HDACs are often associated with transcriptional repression. In addition to histones, other components of the transcription machinery might be acetylated or deacetylated by these enzymes such as STAT proteins themselves and directly affect transcription [125]. Evidence has emerged revealing the role of acetylation in the regulation of STAT1 and STAT3 activities [84].

In chapter 6, I used the HDAC inhibitor TSA to investigate whether STAT3 signaling defects associated with GOF-STAT1 could be corrected by modifying acetylation. My results showed that restoring acetylation with TSA normalized gene transcription levels by decreasing STAT1-induced gene (CXCL10 and IRF1) transcription whilst increasing transcription of STAT3-inducible gene (IL-17, IL-22, c-Fos, SOCS3 and marginally RORc) in cells with GOF-STAT1 mutations. The differentiate regulation of STAT1 and STAT3 transcriptional activity by TSA was not seen with cytokine-induced phosphorylation. These results are consistent with previous reports, in general, acetylation enhances STAT3 signaling whilst negatively regulating STAT1 activity [84]. Although how STAT1 and STAT3 acetylation affects phosphorylation is still a matter of investigation, it has been proposed that acetylation is required for STAT3 dimerization, DNA-binding and gene transcription [126, 127]. Conversely, acetylation impairs STAT1 DNA-binding and transcriptional activity [128, 129]. These observations may provide potential explanations for the opposed regulation of STAT1 and STAT3 gene transcription by TSA in the present study. However, the regulation of STAT gene transcription by acetylation seemed to be gene dependent as IL-10 and c-Myc gene expression was not affected by addition of TSA.

Despite the increased IL-17A gene expression in the presence of TSA, low *C. albicans*-induced IL-17A cytokine production was maintained in AD-CMC patients. The difference in IL-17A gene transcription and cytokine production in the presence of TSA in cells with GOF-STAT1 suggested that the modulation of acetylation involved in STAT signaling is a dynamic and complex process at multiple levels rather than a simple on/off switch and is likely also associated with other post-translational modifications. However, it is might be worth to assess IL-17F gene expression and cytokine production in these AD-CMC patients as the high titers of IL-17F autoantibody

was also detected in APS1 displayed CMC. Importantly, promoting acetylation with TSA in cells of AD-CMC not only increased IL-22 gene expression, but also increased the *C. albicans*-induced IL-22 production. Previous studies have suggested that although IL-17A and IL-22 are structurally and functionally similar Th-17 cell-derived cytokines, IL-22 release is not as strictly limited as IL-17 release [89, 130]. Nevertheless, both of them are essential in fungal immunity. My result indicated that promoting acetylation with HDAC inhibitor increased IL-22 production that could, at least partly, rescue impaired fungal immunity in AD-CMC patients. Class I HDACs (HDAC1, 2 and 3) are known to have a role in STAT1 and STAT3 deacetylation [131]. Gene silencing using HDAC-specific siRNAs confirmed that HDAC1 was involved in modifying STAT3 signaling in this study. This is important because TSA is a broad HDACi, which can affect a range of HDAC members that lacks of specificity. However, whether inhibiting the activity of HDAC1 can eventually rescue low Th-17 cytokine production in AD-CMC patient cells still needs to be addressed in future work.

Interestingly, promoting acetylation had similar and perhaps even stronger effects in healthy controls, suggesting that the altered acetylation may not be the fundamental mechanism that responsible for defective IL-17 immunity in AD-CMC. This issue could be resolved in future work by assessing the acetylation activity of STAT1 and STAT3 in GOF-STAT1 mutant cells. The co-immunoprecipitation assay may provide a better understanding of this issue as it can reveal the interaction between phosphorylation and acetylation of STAT proteins. Nevertheless, promoting acetylation did rescue the defects of STAT3 function caused by these GOF-STAT1 mutations. Indeed, HDAC inhibitors are currently under development for use as anticancer agents [132]. They may also offer new therapeutic approaches for treating CMC patients with GOF-STAT1 mutations.

Although either inhibiting STAT1 with fludarabine or enhancing acetylation with TSA resulted in increased STAT3 transcriptional activity, the synergistic effects of combined TSA and fludarabine on STAT3 gene expression suggested that TSA and fludarabine may act through different pathways to modulate STAT3 signaling.

7.6 Future work

There are a few questions arising from this work that provide a sound basis for further

investigation.

7.6.1 Investigate how GOF-STAT1 mutations alter gene-target DNA-binding for transcription factors STAT1 and STAT3

The defects of STAT3 gene transcription in AD-CMC patients may be due to increased and accumulated phospho-STAT1 in nuclei competing with STAT3 for DNA-binding. Consistent with this, my preliminary data demonstrated the occupancy of STAT3 to its target promoter by ChIP assay was marginally decreased in EBV transformed cells with GOF-STAT1 mutations. However, to further address this issue, ChIP-seq and RNA microarrays should be performed to determine the specificity and functional relevance for STAT1 and STAT3 target-gene binding and transcription. This would provide not only to further understand the fundamental biologic mechanisms underlying impaired fungal immunity in patients with CMC, but also to enhance our knowledge of physiological mechanisms of STAT1/3 interaction and cross-regulate function.

7.6.2 Define the role of STAT protein inhibitors in the regulation of STAT1 and STAT3 activity in GOF-STAT1 mutations

The negative regulation of STAT activity includes the cytoplasmic and/or nuclear proteins families of SOCS [133], PIAS [134] and PTP [81]. The SOCS expressions are inducible by ligands and they inhibit STAT proteins by either suppressing JAKs activity or by competing binding to the docking site at the cytokine receptor, where STATs must bind for their activation. As GOF-STAT1 mutations lead to enhanced STAT1 activation/phosphorylation, it might be worth to investigate the role of SOCS proteins, especially SOCS1 and SOCS3 in CMC patient cells since they can interact directly with phosphorylated STATs through a negative feedback loop. Unlike SOCS proteins, PIAS proteins possess a certain degree of specificity towards STAT members. PIAS1 and PIAS3 bind to and attenuate the transcriptional activity of phosphorylated STAT1 and STAT3 by blocking DNA binding, respectively [81]. Recent study has shown that PIAS1/STAT1 interaction was enhanced in patients with GOF-STAT1 mutations associated with disseminated dimorphic fungal infection [116]. Whether PIAS1/STAT1 and PIAS3/STAT3 interactions play a role in modifying STAT1 and STAT3 signaling

and reducing STAT3-dependent IL-17 production in AD-CMC patients remains to be addressed in future work. In addition, PTPs have been reported to dephosphorylate either JAK and/or STAT proteins. To date, it has been shown that T cell PTP (TC-PTP) and SH2 domain containing PTP-2 (SHP-2) act on STAT1/STAT5 [135] and STAT1/STAT3 [136], respectively. However, how PTPs responsible for the impaired dephosphorylation of STAT1 caused by mutant STAT1 alleles and whether they have any effects on normal phosphorylated STAT3 in AD-CMC patient cells have not yet been identified.

7.6.3 Determine the effects of GOF-STAT1 mutations on post-translational modifications of STAT1 and STAT3

Although, promoting acetylation restored the low IL-17 gene transcription activity in GOF-STAT1 mutant cells, *Candida albicans*-induced IL-17 production was barely seen any changes. These suggested that post-translational modifications of STAT proteins are regulated by far more than phosphorylation and acetylation. Indeed, methylation, ubiquitination, SUMOylation, ISGylation and protein-protein interaction, have all been described to affect the activities of STATs. Previous research has implicated that STAT3 is reversibly dimethylated by histone-modifying enzymes only when it is part of a promoter-bound complex and this modification affects only subsets of STAT3-activated genes [137]. Moreover, a recent report showed the methylation status of STAT1 is hypo-methylated in cells with GOF-STAT1 mutations [116], but the methylation status of STAT3 and its effect on the subsequent gene transcription are not known. Therefore, how the altered methylation status of STAT1 and/or STAT3 contributes to the impaired STAT3 gene transcription and low IL-17 production in cells with GOF-STAT1 mutations needs to be addressed in the future work.

7.6.4 Confirm the mutation-causing mechanisms of CMC

All the results I have presented in this thesis could provide the potential explanations for why GOF-mutations of STAT1 lead to low Th-17 cytokine production and susceptible to fungal infections in CMC. However, to further confirm the mutation-causing mechanisms in these CMC patients, the human U3A STAT1-deficient sarcoma cell lines

need to be used in future work by transfection with either wild type STAT1 allele or GOF-STAT1 mutant alleles that identified in CMC patients.

7.7 Conclusion

Remarkably, profoundly different effects have been identified with respective mutations affecting the same human STAT1 gene, resulting in different infectious diseases through different molecular and cellular mechanisms. Unlike the LOF mutations, which are associated with a predisposition to viral and/or mycobacterial disease, mutations affecting the coiled-coil and DNA-binding domains of STAT1 lead to a gain-of-function and susceptibility to fungal infections. Enhanced initial phosphorylation and impaired dephosphorylation of STAT1 appear to account for its gain-of-function. These GOF-STAT1 mutations have a broad defect on STAT3 gene transcription, which is likely responsible for the decreased Th-17 (IL-17A and IL-22) cytokine production and impaired fungal immunity in AD-CMC patients. The impaired transcriptional activity of STAT3 can be rescued by promoting acetylation and/or inhibiting STAT1 activation through different regulatory mechanisms. Full elucidation of my finding is likely to offer new therapeutic approaches for treating CMC patients with GOF-STAT1 mutations.

Appendix

Table 8.1 Summary of the clinical and genetic data for the patients.

Patients	Gender	Origin	Age at study	Clinical feature of CMC	Autoimmunity	Genotype
Family # 1						
CMCa48	F	UK	58	Nails, Skin, Scalp	None	A267V
CMCa34	M	UK	33	Nails, Skin, Scalp	None	A267V
CMCa37	F	UK	25	Nails, Skin, Scalp	None	A267V
CMCa38	M	UK	26	Nails, Skin, Scalp	None	A267V
CMCc3	F	UK	7	Skin	None	A267V
Family # 2						
CMCa39	F	UK	41	Nails, Oral cavity, Genital mucosa	None	A267V
CMCa42	M	UK	32	Nails, Oral cavity	None	A267V
CMCc43	M	UK	7	Oral cavity	None	A267V
Family # 3						
CMCa32	F	UK	40	Nails, Skin, Scalp, Oral cavity, Oesophagus, Gastro tract, Genital mucosa	None	R274W
CMCc7	F	UK	11	Skin, Oral cavity, Genital mucosa	Thyroid autoimmunity	R274W
CMCc6	M	UK	13	Oral cavity	Thyroid autoimmunity	R274W
Family #4						
CMCc16	M	UK	2	Nails, Skin, Oral cavity	None	R274W
CMCa17	F	UK	19	Nails, Skin, Oral cavity, Genital mucosa	None	R274W
CMCa29	F	UK	47	Nails, Skin, Oral cavity	None	R274W

Family #5							
CMCa31	M	UK	55	Nails, cavity	Oral	None	T288I

Table 8.2 Cell culture reagents and medium used for the research.

Reagent/medium	**Company**	**Catalogue No.**
Phosphate Buffered Saline (PBS)	Lonza	BE10-543F
Hanks Buffered Saline Solution (HBSS)	Lonza	BE17-512F
RPMI 1640 medium	Sigma	R0883
Iscove's Modified Dulbecco's Medium (IMDM)	Sigma	I3390
Dulbecco's Modified Eagle's Medium (DMEM)	Gibco	41965-039
Fetal Calf Serum (FCS)	Lonza	14401F1
KnockOut™ Serum Replacement	Gibco	10828-028
Lymphoprep	Axis-Shield Diag	NYC1114547
200 mM L-glutamine Solution	Sigma	G6392
10x Penicillin-Streptomycin Solution (10^4 units per ml penicillin, 10 mg/ml streptomycin)	Sigma	P0781
Phytohemagglutinin (PHA)	Sigma	L1668
Amphotericin B	Sigma	A2942
RosetteSep® Human $CD4^+$ T Cells Enrichment cocktail	StemCell Tech	15062
CellTiter 96® AQueous Non-Radioactive Cell Proliferation Assay	Promega	G5421
Opti-MEM® I Reduced Serum Medium	Invitrogen	31985-062
Accell siRNA Delivery Media	Thermo Scientific	B-005000
Accell 5x siRNA Buffer	Thermo Scientific	B-002000-UB-100
Attractene Transfection Reagent	Qiagen	1051561

Table 8.3 Chemical and biochemical reagents used for the research.

Chemical/reagent	Company	Catalogue No.
Trichostatin A (TSA)	Sigma	T8552
Sodium Orthovanadate	Sigma	S6508
Fludarabine (Fludara)	Selleckchem	S1491
Staurosporine	Calbiochem	569397
Sandimmune® / Cyclosporine	Sandoz	478967
Yeast Nitrogen Base (YNB)	BD	239210
D-Glucose	Sigma	G8270
CelLytic™ M	Sigma	C2978
Halt™ Phosphatase Inhibitor Cocktail	Thermo Scientific	78420
Complete Protease Inhibitor Mini Tablet	Roche Diagnostics	11836153001
NE-PER Nuclear and Cytoplasmic Extraction Kit	Thermo Scientific	78833
Bradford Ultra™	Expedeon	BFU1L
Albumin from Bovine Serum (BSA)	Sigma	A7030
Bovine Serum Albumin (BSA) Standards	Thermo Scientific	23209
40% Acrylamide/Bis-acrylamide 37.5:1	NBS Biologicals	NBS-3600-05
Ammonium Persulphate (APS)	Sigma	A3678
N,N,N',N'-Tetramethylethylenediamine (TEMED)	Sigma	T22500
Bromophenol Blue	Sigma	B1026
2-Mercaptoethanol	Sigma	M3148
PageRuler Prestained Protein Ladder 10-170kDa	Thermo Scientific	26616
Amersham ECL Detection Reagents	GE Healthcare	RPN2105
Immobilon Western Chemiluminescent HRP Substrate	Millipore	WBKLS0500
iBlot® Transfer Stack, PVDF Regular package	Invitrogen	IB4010-01
Odyssey Infrared EMSA Kit	LiCor Biosciences	829-07910
DL-Dithiothreitol (DTT)	Sigma	43816
Water (DNase, RNase, Protease, free)	Sigma	W4502

BD™ Phosflow Lyse/Fix Buffer (x5)	BD	558049
BD™ Phosflow Perm Buffer III	BD	558050
TransAM STAT3 Kit (human)	Active Motif	45196
TRI® Reagent	Sigma	93289
Superscript II Reverse Transcriptase	Invitrogen	18064022
dNTP Mix	Bioline	BIO-39028
$pd(N)_6$ Random Hexamer 5'-Phophate, Sodium Salt	GE Healthcare	27-2166-01
TaqMan® Gene Expression Master Mix	Life Technologies	4369016
Cignal STAT3 Reporter (luc) Assay Kit	Qiagen	CCS-9028L
Protease Inhibitor Cocktail II	Millipore	539132
Formaldehyde	Sigma	F8775
Glycine	Sigma	G8898
Zysorbin (Staph A membranes)	Invitrogen	10-1051-1
Proteinase K	Sigma	P2308
QIAEX II Gel Extraction Kit	Qiagen	20021
SYBR® Green JumpStart™ *Taq* ReadyMix™	Sigma	S4438
Human IL-17A (homodimer) ELISA Kit	eBioscience	88-7176-22
Human IL-22 ELISA Kit	eBioscience	88-7522-22
O-Phenylenediamine Dihydrochloride (OPD)	Sigma	P4664
ExtrAvidin®-Peroxidase	Sigma	E2886

Table 8.4 Antibodies used for the research.

Protein	Company	Species	Catalogue No.	Dilution	Dilution
STAT3 (79D7)	Cell Signaling	Rabbit	4904	1:2000	WB
Phospho-STAT3 (Tyr705) (D3A7)^{XP}	Cell Signaling	Rabbit	9145	1:1000	WB
Phospho-STAT3 (Ser727)	Cell Signaling	Rabbit	9134	1:1000	WB
STAT1	Cell Signaling	Rabbit	9172	1:1000	WB
Phospho-STAT1 (Tyr701)	Cell Signaling	Rabbit	9171	1:1000	WB
Phospho-STAT1 (Ser727)	Cell Signaling	Rabbit	9177	1:1000	WB
GAPDH (D16H11)^{XP}	Cell Signaling	Rabbit	4134	1:1000	WB
Histone H3 (D1H2)^{XP}	Cell Signaling	Rabbit	4499	1:1000	WB
Lamin A/C	Cell Signaling	Rabbit	2032	1:1000	WB
Immunoglobulin HRP	Dako	Rabbit	P0448	1:2000	WB
HDAC1	Abcam	Rabbit	ab7028	1:1000	WB
HDAC2	Abcam	Rabbit	ab16032	1:1000	WB
HDAC3	Abcam	Rabbit	Ab16047	1:1000	WB
STAT3 (C-20)	Santa-cruz	Rabbit	sc-482	1:1	EMSA/ChIP
STAT1 (E-23)	Santa-cruz	Rabbit	sc-346	1:1	EMSA
Negative ChIP antibody (IgG)	Millipore	Rabbit	PP64B	1:1	ChIP
Alexa Fluor® 647 STAT1 (pY701)	BD Biosciences	Mouse	51-9006596	1:10	Flow Cytometry
Human IL-10 (Capture)	BD Biosciences	Rat	554705	1:1000	ELISA
Human IL-10 (Detection)	BD Biosciences	Rat	554499	1:500	ELISA

Table 8.5 Cytokines used for the research.

Cytokine	Company	Catalogue No.
Recombinant human IL-6	R&D Systems	206-IL
Recombinant human IL-23	R&D Systems	1290-IL
Recombinant human IFN-γ	R&D Systems	285-IF
Recombinant human IL-27	R&D Systems	2526-IL
Recombinant human IL-12	R&D Systems	219-IL
Human IL-21	Cell Signaling	8920
Human IL-2 (Proleukin)	Novartis	n/a
Human IFN-α (IntronA Interferon alfa-2b)	Merck Sharp & Dohme	n/a
Human IL-17A Recombinant protein (1 μg/ml) (ELISA standard)	eBioscience	39-8179-60
Human IL-22 Recombinant protein (1 μg/ml) (ELISA standard)	eBioscience	39-8229-60
Human IL-10 Recombinant protein (100μg/ml) (ELISA standard)	BD Biosciences	554611

Table 8.6 The sequences of STAT probes and competitor oligonucleotides used in the EMSA experiments.

Probe/Competitor	Sequence (5'-3')
hSIE:	5'-GTCGACATTTCCCGTAAATC -3' 5'-GATTTACGGGAAATGTCGAC-3'
IL-17	5'-GTCGACATTTCCGGAAATC-3' 5'-GATTTCCGGAAATGTCGAC-3'
GAS	5'-ATGTATTTCCCAGAAA-3' 5'-TTTCTGGGAAATACAT-3'
ISRE	5'-GATCGGGAAAGGGAAACCGAAACTGAA-3' 5'-TTCAGTTTCGGTTTCCCTTTCCCGATC-3'
STAT3	5'-GATCCTTCTGGGAATTCCTAGATC-3' 5'-GATCTAGGAATTCCCAGAAGGATC-3'

The labeled oligonucleotides were purchased from Eurofins with 5'-DY682 modification, the unlabeled oligonucleotides, as refer to competitors were purchased from Sigma.

Table 8.7 Primers used for TaqMan Real Time PCR gene expression assay.

Gene	Primers
RORc	Applied Biosystems: Assay Number: Hs01076122_m1
IL-22	Applied Biosystems: Assay Number: Hs01574154_m1
IL-17A	Applied Biosystems: Assay Number: Hs00174383_m1
IL-10	Applied Biosystems: Assay Number: Hs00961622_m1
c-Fos	Applied Biosystems: Assay Number: Hs00170630_ml
c-Myc	Applied Biosystems: Assay Number: Hs00153408_m1
SOCS3	Applied Biosystems: Assay Number: Hs02330328_s1
T-bet	Applied Biosystems: Assay Number:Hs00203436_m1
CXCL10	Applied Biosystems: Assay Number:Hs01124251_g1
IRF1	Applied Biosystems: Assay Number:Hs00971960_m1
18S	F 5'-CGAATGGCTCATTAAATCAGTTATGG-3' R 5'-TATTAGCTCTAGAATTACCACAGTTATCC-3' Probe 5'-FAM-TCCTTTGGTCGCTCGCTCCTCTCCC-TAMRA-3'

Table 8.8 siRNA used for gene silencing studies.

siRNA Target Gene	Catalogue Number (Dharmacon)
Accell Non-Targeting siRNA Pool	D-001910-10
SMARTpool Accell HDAC1	E-003493-00-0005
SMARTpool Accell HDAC2	E-003495-00-0005
SMARTpool Accell HDAC3	E-003496-00-0005

Table 8.9 Buffers used for Western blotting.

Buffer alias	Components
Whole Cell Lysis Buffer	10 ml CelLytic M, 100 µl of 100x Halt Phosphatase Inhibitor Cocktail, 1 Complete Protease Inhibitor Mini Tablet
Low Gel Buffer (LGB)	1.5 M Tris, pH 8.8, 0.4% (w/v) SDS
Upper Gel Buffer (UGB)	0.5 M Tris, pH 6.8, 0.4% (w/v) SDS
Stacking Gel Buffer (SGB)	40% Acry/Bis diluted to 4.5% with dH_2O and 4x UGB
10% Acrylamide Gel	1.5 ml 40% Acry/Bis, 1.5 ml 4x LGB, 3 ml dH_2O, 30 µl 20% APS, 10 µl TEMED
Stacking Gel	2.5 ml SGB, 15 µl 20% APS, 5 µl TEMED
Sample Buffer x5	10 ml 10x UGB, 1 g SDS, 8 ml Glycerol, 1.5 ml Bromophenol blue (0.5% made up in EtOH), prior to sample add 200 µl 2-mercaptoethanol into 1 ml aliquots
Running Buffer	250 mM Tris, 2 M Glycine, 10% (w/v) SDS
Tris-Buffered Saline-Tween (TBS/T)	10 mM Tris-HCl, pH 7.4, 0.15 M NaCl and 0.2% (v/v) Tween-20

Table 8.10 Buffers used for EMSA.

Buffer alias	Components
Hypotonic Buffer	10 mM HEPES, pH7.6, 1.5 mM $MgCl_2$, 10 mM KCl, 1 mM DTT, 10 mM NaF, 1 mM Na_3VO_4, 0.1% Nonidet P-40 alternative (v/v), 1 Complete protease inhibitor Mini Tablet per 50 ml
High Salt Buffer	20 mM HEPES, pH7.9, 420 mM NaCl, 20% Glycerol (v/v), 1 mM DTT, 10 mM NaF, 1 mM Na_3VO_4, 1 Complete protease inhibitor Mini Tablet per 50 ml
Annealing Buffer	10 mM Tris, pH 7.5-8.0, 50 mM NaCl, 1 mM EDTA
Tris/Borate/EDTA (TBE) x5	0.445 M Tris-base, 0.445 M Boric acid, 0.01 M EDTA
Running Buffer (0.5xTBE)	44.5 mM Tris-base, 44.5 mM Boric acid, 1 mM EDTA
Non-denaturing Polyacrylamide gel (5%)	2.6 ml 5x TBE, 3.2 ml 40 % Acry/Bis, 19.1 ml dH_2O, 88 µl 20% APS, 25 µl TEMED
STAT Protein Optimal Binding Reaction	1x Binding Buffer, 1 mM DTT, 1 mM EDTA, 50 mM Tris-HCl pH8.0, 210 mM NaCl, 10% glycerol, 1 µg Poly (dI-dC), 0.5 µg Salmon Sperm, 1 pmol labelled probe and 10 µg nuclear extract

Table 8.11 Buffers used for ChIP assay.

Buffer alias	Components
SDS Lysis Buffer	1% (w/v) SDS, 10 mM EDTA, 50 mM Tris pH8.1
Dilution Buffer	1.1% (v/v) Triton, 1.2 mM EDTA, 16.7 mM Tris-HCl pH8.1, 167 mM NaCl
Low Salt Buffer	1% (v/v) Triton, 2 mM EDTA, 20 mM Tris-HCl pH8.1, 150 mM NaCl
High Salt Buffer	1% (v/v) Triton, 2 mM EDTA, 20 mM Tris-HCl pH8.1, 500 mM NaCl
LiCl Wash Buffer	0.25 mM LiCl, 1% (v/v) NP40, 1 mM EDTA, 10 mM Tris-HCl pH8.1
Elution Buffer	0.084g $NaHCO_3$ in 9 ml water
TE Buffer	10 mM Tris-HCl pH8.1, 1 mM EDTA

All buffers (except elution and TE buffer) were added protease inhibitors (Millipore) before using at final concentration of 4 μl/ml.

Table 8.12 Buffers used for ELISA.

Buffer alias	Components
Coating Buffer	15 mM Na_2HPO_4, 20 mM $NaH_2PO_4.H_2O$
Wash Buffer	PBS pH7.2, 0.1% (v/v) Tween-20
Blocking Buffer	PBS pH7.2, 1% (w/v) BSA
Diluent Buffer	PBS pH7.2, 1% (w/v) BSA, 0.1% (v/v) Tween-20
Citrate Phosphate Buffer	25 mM Citric acid, 50 mM Na_2HPO_4, 20 mM $Na_2HPO_4.2H_2O$
Substrate	1 tablet OPD, 13 ml Citrate Phosphate Buffer, 6 μl H_2O_2

Table 8.13 Presentations generated from this study.

Conference	Title	Date	Venue
Oral presentation			
North East Postgraduate Conference	Gain-of-function STAT1 mutation decreases STAT3-inducible gene transcription in patients with Chronic Mucocutaneous Candidiasis	October 2013	Newcastle University, UK
British Society for Medical Mycology	Decreased STAT3-inducible gene transcription in patients with gain-of-function STAT1 mutations	April 2013	Newcastle, UK
North East Postgraduate Conference	Gain-of-function STAT1 mutations alter STAT3 activation	October 2012	Newcastle University, UK
Poster presentation			
British Society for Immunology Congress	Gain-of-function STAT1 mutation decreases STAT3-inducible gene transcription in patients with Chronic Mucocutaneous Candidiasis	December 2013	Liverpool, UK
British Society for Immunology Summer School	Decreased STAT3-inducible gene transcription in patients with gain-of-function STAT1 mutations	August 2013	Newcastle University, UK
Institute of Cellular Medicine Research Day	Decreased STAT3-inducible gene transcription in patients with gain-of-function STAT1 mutations	June 2013	Newcastle University, UK
15th Biennial Meeting of the European Society of Immunodeficiencies	Gain-of-function STAT1 mutations alter STAT3 activation	October 2012	Florence, Italy
Institute of Cellular Medicine Research Day	Gain-of-function STAT1 mutations alter STAT3 activation	June 2012	Newcastle University, UK
British Society for Immunology Congress	Effect of cytokine-induced STAT1 signaling on STAT3 activation and binding	December 2011	Liverpool, UK
North East Postgraduate Conference	Effect of cytokine-induced STAT1 signaling on STAT3 activation and binding	October 2011	Newcastle University, UK

REFERENCE

1. Lilic D and Haynes K, *Candida*. Immunology of Fungal Infections, ed. Brown GD and Netea MG. 2007: Springer. 361-382.
2. Perfect JR, *The impact of the host on fungal infections.* Am J Med, 2012. **125**(1 Suppl): p. S39-51.
3. Chapel H, *Classification of primary immunodeficiency diseases by the International Union of Immunological Societies (IUIS) Expert Committee on Primary Immunodeficiency 2011.* Clin Exp Immunol, 2012. **168**(1): p. 58-9.
4. Antachopoulos C, Walsh TJ, and Roilides E, *Fungal infections in primary immunodeficiencies.* Eur J Pediatr, 2007. **166**(11): p. 1099-117.
5. Vinh DC, *Insights into human antifungal immunity from primary immunodeficiencies.* Lancet Infect Dis, 2011. **11**(10): p. 780-92.
6. de Repentigny L, Lewandowski D, and Jolicoeur P, *Immunopathogenesis of oropharyngeal candidiasis in human immunodeficiency virus infection.* Clin Microbiol Rev, 2004. **17**(4): p. 729-59, table of contents.
7. Ramos ESM, Lima CM, Schechtman RC, et al., *Superficial mycoses in immunodepressed patients (AIDS).* Clin Dermatol, 2010. **28**(2): p. 217-25.
8. Grubb SE, Murdoch C, Sudbery PE, et al., *Candida albicans-endothelial cell interactions: a key step in the pathogenesis of systemic candidiasis.* Infect Immun, 2008. **76**(10): p. 4370-7.
9. Kirkpatrick CH, *Chronic mucocutaneous candidiasis.* Pediatr Infect Dis J, 2001. **20**(2): p. 197-206.
10. Lilic D, *New perspectives on the immunology of chronic mucocutaneous candidiasis.* Curr Opin Infect Dis, 2002. **15**(2): p. 143-7.
11. Casanova JL, Fieschi C, Bustamante J, et al., *From idiopathic infectious diseases to novel primary immunodeficiencies.* J Allergy Clin Immunol, 2005. **116**(2): p. 426-30.
12. Blanco JL and Garcia ME, *Immune response to fungal infections.* Vet Immunol Immunopathol, 2008. **125**(1-2): p. 47-70.

13. Huppler AR, Bishu S, and Gaffen SL, *Mucocutaneous candidiasis: the IL-17 pathway and implications for targeted immunotherapy.* Arthritis Res Ther, 2012. **14**(4): p. 217.
14. Janeway CA, Jr. and Medzhitov R, *Innate immune recognition.* Annu Rev Immunol, 2002. **20**: p. 197-216.
15. Netea MG, Brown GD, Kullberg BJ, et al., *An integrated model of the recognition of Candida albicans by the innate immune system.* Nat Rev Microbiol, 2008. **6**(1): p. 67-78.
16. Medzhitov R, *Recognition of microorganisms and activation of the immune response.* Nature, 2007. **449**(7164): p. 819-26.
17. Akira S, Uematsu S, and Takeuchi O, *Pathogen recognition and innate immunity.* Cell, 2006. **124**(4): p. 783-801.
18. Netea MG and Marodi L, *Innate immune mechanisms for recognition and uptake of Candida species.* Trends Immunol, 2010. **31**(9): p. 346-53.
19. Beutler BA, *TLRs and innate immunity.* Blood, 2009. **113**(7): p. 1399-407.
20. Wang JE, Warris A, Ellingsen EA, et al., *Involvement of CD14 and toll-like receptors in activation of human monocytes by Aspergillus fumigatus hyphae.* Infect Immun, 2001. **69**(4): p. 2402-6.
21. Villamon E, Gozalbo D, Roig P, et al., *Toll-like receptor 2 is dispensable for acquired host immune resistance to Candida albicans in a murine model of disseminated candidiasis.* Microbes Infect, 2004. **6**(6): p. 542-8.
22. Netea MG, Van der Graaf C, Van der Meer JW, et al., *Recognition of fungal pathogens by Toll-like receptors.* Eur J Clin Microbiol Infect Dis, 2004. **23**(9): p. 672-6.
23. Netea MG, Van Der Graaf CA, Vonk AG, et al., *The role of toll-like receptor (TLR) 2 and TLR4 in the host defense against disseminated candidiasis.* J Infect Dis, 2002. **185**(10): p. 1483-9.
24. Jouault T, Ibata-Ombetta S, Takeuchi O, et al., *Candida albicans phospholipomannan is sensed through toll-like receptors.* J Infect Dis, 2003. **188**(1): p. 165-72.
25. Netea MG, Gow NA, Munro CA, et al., *Immune sensing of Candida albicans*

requires cooperative recognition of mannans and glucans by lectin and Toll-like receptors. J Clin Invest, 2006. **116**(6): p. 1642-50.

26. Miyazato A, Nakamura K, Yamamoto N, et al., *Toll-like receptor 9-dependent activation of myeloid dendritic cells by Deoxynucleic acids from Candida albicans.* Infect Immun, 2009. **77**(7): p. 3056-64.
27. Netea MG, van de Veerdonk F, Verschueren I, et al., *Role of TLR1 and TLR6 in the host defense against disseminated candidiasis.* FEMS Immunol Med Microbiol, 2008. **52**(1): p. 118-23.
28. Geijtenbeek TB and Gringhuis SI, *Signalling through C-type lectin receptors: shaping immune responses.* Nat Rev Immunol, 2009. **9**(7): p. 465-79.
29. Ferwerda B, Ferwerda G, Plantinga TS, et al., *Human dectin-1 deficiency and mucocutaneous fungal infections.* N Engl J Med, 2009. **361**(18): p. 1760-7.
30. Glocker EO, Hennigs A, Nabavi M, et al., *A homozygous CARD9 mutation in a family with susceptibility to fungal infections.* N Engl J Med, 2009. **361**(18): p. 1727-35.
31. Robinson MJ, Osorio F, Rosas M, et al., *Dectin-2 is a Syk-coupled pattern recognition receptor crucial for Th17 responses to fungal infection.* J Exp Med, 2009. **206**(9): p. 2037-51.
32. Goodridge HS and Underhill DM, *Fungal Recognition by TLR2 and Dectin-1*. Handb Exp Pharmacol, 2008(183): p. 87-109.
33. Romani L, *Immunity to fungal infections.* Nat Rev Immunol, 2011. **11**(4): p. 275-88.
34. Romani L, *Innate and adaptive immunity in Candida albicans infections and saprophytism.* J Leukoc Biol, 2000. **68**(2): p. 175-9.
35. Lilic D, Gravenor I, Robson N, et al., *Deregulated production of protective cytokines in response to Candida albicans infection in patients with chronic mucocutaneous candidiasis.* Infect Immun, 2003. **71**(10): p. 5690-9.
36. Harrington LE, Hatton RD, Mangan PR, et al., *Interleukin 17-producing CD4+ effector T cells develop via a lineage distinct from the T helper type 1 and 2 lineages.* Nat Immunol, 2005. **6**(11): p. 1123-32.
37. Oppmann B, Lesley R, Blom B, et al., *Novel p19 protein engages IL-12p40 to*

form a cytokine, IL-23, with biological activities similar as well as distinct from IL-12. Immunity, 2000. **13**(5): p. 715-25.

38. van de Veerdonk FL, Gresnigt MS, Kullberg BJ, et al., *Th17 responses and host defense against microorganisms: an overview.* BMB Rep, 2009. **42**(12): p. 776-87.
39. Puel A, Picard C, Cypowyj S, et al., *Inborn errors of mucocutaneous immunity to Candida albicans in humans: a role for IL-17 cytokines?* Curr Opin Immunol, 2010. **22**(4): p. 467-74.
40. Bettelli E, Oukka M, and Kuchroo VK, *T(H)-17 cells in the circle of immunity and autoimmunity.* Nat Immunol, 2007. **8**(4): p. 345-50.
41. Puel A, Cypowyj S, Marodi L, et al., *Inborn errors of human IL-17 immunity underlie chronic mucocutaneous candidiasis.* Curr Opin Allergy Clin Immunol, 2012. **12**(6): p. 616-22.
42. Gaffen SL, Hernandez-Santos N, and Peterson AC, *IL-17 signaling in host defense against Candida albicans.* Immunol Res, 2011. **50**(2-3): p. 181-7.
43. Heropolitanska-Pliszka E, Pietrucha B, Mikoluc B, et al., *Hyper-IgE syndrome with mutation in STAT3 gene - case report and literature review.* Med Wieku Rozwoj, 2009. **13**(1): p. 19-25.
44. Minegishi Y, *Hyper-IgE syndrome.* Curr Opin Immunol, 2009. **21**(5): p. 487-92.
45. Holland SM, DeLeo FR, Elloumi HZ, et al., *STAT3 mutations in the hyper-IgE syndrome.* N Engl J Med, 2007. **357**(16): p. 1608-19.
46. Minegishi Y, Saito M, Tsuchiya S, et al., *Dominant-negative mutations in the DNA-binding domain of STAT3 cause hyper-IgE syndrome.* Nature, 2007. **448**(7157): p. 1058-62.
47. Ma CS, Chew GY, Simpson N, et al., *Deficiency of Th17 cells in hyper IgE syndrome due to mutations in STAT3.* J Exp Med, 2008. **205**(7): p. 1551-7.
48. Milner JD, Brenchley JM, Laurence A, et al., *Impaired T(H)17 cell differentiation in subjects with autosomal dominant hyper-IgE syndrome.* Nature, 2008. **452**(7188): p. 773-6.
49. Conti HR, Shen F, Nayyar N, et al., *Th17 cells and IL-17 receptor signaling are essential for mucosal host defense against oral candidiasis.* J Exp Med, 2009.

206(2): p. 299-311.

50. Liu X, Lee YS, Yu CR, et al., *Loss of STAT3 in CD4+ T cells prevents development of experimental autoimmune diseases.* J Immunol, 2008. **180**(9): p. 6070-6.
51. Zhang Q, Davis JC, Lamborn IT, et al., *Combined immunodeficiency associated with DOCK8 mutations.* N Engl J Med, 2009. **361**(21): p. 2046-55.
52. Engelhardt KR, McGhee S, Winkler S, et al., *Large deletions and point mutations involving the dedicator of cytokinesis 8 (DOCK8) in the autosomal-recessive form of hyper-IgE syndrome.* J Allergy Clin Immunol, 2009. **124**(6): p. 1289-302 e4.
53. Milner JD and Holland SM, *The cup runneth over: lessons from the ever-expanding pool of primary immunodeficiency diseases.* Nat Rev Immunol, 2013. **13**(9): p. 635-48.
54. Minegishi Y, Saito M, Morio T, et al., *Human tyrosine kinase 2 deficiency reveals its requisite roles in multiple cytokine signals involved in innate and acquired immunity.* Immunity, 2006. **25**(5): p. 745-55.
55. Al Khatib S, Keles S, Garcia-Lloret M, et al., *Defects along the T(H)17 differentiation pathway underlie genetically distinct forms of the hyper IgE syndrome.* J Allergy Clin Immunol, 2009. **124**(2): p. 342-8, 348 e1-5.
56. Kilic SS, Hacimustafaoglu M, Boisson-Dupuis S, et al., *A patient with tyrosine kinase 2 deficiency without hyper-IgE syndrome.* J Pediatr, 2012. **160**(6): p. 1055-7.
57. LeibundGut-Landmann S, Gross O, Robinson MJ, et al., *Syk- and CARD9-dependent coupling of innate immunity to the induction of T helper cells that produce interleukin 17.* Nat Immunol, 2007. **8**(6): p. 630-8.
58. Puel A, Cypowyj S, Bustamante J, et al., *Chronic mucocutaneous candidiasis in humans with inborn errors of interleukin-17 immunity.* Science, 2011. **332**(6025): p. 65-8.
59. de Beaucoudrey L, Samarina A, Bustamante J, et al., *Revisiting human IL-12Rbeta1 deficiency: a survey of 141 patients from 30 countries.* Medicine (Baltimore), 2010. **89**(6): p. 381-402.

60. de Beaucoudrey L, Puel A, Filipe-Santos O, et al., *Mutations in STAT3 and IL12RB1 impair the development of human IL-17-producing T cells.* J Exp Med, 2008. **205**(7): p. 1543-50.

61. Nagamine K, Peterson P, Scott HS, et al., *Positional cloning of the APECED gene.* Nat Genet, 1997. **17**(4): p. 393-8.

62. Puel A, Doffinger R, Natividad A, et al., *Autoantibodies against IL-17A, IL-17F, and IL-22 in patients with chronic mucocutaneous candidiasis and autoimmune polyendocrine syndrome type I.* J Exp Med, 2010. **207**(2): p. 291-7.

63. Kisand K, Boe Wolff AS, Podkrajsek KT, et al., *Chronic mucocutaneous candidiasis in APECED or thymoma patients correlates with autoimmunity to Th17-associated cytokines.* J Exp Med, 2010. **207**(2): p. 299-308.

64. Nehme NT, Pachlopnik Schmid J, Debeurme F, et al., *MST1 mutations in autosomal recessive primary immunodeficiency characterized by defective naive T-cell survival.* Blood, 2012. **119**(15): p. 3458-68.

65. Abdollahpour H, Appaswamy G, Kotlarz D, et al., *The phenotype of human STK4 deficiency.* Blood, 2012. **119**(15): p. 3450-7.

66. Boisson B, Wang C, Pedergnana V, et al., *An ACT1 mutation selectively abolishes interleukin-17 responses in humans with chronic mucocutaneous candidiasis.* Immunity, 2013. **39**(4): p. 676-86.

67. van de Veerdonk FL, Plantinga TS, Hoischen A, et al., *STAT1 mutations in autosomal dominant chronic mucocutaneous candidiasis.* N Engl J Med, 2011. **365**(1): p. 54-61.

68. Liu L, Okada S, Kong XF, et al., *Gain-of-function human STAT1 mutations impair IL-17 immunity and underlie chronic mucocutaneous candidiasis.* J Exp Med, 2011. **208**(8): p. 1635-48.

69. Smeekens SP, Plantinga TS, van de Veerdonk FL, et al., *STAT1 hyperphosphorylation and defective IL12R/IL23R signaling underlie defective immunity in autosomal dominant chronic mucocutaneous candidiasis.* PLoS One, 2011. **6**(12): p. e29248.

70. Averbuch D, Chapgier A, Boisson-Dupuis S, et al., *The clinical spectrum of patients with deficiency of Signal Transducer and Activator of Transcription-1.*

Pediatr Infect Dis J, 2011. **30**(4): p. 352-5.

71. Takezaki S, Yamada M, Kato M, et al., *Chronic mucocutaneous candidiasis caused by a gain-of-function mutation in the STAT1 DNA-binding domain.* J Immunol, 2012. **189**(3): p. 1521-6.
72. Toth B, Mehes L, Tasko S, et al., *Herpes in STAT1 gain-of-function mutation.* Lancet, 2012. **379**(9835): p. 2500.
73. Boisson-Dupuis S, Kong XF, Okada S, et al., *Inborn errors of human STAT1: allelic heterogeneity governs the diversity of immunological and infectious phenotypes.* Curr Opin Immunol, 2012. **24**(4): p. 364-78.
74. Soltesz B, Toth B, Shabashova N, et al., *New and recurrent gain-of-function STAT1 mutations in patients with chronic mucocutaneous candidiasis from Eastern and Central Europe.* J Med Genet, 2013. **50**(9): p. 567-78.
75. Ng WF, von Delwig A, Carmichael AJ, et al., *Impaired T(H)17 responses in patients with chronic mucocutaneous candidiasis with and without autoimmune polyendocrinopathy-candidiasis-ectodermal dystrophy.* J Allergy Clin Immunol, 2010. **126**(5): p. 1006-15, 1015 e1-4.
76. Ihle JN, *The Stat family in cytokine signaling.* Curr Opin Cell Biol, 2001. **13**(2): p. 211-7.
77. Leonard WJ, *Role of Jak kinases and STATs in cytokine signal transduction.* Int J Hematol, 2001. **73**(3): p. 271-7.
78. Levy DE and Darnell JE, Jr., *Stats: transcriptional control and biological impact.* Nat Rev Mol Cell Biol, 2002. **3**(9): p. 651-62.
79. Casanova JL, Holland SM, and Notarangelo LD, *Inborn errors of human JAKs and STATs.* Immunity, 2012. **36**(4): p. 515-28.
80. Mitchell TJ and John S, *Signal transducer and activator of transcription (STAT) signalling and T-cell lymphomas.* Immunology, 2005. **114**(3): p. 301-12.
81. Lim CP and Cao X, *Structure, function, and regulation of STAT proteins.* Mol Biosyst, 2006. **2**(11): p. 536-50.
82. Benekli M, Baer MR, Baumann H, et al., *Signal transducer and activator of transcription proteins in leukemias.* Blood, 2003. **101**(8): p. 2940-54.
83. Shuai K and Liu B, *Regulation of JAK-STAT signalling in the immune system.*

Nat Rev Immunol, 2003. **3**(11): p. 900-11.

84. Zhuang S, *Regulation of STAT signaling by acetylation.* Cell Signal, 2013. **25**(9): p. 1924-31.

85. Platanias LC, *Mechanisms of type-I- and type-II-interferon-mediated signalling.* Nat Rev Immunol, 2005. **5**(5): p. 375-86.

86. O'Shea JJ, Lahesmaa R, Vahedi G, et al., *Genomic views of STAT function in CD4+ T helper cell differentiation.* Nat Rev Immunol, 2011. **11**(4): p. 239-50.

87. Yang XO, Panopoulos AD, Nurieva R, et al., *STAT3 regulates cytokine-mediated generation of inflammatory helper T cells.* J Biol Chem, 2007. **282**(13): p. 9358-63.

88. Chen Z, Laurence A, Kanno Y, et al., *Selective regulatory function of Socs3 in the formation of IL-17-secreting T cells.* Proc Natl Acad Sci U S A, 2006. **103**(21): p. 8137-42.

89. Eyerich S, Eyerich K, Cavani A, et al., *IL-17 and IL-22: siblings, not twins.* Trends Immunol, 2010. **31**(9): p. 354-61.

90. Durant L, Watford WT, Ramos HL, et al., *Diverse targets of the transcription factor STAT3 contribute to T cell pathogenicity and homeostasis.* Immunity, 2010. **32**(5): p. 605-15.

91. Regis G, Pensa S, Boselli D, et al., *Ups and downs: the STAT1:STAT3 seesaw of Interferon and gp130 receptor signalling.* Semin Cell Dev Biol, 2008. **19**(4): p. 351-9.

92. Montgomery DC, *Design and analysis of experiments*. 2006: Wiley. com.

93. Dupuis S, Dargemont C, Fieschi C, et al., *Impairment of mycobacterial but not viral immunity by a germline human STAT1 mutation.* Science, 2001. **293**(5528): p. 300-3.

94. Dupuis S, Jouanguy E, Al-Hajjar S, et al., *Impaired response to interferon-alpha/beta and lethal viral disease in human STAT1 deficiency.* Nat Genet, 2003. **33**(3): p. 388-91.

95. Chapgier A, Kong XF, Boisson-Dupuis S, et al., *A partial form of recessive STAT1 deficiency in humans.* J Clin Invest, 2009. **119**(6): p. 1502-14.

96. Acosta-Rodriguez EV, Rivino L, Geginat J, et al., *Surface phenotype and*

antigenic specificity of human interleukin 17-producing T helper memory cells. Nat Immunol, 2007. **8**(6): p. 639-46.

97. Lilic D, *Unravelling fungal immunity through primary immune deficiencies.* Curr Opin Microbiol, 2012. **15**(4): p. 420-6.

98. Pensa S, Regis G, Boselli D, et al., *STAT1 and STAT3 in Tumorigenesis: Two Sides of the Same Coin?* JAK-STAT Pathway in Disease, ed. Stephanou A. 2009. 100-121.

99. Katze MG, He Y, and Gale M, Jr., *Viruses and interferon: a fight for supremacy.* Nat Rev Immunol, 2002. **2**(9): p. 675-87.

100. Kalliolias GD and Ivashkiv LB, *IL-27 activates human monocytes via STAT1 and suppresses IL-10 production but the inflammatory functions of IL-27 are abrogated by TLRs and p38.* J Immunol, 2008. **180**(9): p. 6325-33.

101. Sato T, Selleri C, Young NS, et al., *Inhibition of interferon regulatory factor-1 expression results in predominance of cell growth stimulatory effects of interferon-gamma due to phosphorylation of Stat1 and Stat3.* Blood, 1997. **90**(12): p. 4749-58.

102. Lemmink HH, Tuyt L, Knol G, et al., *Identification of LIL-STAT in monocytic leukemia cells and monocytes after stimulation with interleukin-6 or interferon gamma.* Blood, 2001. **98**(13): p. 3849-52.

103. Murray PJ, *The primary mechanism of the IL-10-regulated antiinflammatory response is to selectively inhibit transcription.* Proc Natl Acad Sci U S A, 2005. **102**(24): p. 8686-91.

104. O'Shea JJ and Murray PJ, *Cytokine signaling modules in inflammatory responses.* Immunity, 2008. **28**(4): p. 477-87.

105. Torella D, Curcio A, Gasparri C, et al., *Fludarabine prevents smooth muscle proliferation in vitro and neointimal hyperplasia in vivo through specific inhibition of STAT-1 activation.* Am J Physiol Heart Circ Physiol, 2007. **292**(6): p. H2935-43.

106. Frank DA, Mahajan S, and Ritz J, *Fludarabine-induced immunosuppression is associated with inhibition of STAT1 signaling.* Nat Med, 1999. **5**(4): p. 444-7.

107. Icardi L, De Bosscher K, and Tavernier J, *The HAT/HDAC interplay: multilevel*

control of STAT signaling. Cytokine Growth Factor Rev, 2013. **23**(6): p. 283-91.

108. Drummond DC, Noble CO, Kirpotin DB, et al., *Clinical development of histone deacetylase inhibitors as anticancer agents.* Annu Rev Pharmacol Toxicol, 2005. **45**: p. 495-528.

109. Kisand K, Lilic D, Casanova JL, et al., *Mucocutaneous candidiasis and autoimmunity against cytokines in APECED and thymoma patients: clinical and pathogenetic implications.* Eur J Immunol, 2011. **41**(6): p. 1517-27.

110. Chapgier A, Wynn RF, Jouanguy E, et al., *Human complete Stat-1 deficiency is associated with defective type I and II IFN responses in vitro but immunity to some low virulence viruses in vivo.* J Immunol, 2006. **176**(8): p. 5078-83.

111. Vairo D, Tassone L, Tabellini G, et al., *Severe impairment of IFN-{gamma} and IFN-{alpha} responses in cells of a patient with a novel STAT1 splicing mutation.* Blood, 2011. **118**(7): p. 1806-17.

112. Sampaio EP, Bax HI, Hsu AP, et al., *A novel STAT1 mutation associated with disseminated mycobacterial disease.* J Clin Immunol, 2012. **32**(4): p. 681-9.

113. Chapgier A, Boisson-Dupuis S, Jouanguy E, et al., *Novel STAT1 alleles in otherwise healthy patients with mycobacterial disease.* PLoS Genet, 2006. **2**(8): p. e131.

114. Hirata O, Okada S, Tsumura M, et al., *Heterozygosity for the Y701C STAT1 mutation in a multiplex kindred with multifocal osteomyelitis.* Haematologica, 2013. **98**(10): p. 1641-9.

115. Tsumura M, Okada S, Sakai H, et al., *Dominant-negative STAT1 SH2 domain mutations in unrelated patients with Mendelian susceptibility to mycobacterial disease.* Hum Mutat, 2012. **33**(9): p. 1377-87.

116. Sampaio EP, Hsu AP, Pechacek J, et al., *Signal transducer and activator of transcription 1 (STAT1) gain-of-function mutations and disseminated coccidioidomycosis and histoplasmosis.* J Allergy Clin Immunol, 2013. **131**(6): p. 1624-34.

117. Uzel G, Sampaio EP, Lawrence MG, et al., *Dominant gain-of-function STAT1 mutations in FOXP3 wild-type immune dysregulation-polyendocrinopathy-enteropathy-X-linked-like syndrome.* J

Allergy Clin Immunol, 2013. **131**(6): p. 1611-23.

118. Zola H and Flego L, *Expression of interleukin-6 receptor on blood lymphocytes without in vitro activation.* Immunology, 1992. **76**(2): p. 338-40.

119. Floss DM, Mrotzek S, Klocker T, et al., *Identification of canonical tyrosine-dependent and non-canonical tyrosine-independent STAT3 activation sites in the intracellular domain of the interleukin 23 receptor.* J Biol Chem, 2013. **288**(27): p. 19386-400.

120. Anastasov N, Klier M, Koch I, et al., *Efficient shRNA delivery into B and T lymphoma cells using lentiviral vector-mediated transfer.* J Hematop, 2009. **2**(1): p. 9-19.

121. Guven H, Konstantinidis KV, Alici E, et al., *Efficient gene transfer into primary human natural killer cells by retroviral transduction.* Exp Hematol, 2005. **33**(11): p. 1320-8.

122. Huang H, Pannetier C, Hu-Li J, et al., *Transient transfection of primary T helper cells by particle-mediated gene transfer.* J Immunol Methods, 1998. **215**(1-2): p. 173-7.

123. Vitolo JM, Thiriet C, and Hayes JJ, *The H3-H4 N-terminal tail domains are the primary mediators of transcription factor IIIA access to 5S DNA within a nucleosome.* Mol Cell Biol, 2000. **20**(6): p. 2167-75.

124. Lee KK and Workman JL, *Histone acetyltransferase complexes: one size doesn't fit all.* Nat Rev Mol Cell Biol, 2007. **8**(4): p. 284-95.

125. Spange S, Wagner T, Heinzel T, et al., *Acetylation of non-histone proteins modulates cellular signalling at multiple levels.* Int J Biochem Cell Biol, 2009. **41**(1): p. 185-98.

126. Yuan ZL, Guan YJ, Chatterjee D, et al., *Stat3 dimerization regulated by reversible acetylation of a single lysine residue.* Science, 2005. **307**(5707): p. 269-73.

127. Wang R, Cherukuri P, and Luo J, *Activation of Stat3 sequence-specific DNA binding and transcription by p300/CREB-binding protein-mediated acetylation.* J Biol Chem, 2005. **280**(12): p. 11528-34.

128. Kramer OH and Heinzel T, *Phosphorylation-acetylation switch in the regulation*

of STAT1 signaling. Mol Cell Endocrinol, 2010. **315**(1-2): p. 40-8.

129. Guo L, Guo H, Gao C, et al., *Stat1 acetylation inhibits inducible nitric oxide synthase expression in interferon-gamma-treated RAW264.7 murine macrophages.* Surgery, 2007. **142**(2): p. 156-62.

130. Trifari S, Kaplan CD, Tran EH, et al., *Identification of a human helper T cell population that has abundant production of interleukin 22 and is distinct from T(H)-17, T(H)1 and T(H)2 cells.* Nat Immunol, 2009. **10**(8): p. 864-71.

131. Villagra A, Sotomayor EM, and Seto E, *Histone deacetylases and the immunological network: implications in cancer and inflammation.* Oncogene, 2010. **29**(2): p. 157-73.

132. West AC and Johnstone RW, *New and emerging HDAC inhibitors for cancer treatment.* J Clin Invest, 2014. **124**(1): p. 30-9.

133. Tamiya T, Kashiwagi I, Takahashi R, et al., *Suppressors of cytokine signaling (SOCS) proteins and JAK/STAT pathways: regulation of T-cell inflammation by SOCS1 and SOCS3.* Arterioscler Thromb Vasc Biol, 2011. **31**(5): p. 980-5.

134. Shuai K, *Regulation of cytokine signaling pathways by PIAS proteins.* Cell Res, 2006. **16**(2): p. 196-202.

135. Meyer T, Marg A, Lemke P, et al., *DNA binding controls inactivation and nuclear accumulation of the transcription factor Stat1*. Genes Dev, 2003. **17**(16): p. 1992-2005.

136. Wu TR, Hong YK, Wang XD, et al., *SHP-2 is a dual-specificity phosphatase involved in Stat1 dephosphorylation at both tyrosine and serine residues in nuclei.* J Biol Chem, 2002. **277**(49): p. 47572-80.

137. Yang J, Huang J, Dasgupta M, et al., *Reversible methylation of promoter-bound STAT3 by histone-modifying enzymes.* Proc Natl Acad Sci U S A, 2010. **107**(50): p. 21499-504.